DEEP DECK AND CELLULAR DECK DIAPHRAGM STRENGTH AND STIFFNESS EVALUATION

By

Jonathan M. Bagwell

A Thesis submitted to the faculty of the Virginia Polytechnic Institute and State University in partial fulfillment of the requirements for the degree of

MASTER OF SCIENCE
In
Civil Engineering

APPROVED:

W. Samuel Easterling, Chair

Thomas M. Murray

Carin Roberts-Wollmann

June 2007
Blacksburg, Virginia 24061

Keywords: Diaphragm Stiffness, Diaphragm Strength, Cellular Deck, Deep Deck, Cold Formed Steel

DEEP DECK AND CELLULAR DECK DIAPHRAGM STRENGTH AND STIFFNESS EVALUATION

by:

Jonathan M. Bagwell

Abstract

Twenty cantilever diaphragm tests were performed in the Structures and Materials Laboratory at Virginia Tech. The tests included both deep deck and cellular deck profiles with varying structural and side-lap connections. The tests were conducted with three different structural connections: screws, pins and welds and two different side-lap connections: screws and button punch.

The tests were conducted and both load and deflection of the diaphragms were recorded. The current International Code Council, ICC, evaluation procedure shows that there are two different methods for measuring diaphragm deflection. The first method was by measuring specific corner displacements and making corrections to remove any rigid body motion. The second method is by measuring the deflection of the diagonals of the diaphragm. In this study both measurements were taken to do a comparison of the results that were obtained.

Both strength and stiffness values were calculated based on the Steel Deck Institute (SDI) Diaphragm Design Manual (2004) and modifications described by Luttrell (2005). The paper by Luttrell (2005) only recommends modifications for the calculation of diaphragm stiffness. The data obtained from the tests were compared to the SDI calculations to distinguish any noticeable trends. Modifications are recommended regarding diaphragm strength and further research is suggested to create a better stiffness prediction of diaphragms.

Acknowledgements

I would like to express my gratitude to Dr. W. Samuel Easterling for his guidance and assistance with this research study. I appreciate the opportunity he gave me to do this research. I have learned and accomplished many things that I feel will help me better develop my professional career. I am also thankful for the assistance provided to me by my additional committee members, Dr. Carin Roberts-Wollmann and Dr. Thomas Murray.

I would also like to thank the American Iron and Steel Institute and the Steel Deck Institute for providing the funding for this study. I also would like to thank Consolidated Systems, United Steel Deck, Vulcraft, Wheeling Corrugating and Hilti for the materials they provided. Without these materials this research would not have been possible. A particular thanks goes to Nucor Research and Development for providing the structural steel needed to fabricate the test frame.

In this project I was also given much assistance in consulting by Dr. Larry Luttrell which was much appreciated. His explanations and expertise were utilized to better understand the development of the current SDI design manuals. I appreciate the assistance given by Pierre Gignac, chair of SDI Diaphragm committee, in the organization and development of this research study.

Thank you to Brett Farmer, Dennis Huffman and Clark Brown at the Virginia Tech Structures and Material Laboratory. All of your technical assistance for the completion of my project was greatly appreciated. I would like to thank Adam Bowland for his help in the construction of many of my test specimens. Without his help my research would have been much more difficult.

Most importantly I would like to thank my parents and grandparents for all of their love and support. They have been there to encourage me to succeed and continue with my education. Without their help I would not have gotten where I am today. Thanks for always being there.

Table of Contents

List of Figures

List of Tables

CHAPTER 1 - INTRODUCTION

1.1 Overview

In the design of any structure, the determination of proper loads is essential in the design process. The two types of loads common to any structure are vertical and horizontal. Vertical loads come from the application of live loads and the presence of dead loads that are within the structure. Horizontal loads come from external forces, such as wind or earthquakes, which are applied perpendicular to the exterior of the building. Once these loads are quantified the building components must be designed to withstand the stresses that will ensue. Some of the common building components are beams, columns, connections, roof and floor sheathing, and horizontal load resisting systems. Horizontal load resisting systems can include thing such as x-bracing, shear walls and diaphragms.

Horizontal load resisting systems are placed in a building at locations that are most advantageous for their purpose. This advantage comes from the floor and roof systems ability to act as a deep beam or diaphragm to transfer the loads. The typical floor and roof bracing systems in steel buildings that are used to accomplish this are x-bracing, concrete slabs, light gage cold-formed steel deck, and steel deck reinforced concrete slabs. Light gage cold-formed steel deck's use as a diaphragm system is the focus of this thesis with special interest in the effect of deep deck systems.

1.2 Scope of Research

The goal of this research was to examine the performance of deep deck and cellular deck diaphragms. Most of the diaphragm research conducted from the late 1950s to date was done with decks ranging in depth from 9/16 in. to 3 in. In this study, narrow rib decks, N-decks, with a depth greater than 3 in. and cellular decks 3 in. or greater were considered. Cellular decks have similar profiles to N-decks with the addition of a flat sheet on the bottom of the profile. This flat sheet benefits the profile in several ways. It increases the flexural strength of the profile enabling it to span longer distances. It also decreases the warping distortion that occurs at the end of the sheet. Also the flat sheet helps increase the shear strength of the section in-plane by increasing the shear area. The

research program consisted of 20 diaphragm tests and sixty tensile coupon tests representing each unique component of the different deck sections. This test program utilized three types of sheet to structural connectors and two types of sheet-to-sheet connections. Nine tests were conducted with screws used for the structural connections, eight tests with Hilti powder-actuated fasteners used for the structural connections, and three tests with welds used for the structural connections.

The experimental results were analyzed to determine both the strength and stiffness of the system. The experimental values were compared to those predicted by the SDIDDM03 (Luttrell 2004) including the modifications described by Luttrell (2005) that pertain to deep deck and cellular deck profiles. Once the comparisons were made recommendations were developed for modifications to the SDI design method.

1.3 Research Outline

To better understand the research topics a brief outline will be given that describes the topics that will be covered. Chapter 2 is a review of the past research that has been done in the field of cold-formed steel diaphragms. This review, however, will be about general diaphragm behavior not pertaining to deep decks. This is because the information is not available, hence, the reason for this study. The methodology behind the SDIDDM03 is also presented in Chapter 2.

In Chapter 3, the experimental test program is described in detail. A designation was established for each test to distinguish the connection configuration being used. The test frame configuration is shown to illustrate how the diaphragm test setups were arranged. The loading and measurements taken for each test are described in detail. Also included in the test program are coupon tests. The process used for their testing is also described.

Detailed descriptions of the diaphragm strength and stiffness calculations from the SDIDDM03 are presented in Chapter 4. Along with a description of the calculation procedure, example calculations are given. A comparison of the calculated strength and stiffness with the observed test strength and stiffness are presented.

In Chapter 5 a summary of the significant findings from the test program are presented. Along with these findings any potential conclusions and recommendations

regarding the SDIDDM03 design method are also presented. Suggestions for further research are also listed.

1.4 Definitions

Panel – An individual cold-formed steel deck unit ranging in width from 12 in. to 36 in. Each panel can either be single span or multiple spans depending upon the application.

Cover Width – The width of each panel of a cold-formed steel deck.

Structural Connection – Any connection used to attach the cold-formed steel deck to the main support elements of a structure.

Puddle Welds – A type of welded connection that is used to secure deck panels to the supporting steel structure. These welds are made by burning a hole in the deck panel and filling in the hole with weld metal in a continuous process. The typical puddle weld used in this project was ¾ in. visible diameter.

Powder Actuated Fasteners – A specialized mechanical fastener used to secure the deck panels to the supporting steel structure. The fastener is installed by firing the pin from a specialized gun with a powder charge into the structural steel. The powder actuated fastener used in this project was a Hilti Pin X-ENP-19 L15.

Side-Lap Connection – The side-lap is the interface where two panels connect parallel to the span of the deck. This connection can be made by: seam welds, screws, or button punch. In this project these connections were made with either screws or button punch.

Button Punch – A mechanical side-lap connection made by crimping the longitudinal hooks between the adjacent panels. This is done with a specialized tool that is produced by a manufacturer specifically for their deck profiles.

Pitch – The width of a single flute or cell in a diaphragm profile.

CHAPTER 2 –LITERATURE REVIEW

2.1 Previous Research

The first research work on light gage steel shear diaphragms in the United States was done by Arthur Nilson at Cornell University. From 1956 to 1960 he tested 46 full-scale diaphragms with the cantilever test method. Originally, the tests were conducted with three connected bays loaded at the third points but it was determined that an individual bay could be tested simply for shear strength. The middle bay in the original tests was eliminated because even though some moment was transferred through the system only the total deflection was changed (Nilson, 1960 a). During the testing of steel diaphragms at Cornell University the most efficient and economical ways to connect to the frame and to join the panels were established. A special type of welding was determined to be the most efficient and has since become a part of standard industry practice. For the different connection scenarios four basic types of welds were established. These welds are puddle welds at panel ends, fillet welds at panel edges, seam weld used for concave-upward hook joint, and a different seam weld used for concave-downward hook joint (Nilson, 1960 b). The cantilever test method has been used for many years and has become the American Iron and Steel Institute, AISI, standard (AISI, 2002). Luttrell followed Nilson's work and derived a semi-empirical equation to determine the shear stiffness of standard corrugated diaphragms (Luttrell, 1965 a). One of Luttrell's main findings was that the panel length has a strong influence on stiffness but not on the overall ultimate strength. Apparao (1966) supported many of the observations that Luttrell had reported. The observations showed that length of the diaphragm, fastener type, and connector spacing are the major influences on shear stiffness (Apparao, 1966).

Luttrell (1967) reported on many tests of steel deck diaphragms conducted at Cornell University. The main components that he studied were intermediate side-lap fasteners, panel cover width, deck thickness, panel length, material strength, and frame flexibility. Luttrell observed a moderate influence on the ultimate strength of the diaphragms from the frame flexibility. An interesting point was that no constant correlation was found between number of side-lap fasteners and the diaphragm shear

strength. However, additional side-lap fasteners between purlins were found to impact stiffness more than strength. Luttrell found that strength increased nearly linearly as deck thickness increased. Panel cover width data was not conclusive. However, it pointed to a doubled stiffness for an increase of only 50% in cover width. The panel length was found to have a small effect on the shear strength but could have a large effect on the shear stiffness. The stiffness increase is due to the percentage of corrugation length that is not warped when load is applied (Luttrell, 1967).

Ellifritt and Luttrell (1970) reported over 100 full-scale diaphragm tests. These tests were used to determine the main components that affect diaphragm performance. Once these components were identified, then proper design criteria for both ultimate strength and shear stiffness were developed. Some of the components that were evaluated were: material yield strength, thickness, panel width, extra end weld, purlin spacing, deck profile, side lap fasteners and structural fasteners. The investigation on material yield strength found that its change did not correspond to a linear variation in strength. To account for a material thickness change, a separate equation had to be developed. The equations, which are based on profile dimensions, compute the strength and stiffness of the diaphragm. These equations needed an additional equation to act as a conversion factor which accounts for the thickness change.

For the panel width component, it was noticed that an increase in strength came with wider panels. This was the same finding made by Luttrell (1967). However, this increase was not found to be as significant as the addition of extra welds (Ellifritt and Luttrell, 1970). For the extra end weld, the test results showed that the strength only needed to be modified by a coefficient. This coefficient was related to the gage, profile of the diaphragm, and the spacing of the welds. From the purlin spacing variation it was noticed that as the purlins got closer, the ultimate strength was increased. This was due to the increase in number of fasteners and the reduction of the possibility of out-of-plane buckling of the diaphragm.

Also several different profiles were examined to determine their strength. The different profiles that were evaluated were narrow rib, intermediate rib, and wide rib sections. Because narrow rib was the weakest it was normalized and the other profiles were ranked accordingly. The wide rib profile was found to be the strongest with an

average strength and stiffness increased by 25 percent over the other profiles. Only a small number of screw-connected diaphragms were tested but results showed that if welds were replaced with screws, then the stiffness would decrease slightly but the ultimate strength was not affected much (Ellifritt and Luttrell, 1970).

In 1978 a group of researchers in Canada wanted to compare a few of the existing analytical methods for predicting the shear behavior of diaphragms. The methods that were compared were the ones proposed by Bryan (1972), and Davies (1974). All of these methods were used to describe observed behavior and failures of diaphragms with fasteners other than welding. In this study, comparisons of specific tests would be used to compare the different methods to determine their validity when welds were used as the fasteners for the diaphragms. In the tests that were done, the side-laps of each sheet were attached with a button punch. The end fasteners were done with ¾ in. puddle welds.

In England, diaphragm design was based largely off of the work of Bryan (1972). For each type of diaphragm described in Bryan's work a simple distribution of the forces on the fasteners was used. Through a basic comparison of Bryan's calculations and the test results, it was shown that the method dramatically underestimated the strength of the welded system by approximately four times.

Next Davies method was compared with its improved internal force distribution for the fasteners. Davies method came much closer to the tested strength but was still approximately 30% lower. Davies equations were derived for a specific fastener arrangement and it was noted that care would have to be taken to modify them accordingly (Fazio et al, 1979).

Fazio et al (1979) showed a simplified approach to the problem at hand. This approach was based on the assumption that the seam fasteners were subjected only to longitudinal forces parallel to the panel, the end fasteners are symmetrical to the panel centerline and carry both longitudinal forces and transverse forces, intermediate girt fasteners were symmetrical to the panel center line and carry forces perpendicular to the girt, and the load-slip curves for the end fasteners and the seam fasteners may be assumed to be elasto-plastic (Fazio et al, 1979). With the test that was performed, the simplified method was only approximately 8% off of the tested result. This method was then compared to many other diaphragm tests. The results of this comparison showed a close

correlation to the new method except for in a few cases where the new method was shown to be unconservative (Fazio et al, 1979).

Ameen (1990) did an analytical study of the effects of Z-member end closures being used to increases system stiffness. This study was based off the assumption that with smaller the end warping the overall system stiffness could be increased. To accomplish the analysis the current SDI formulas were modified to account for the added stiffness of the Z-member end closures. From the modified formulas, both the shear strength and the stiffness were predicted and design tables were prepared. Once the preliminary analysis was done, five experimental tests were done to see if the predicted formulas would accurately predict the real behavior of the system. Each test setup was done both with and without the end Z-member end closures. Also different fastener types were used to connect the Z-member to the diaphragm. With the fasteners in every valley and a Z-member being used that had a 2 in. flange, increased the strength varying from 10% to 107%. This variation was dependent on the panel thicknesses and the type and number of stitch connectors. For a Z-member being used that had a 4 in. flange, the strength variation was from 25% to 133%. From these test results, a close agreement was found between the developed equations and the experimental tests of approximately one percent (Ameen, 1990).

In 1990 Chris Glatt did a comparative study to determine the differences between the Tri-Services Manual (TM) and the Structural Deck Institute (SDI) manual for calculating capacities of steel diaphragms. Because the study was done in Kansas it was limited to the materials typically used in the Midwest. (Glatt, 1990) The typical diaphragm was a 22 gage narrow rib deck with 36/4 framing weld pattern, and 2 seam welds per span. Because a diaphragm is a system of small parts that work together to form a larger system, each method was tested for its sensitivity to changes. In the study six different variations were made to determine the methods' response (Glatt, 1990).

The first thing that was tested was the effect of deck thickness. From the comparison it showed that the shape and slope of the curves for design shear to diaphragm span were similar. However, the TM values increased substantially more. The range of difference in the values for the two methods was 10% to 30% greater for the TM. The second study considered the type of deck. SDI strengths apply to all deck types

because deck type is not a variable in the equations. The TM values increase for wide rib decks in comparison to narrow rib decks. The TM equation 5-9 has the most significance affect on local buckling limits of the panel edge flute. SDI equation 2.2-4, Eq. 2.2 in this document, is supposed to account for the same behavior (Glatt, 1990). It was shown that the equations were increasingly sensitive as the decks got thicker.

The third effect studied was the framing weld pattern. The 22 gage deck tests showed that the TM and the SDI was practically unchanged with the TM values averaging 25% below the SDI values. However, the 18 gage deck tests showed that the SDI equations tended to stay along the same trend and the TM values were greatly affected by the change in weld pattern. The fourth parameter considered was the panel width. This was difficult to compare but a full weld pattern of 36/7 and 30/6 which is a weld pattern of 6 in. on center for both. Both methods were shown to predict strengths that were less than 5% below the 36/7 pattern for the 30/6. The next study was done on seam weld spacing. With using just one seam weld per span the methods were pretty comparable with similar graphs of design shear to diaphragm span. However, when five seam welds were used, an increase in strength of 75% was shown for SDI whereas the TM only showed a 40% increase. This showed that the SDI equations were more sensitive to the seam weld spacing (Glatt, 1990).

These studies were done not to discredit either method, but simply to do comparisons of each methods' variables. One of the major disadvantages of the TM is that it was based on 80 full-scale tests done in the sixties that only used welds. Also these welds were done by highly skilled welders that made sure to get the best strength possible out of each weld. This is not a typical field practice and therefore not the best comparison for calculation purposes. The SDI equations were developed with hundreds of full-scale tests that not only did welded connections but rivets and power-driven pins. This makes the SDI equations more versatile for the typical engineering project (Glatt, 1990).

The research presented in this section lead to the development of the current diaphragm strength and stiffness evaluation procedures. Many different factors were tested that affected diaphragms. However, all of this research was limited to depths of 3 in. or less and there were no cellular profiles included. Some research has been done on deep deck and cellular profiles that were available in open literature. However, many of

these tests were done in the late 1950's and 1960's. Consequentially there are not many copies of this literature available. Luttrell has compared his calculation procedures to as many of these test results as could be found. This test study was done to have more data to compare Luttrell's modified design method presented in the white paper (Luttrell, 2005).

2.2 SDI Diaphragm Design Manual Calculation Procedure

The first SDI diaphragm design manual, SDIDDM01, was published in January 1981 by Dr. Larry Luttrell from the Department of Civil Engineering at West Virginia University (Luttrell, 1981). With regards to ultimate strength of steel shear diaphragms the manual focuses on the type and quality of the connections used to attach the panels to each other and to the structural system. The SDIDDM01 was based on 153 full scale diaphragm tests and many strength tests done on different connections types to come up with the theoretical strength formulas (Luttrell, 1981).

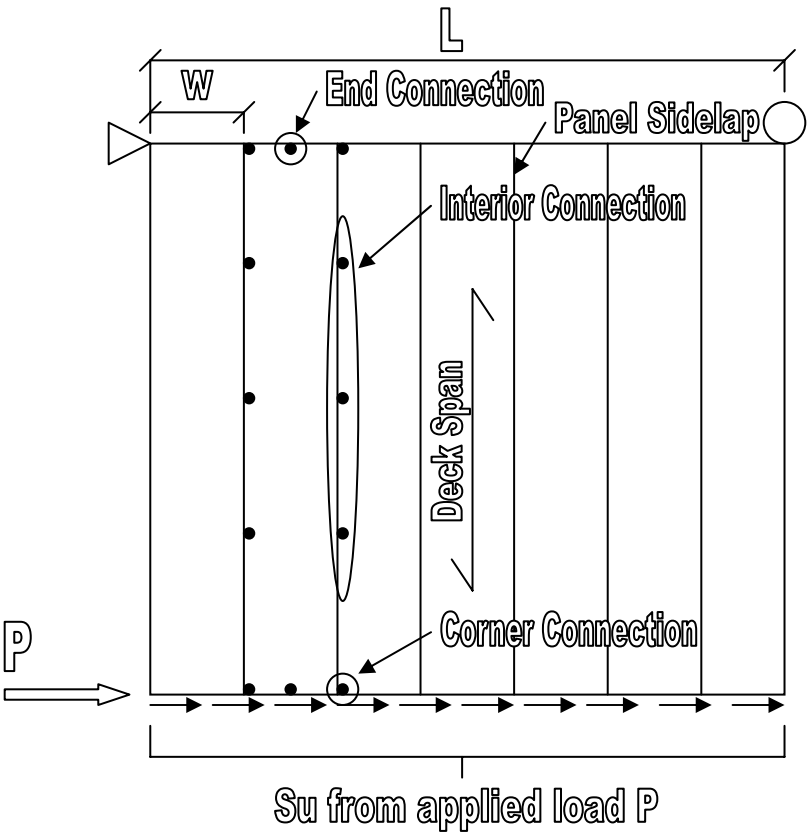

Figure 2-1: Diaphragm Layout Schematic

The design formulas have three scenarios as the potential limiting factors for strength. The first is at the termination of the diaphragm along a panel edge. The strength represented in pounds per foot for this limits is as follows:

$$S_u = \left(2\alpha_1 + n_p \cdot \alpha_2 + n_e\right) \cdot \frac{Q_f}{L} \tag{2.1}$$

Where:

$\alpha_1 = \frac{1}{w} \cdot \sum_{e=1}^{n} x_e$ the end distribution factor per panel

x_e = distance from panel centerline to any fastener in a panel along the end support member

n_p = number of purlins or joists excluding supports at panel ends

α_2 = purlin distribution factor similar to α_1

n_e = total number of edge connectors along the edge excluding those at the purlins or joists and ends

Q_f = shear strength of sheet-to-frame connection

L = total length of the diaphragm

w = panel cover width

The second limitation is at the side-laps along the length of the panels. At this location there is a shear transfer, from the connections, that helps the individual panels act as a system. The strength represented in pounds per foot for this limit is as follows:

$$S_u = \left[2\left(\lambda_1 - 1\right) + n_s \cdot \alpha_s + \frac{1}{w^2} \cdot \left(2 \cdot n_p \cdot \sum_{p=1}^{n} x_p^{\,2} + 4 \cdot \sum_{e=1}^{n} x_e^{\,2} \right) \right] \cdot \frac{Q_f}{L} \tag{2.2}$$

Where:

$\lambda_1 = \frac{1}{1 + \left(\frac{L_s}{135}\right)^2}$ This factor is a measure of the edge flute's tendency to deflect normal to the diaphragm plane. The factor shown is for a

typical panel with a nominal 1.5 in. depth.

n_s = number of side-lap connectors not at purlins or joists

$$\alpha_s = \frac{Q_s}{Q_f}$$ The relative fastener strength

Q_s = shear strength of sheet-to-sheet connection

w = panel cover width

x_p = distance from panel centerline to any fastener in a panel along an interior purlin support member

The third limitation is at the panel ends of the diaphragm at extreme edges of the diaphragm. These are the connectors located at the corners of the diaphragm. The strength represented in pounds per foot for this limit is as follows:

$$S_u = \frac{Q_f}{C_1} = \frac{Q_f \cdot N \cdot B}{\sqrt{B^2 + N^2 \cdot L^2}} \qquad (2.3)$$

Where:

N = the average number of fasteners per foot across panel ends

$$B = n_s \cdot \alpha_s + \frac{1}{w^2} \cdot \left(2 \cdot n_p \cdot \sum_{p=1}^{n} x_p^{\,2} + 4 \cdot \sum_{e=1}^{n} x_e^{\,2} \right)$$

$$C_1 = \sqrt{\left(\frac{1}{N}\right)^2 + \left[\frac{L}{n_s \cdot \alpha_s + \frac{1}{w^2}\left[2 n_p \cdot \left(\sum_{p=1}^{n} x_p^{\,2} \right) + 4 \cdot \sum_{e=1}^{n} x_e^{\,2} \right]} \right]^2}$$

The smallest value from Eq 2.1 through 2.3 is the controlling strength of the diaphragm (Luttrell, 1981).

As far as stiffness of the system is concerned the Steel Deck Institute Diaphragm Design Manual first edition, SDIDDM01, treats the general stiffness of the system to be represented by:

$$G' = \frac{P}{\Delta} \cdot \frac{a}{L} \tag{2.4}$$

where P is taken at or below $0.4P_u$ and Δ is the corresponding shear displacement (Luttrell, 1981). P_u is the maximum load the diaphragm can resist. The deflection of the system, Δ, comes from several different places and is summed to determine the total displacement. The deflection of the system comes from: shear displacement Δ_s, warping displacement Δ_d, relative slip at panel edge Δ_c, and other miscellaneous effects. The general stiffness equation used to determine the system stiffness is:

$$G' = \frac{E \cdot t}{2 \cdot (1 + \nu) \cdot \frac{s}{d} + D_n + C} \tag{2.5}$$

Where:

s = Developed width of plate per pitch, d

D_n = panel warping constant

C = slip relaxation constant

E = modulus of elasticity

ν = Poison's ratio

t = sheet steel thickness

All of the unknowns in Eq 2.5 are essentially given once the profile is selected and the connection pattern is determined. The only thing that is unknown for Eq 2.5 then is the slip relaxation constant, C, which is a function of the structural and side-laps connection flexibility. The slip relaxation constant, C, for the case in this project is when the number of sheets times the width equals the system width a.

$$C = \frac{2E \cdot t \cdot L}{w} \cdot S_f \left(\frac{1}{2 \cdot \alpha_1 + n_p \cdot \alpha_2 + 2 \cdot n_s \cdot \frac{S_f}{S_s}} \right) \tag{2.6}$$

Where:

S_f = flexibility of the sheet-to-frame connection

S_s = flexibility of the sheet-to-sheet connection

The second SDI diaphragm design manual, SDIDDM02, was published in 1987 (Luttrell, 1987). It was also prepared by Dr. Larry Luttrell from West Virginia University, as was the first diaphragm design manual. The strength and stiffness theories for diaphragm design are the same as the previous manual with a few modifications. As far as the strength is concerned the main change came with a general equation for λ, (Luttrell, 1987).

$$\lambda = 1 - \frac{DL_V}{240\sqrt{t}} \tag{2.7}$$

Where:

D = panel depth, in.

L_v = purlin spacing, ft

As can be seen, this new equation is made to accommodate any depth of deck whereas the previous λ_1 equation was given specifically for 1.5 in decks only. This new equation provides more diversity to the engineers' using the SDIDDM02. Also in the SDIDDM02 a stability check was added that takes into consideration the overall buckling of the diaphragm plate. Two scenarios are shown, one with many spans and another with fewer spans. The SDIDDM02 equation with fewer spans, Eq. 2.4-2, is the one that would pertain to this project. With this equation let $L = 2L_v$ (Luttrell, 1987).

$$S_c = \frac{3250}{L_v^2} \cdot \sqrt[4]{I^3 \cdot t^3 \frac{d}{s}} \tag{2.8}$$

Where:

I = panel moment of inertia, in^4/ft of width

d = corrugation pitch, in.

s = developed flute width, in.

L = design length, ft

The third SDI diaphragm design manual, SDIDDM03, was published in September 2004. All of the major analytical theory behind the strength and stiffness evaluation of diaphragms are the same. Only one small modification was made that would apply to this project. The λ equation was given a limit that its value would always be taken as greater than or equal to 0.7.

In 2005 Dr. Luttrell prepared a document as an addendum to the SDIDDM03 titled, Deeper Steel Deck and Cellular Diaphragms (Luttrell, 2005). This white paper addresses the issues related to the decks listed in the title. The adjustments made to the equations that are typically used in the SDIDDM03 were based upon tests done by Arthur Nilson (1956) on deep decks and testing done by Fenestra Company and Mahon Steel in the 1950's. The main change to the SDIDDM03 is present in Eq 2.5 for calculating the diaphragm stiffness. The new equation for diaphragm stiffness is:

$$G' = \frac{E \cdot t}{A_A + \left(\frac{D_n}{3 \cdot D_d \left(\frac{t_b}{t} \right)^3} \right) + C} \tag{2.9}$$

Where:

$$A_A = \frac{2.6 \cdot D_{DL}}{\left(1 + D_{DL} \cdot \frac{t_b}{t} \right)} \tag{2.10}$$

D_d = depth of deck, in.

D_{DL} = cell width/d, developed width of hat per cell, in.

With the increased torsional stiffness in a cellular system due to the bottom plate a need arose to modify the denominator of the previously used equations to increase the stiffness values obtained. The A_A term accounts for the shear path that a panel has when it involves both the top hat and a flat bottom sheet. The flat sheet has a much smaller shear width than the top hat therefore it is the stiffer element in the profile. The second

term in the denominator is the warping portion. Because the section is now tubular instead of an open flute the torsional stiffness of the section is greatly increased which makes panel warping effects a much smaller portion of the stiffness.

Luttrell developed these modifications from cellular diaphragm tests reported by: Nilson (1960a), Nilson (1960b), Nilson (1969a), Nilson (1969b) and S.B. Barnes and Associates (1959). The results for these tests strength and stiffness have been compiled into Table 2-1. These test results were compared in the white paper (Luttrell, 2005) with the new calculation method and seem to have a good correlation for both the strength and stiffness, as reflected by the mean and standard deviation shown in Table 2-1.

Table 2-1: Cellular Diaphragm Test Data

Test Number	Test S_u (k/ft)	Theoretical S_u (k/ft)	Test G` (k/in)	Theoretical G` (k/in)	Strength (Test/Calc)	Stiffness (Test/Calc)
1	2.03	2.02	83	82	1.005	1.012
2	1.46	2.02	84	82	0.723	1.024
3	3.23	3.08	230	248	1.049	0.927
4	3.22	3.08	322	248	1.045	1.298
5	2.91	2.66	189	232	1.094	0.815
6	2.67	2.47	276	220	1.081	1.255
7	2.57	2.47	247	220	1.040	1.123
8	3.19	2.88	150	241	1.108	0.622
9	2.29	2.47	205	220	0.927	0.932
10	2.13	2.47	191	219	0.862	0.872
11	2.73	2.47	218	219	1.105	0.995
12	2.08	2.44	176	220	0.852	0.800
13	2.38	2.11	167	204	1.128	0.819
14	2.03	2.02	83	82	1.005	1.012
15	2.15	2.02	118	82	1.064	1.439
16	1.77	2.02	109	82	0.876	1.329
17	1.46	2.02	84	82	0.723	1.024
18	0.97	1.07	35	39	0.907	0.897
19	1.48	1.69	64	69	0.876	0.928
20	1.23	1.42	49	58	0.866	0.845
21	0.90	1.04	25	42	0.865	0.595
22	3.42	3.73	178	214	0.917	0.832
23	3.55	3.73	163	212	0.952	0.769
24	2.30	1.95	177	127	1.179	1.394
25	2.00	2.27	160	145	0.881	1.103
26	0.71	0.70	21	22	1.016	0.955
27	7.75	7.43	430	490	1.043	0.878
28	12.95	15.96	720	600	0.811	1.200
29	2.30	2.20	187	217	1.045	0.862
				Mean	0.967	0.985
				σ	0.120	0.213

CHAPTER 3 – EXPERIMENTAL TESTING

3.1 Overview

A series of twenty cantilever diaphragm tests were conducted at the Virginia Tech Structures and Material Science Laboratory in Blacksburg, Virginia. These tests were performed to determine the validity of diaphragm strength and stiffness equations prepared by Luttrell (2005). The equations are for use with the current Steel Deck Institute (SDI) diaphragm design manual (Luttrell 2004) and were developed to enable the design of deep deck and cellular deck diaphragms. These tests were conducted in accordance with the International Code Council, ICC, Evaluation Criteria for Steel Deck Roof and Floor Systems. (ICC)

Nine of the diaphragms used screws for the structural connection, eight of the diaphragms used Hilti X-ENP-19 L15 powder actuated fasteners for the structural connection, and three of the diaphragms used ¾ in. visible diameter puddle welds for the structural connection. One of the goals during these tests was to evaluate measurements of both the corner and the diagonal displacements to show a comparison of the two displacements. These displacements are very important in the process of evaluating the stiffness of the diaphragm system. These two procedures will be explained later in the report.

Each test setup consisted of panels, varying in widths depending on the manufacturer, from 12 in. to 24 in. spanning 24 ft and making a total test width of 24 ft. Once the diaphragm was placed on the test frame each panel was connected to the adjacent panel at the side-lap and at the end to the frame. Then the frame was loaded by a hydraulic ram placed at the free end of the cantilever test frame. Displacement transducers were placed at all of the corners to monitor the x and y displacements. Also, displacement transducers were placed at the corners to monitor the diagonal displacements of the frame. Figure 3.1 shows a typical test setup.

Figure 3-1: Typical Test Setup

3.2 Test Details

3.2.1 Test Designation

Each test was given a designation to identify the unique aspects of each test. Each term in the designation represents a different aspect of the test. An example of one of the test designations is: WH-4.5-N-20-S-S. The first term of the designation is the manufacturer of the deck. The second term represents the depth in inches of the deck. The third term is the type of deck which can either be cellular, N-Deck, or 2xN. The fourth term is the gage of the deck for that particular test. This can either be a single number as shown or can be two numbers separated by a backslash. The number before the slash represents the hat gage and the number after the slash represents the flat sheet gage. The fifth term of the designation represents the structural fastener used. This can be a screw, powder actuated fastener or weld. The sixth term of the designation represents the side-lap, also referred to as stitch, fastener used for the test. Table 3.1 shows the full test break down with the designations for each test and the fastener configuration used.

Table 3-1: Test Configurations

Test No.	Test Designation	Structural Fastener Configuration	Stitch Fastener	Cover Width (in)
1	WH-4.5-N-20-S-S	1 screw/rib at ends, 1 screw/ft at sides	#12, 36 in. o/c	24
2	USD-4.5-C-20/20-S-S	1 screw/rib at ends, 1 screw/ft at sides	#12, 36 in. o/c	24
3	CSI-7.5-N-18-S-S	1 screw/rib at ends, 1 screw/ft at sides	#12, 36 in. o/c	12
4	USD-4.5-C-18/18-S-S	1 screw/rib at ends, 1 screw/ft at sides	#12, 36 in. o/c	24
5	USD-7.5-C-18/20-S-S	1 screw/rib at ends, 1 screw/ft at sides	#12, 36 in. o/c	24
6	CSI-7.5-N-16-S-S	1 screw/rib at ends, 1 screw/ft at sides	#12, 36 in. o/c	12
7	WH-4.5-N-20-P-S	1 pin/rib at ends, 1 pin/ft at sides	#12, 36 in. o/c	24
8	WH-4.5-N-16-P-S	1 pin/rib at ends, 1 pin/ft at sides	#12, 36 in. o/c	24
9	CSI-7.5-N-18-P-S	1 pin/rib at ends, 1 pin/ft at sides	#12, 36 in. o/c	12
10	USD-7.5-C-18/20-P-S	1 pin/rib at ends, 1 pin/ft at sides	#12, 36 in. o/c	24
11	USD-7.5-C-16/18-P-S	1 pin/rib at ends, 1 pin/ft at sides	#12, 36 in. o/c	24
12	WH-4.5-N-18-W-S	1 weld/rib at ends, 1 weld/ft at sides	#12, 12 in. o/c	24
13	USD-4.5-C-20/20-W-S	1 weld/rib at ends, 1 weld/ft at sides	#12, 12 in. o/c	24
14	WH-3-M-20/20-W-S	1 weld/rib at ends, 1 weld/ft at sides	#12, 12 in. o/c	24
15	VC-3-C-16/16-P-BP	1 pin/rib at ends, 1 pin/ft at sides	BP, 12 in. o/c	24
16	VC-3-C-20/20-P-BP	1 pin/rib at ends, 1 pin/ft at sides	BP, 12 in. o/c	24
17	WH-3-M-16/16-P-S	1 pin/rib at ends, 1 pin/ft at sides	#12, 12 in. o/c	24
18	VC-3-C-18/18-S-S	1 screw/rib at ends, 1 screw/ft at sides	#10, 12 in. o/c	24
19	VC-3-C-20/20-S-S	1 screw/rib at ends, 1 screw/ft at sides	#10, 12 in. o/c	24
20	WH-3-M-20/20-S-S	1 screw/rib at ends, 1 screw/ft at sides	#10, 12 in. o/c	24

S - Screw	WH - Wheeling	C - Cellular
P - Pin	CSI - Consolidated Systems Inc.	N - N Deck
W - Weld	VC - Vulcraft	M – 2xN Deck
BP - Button Punch	USD - United Steel Deck	

3.2.2 Test Frame Configuration

The cantilever diaphragm test frame, as illustrated in Figure 3-2 was constructed with four W12x87 perimeter beams. The perimeter beams were spaced, from center-to-center, at 24 ft by 24 ft from the opposing webs centerline of the members as shown in Figure 3-2. On top of each beam a system of channels and angles were attached to the top flange, as illustrated in Figure 3-3.

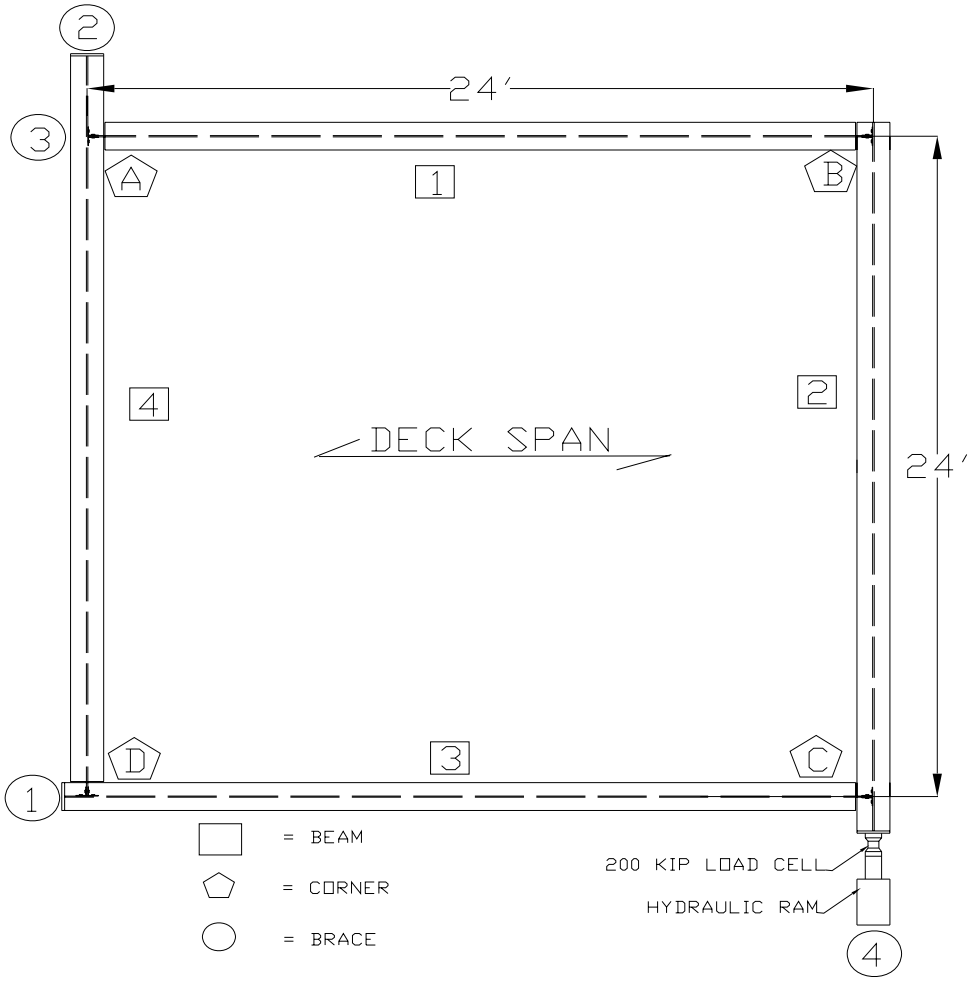

Figure 3-2: 24 ft Span Test Setup

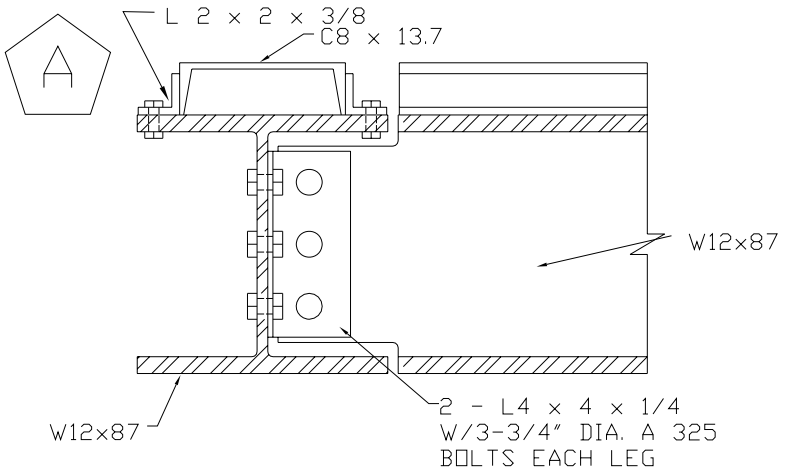

Figure 3-3: Beam-to-Beam Connection

These channels and angles were used to help maintain the structural integrity of the test frame. The channels and angles are meant to be changed once a sufficient amount of damage has occurred to the web of the channel making it difficult to attach any further diaphragm specimens.

The perimeter members were connected with double angle connections at corners A through D as can be seen in Figure 3-3. Beam 2 in the frame was set on roller supports at each end to allow the frame to move freely on a level plane as shown in Figure 3-4. Also a roller system was used along Beam 2 to resist any uplift of the system during the loading process, as illustrated in Figure 3-4.

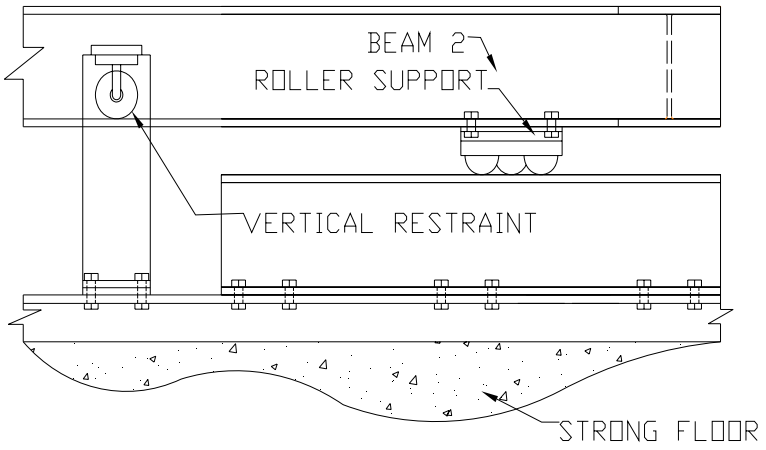

Figure 3-4: Restraint and Roller System

Each brace of the cantilever diaphragm system was different and had to account for the reaction forces from the applied load. As can be seen in Figure 3-5 the Corner 1 bracing was used to account for the tension force caused by the couple on the system. The main concern was keeping the flanges of the upright W-section from deforming, so several intermediate stiffeners were welded in place to eliminate the flange deformation. The system for brace 2 and brace 3, Figures 3-6 and 3-7 respectively, were very similar because these were designed to account for compressive force from the applied force and the compression portion of the couple on the system respectively. Brace 4, Figure 3-6,

was designed as the point where the hydraulic ram would apply the load onto the system. A support angle was welded onto the face of the frame to rest the compression load cell on until the loading cycle was started. Between the load cell and the frame a swivel head was placed to keep the applied load perpendicular to the load frame.

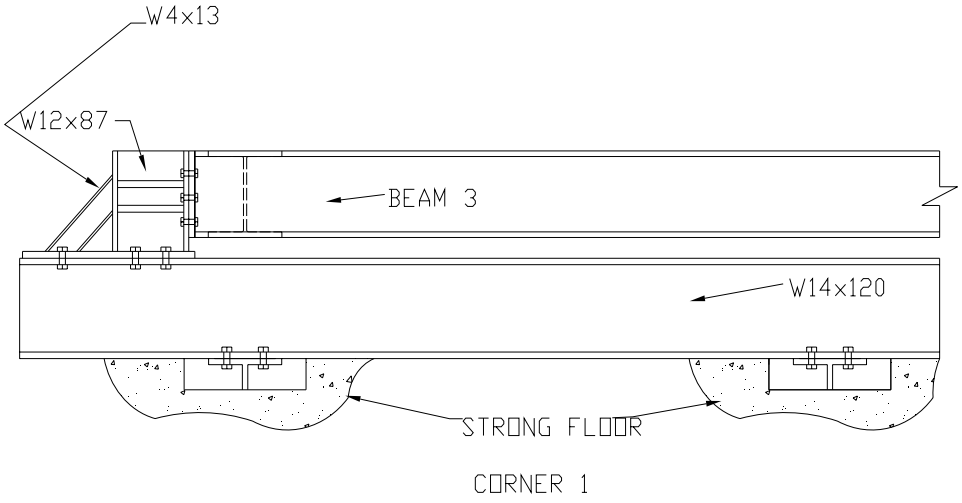

Figure 3-5: Corner 1 Brace

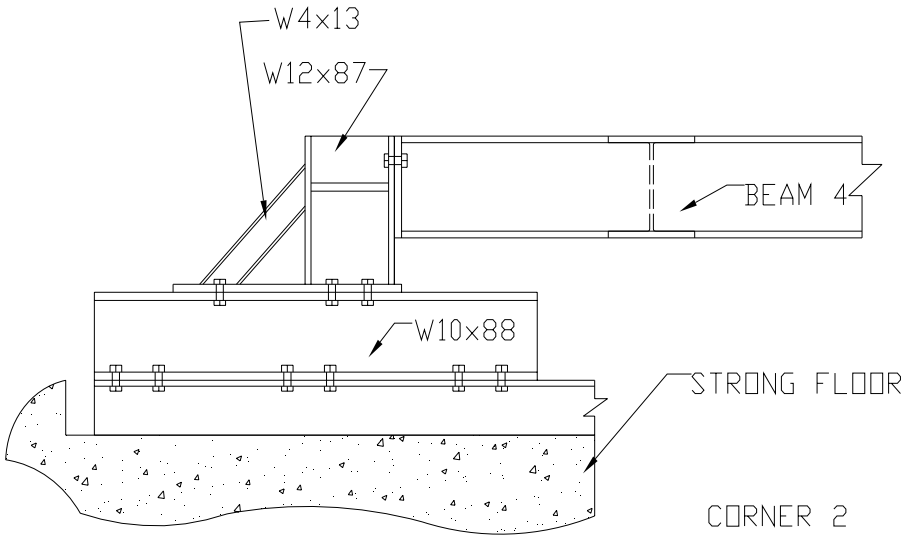

Figure 3-6: Corner 2 Brace

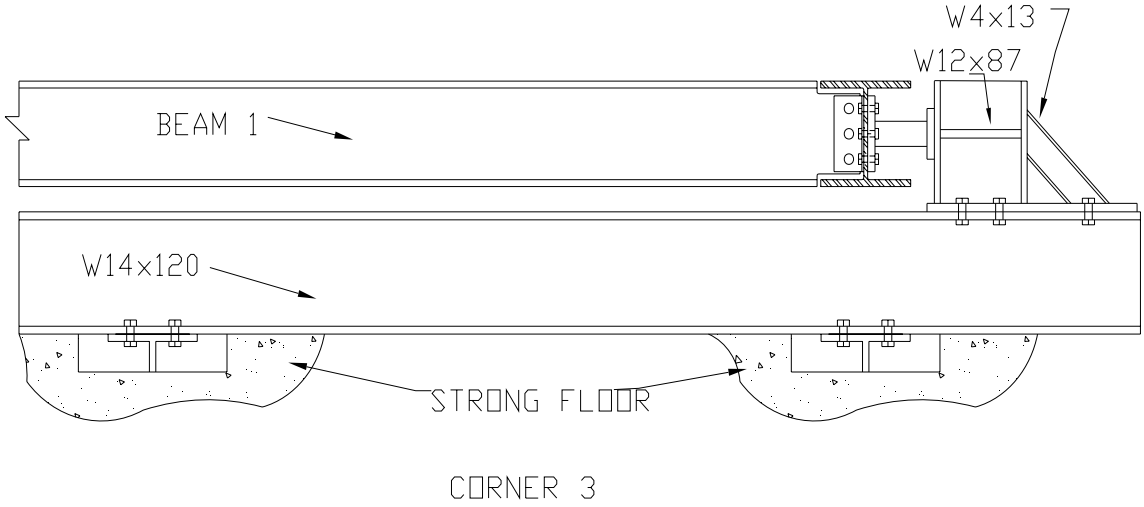

Figure 3-7: Corner 3 Brace

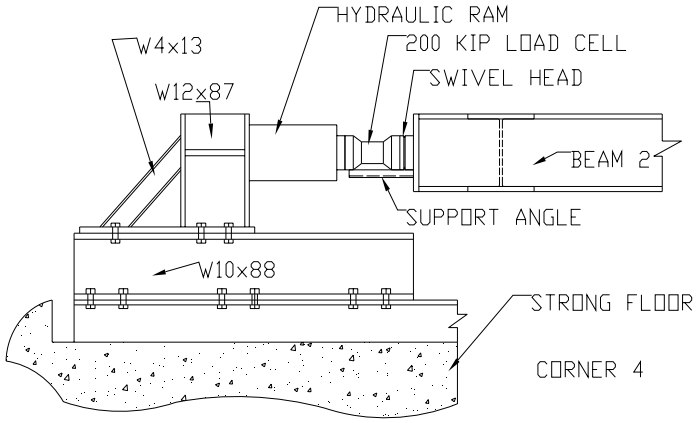

Figure 3-8: Corner 4 Brace

3.2.3 Test Specimen Configuration

The framing configuration for the diaphragm systems was the test setup shown in Figure 3-2. All of the diaphragm specimens spanned the full 24 ft and were composed of the appropriate number of panels to make a 24 ft wide specimen as illustrated in Figure

3-9. Some of the specimens had a 12 in. cover width while the majority had a 24 in. cover width. The specimens that were used ranged in thickness from 0.0359in (20 ga.) to 0.0598in. (16 ga.).

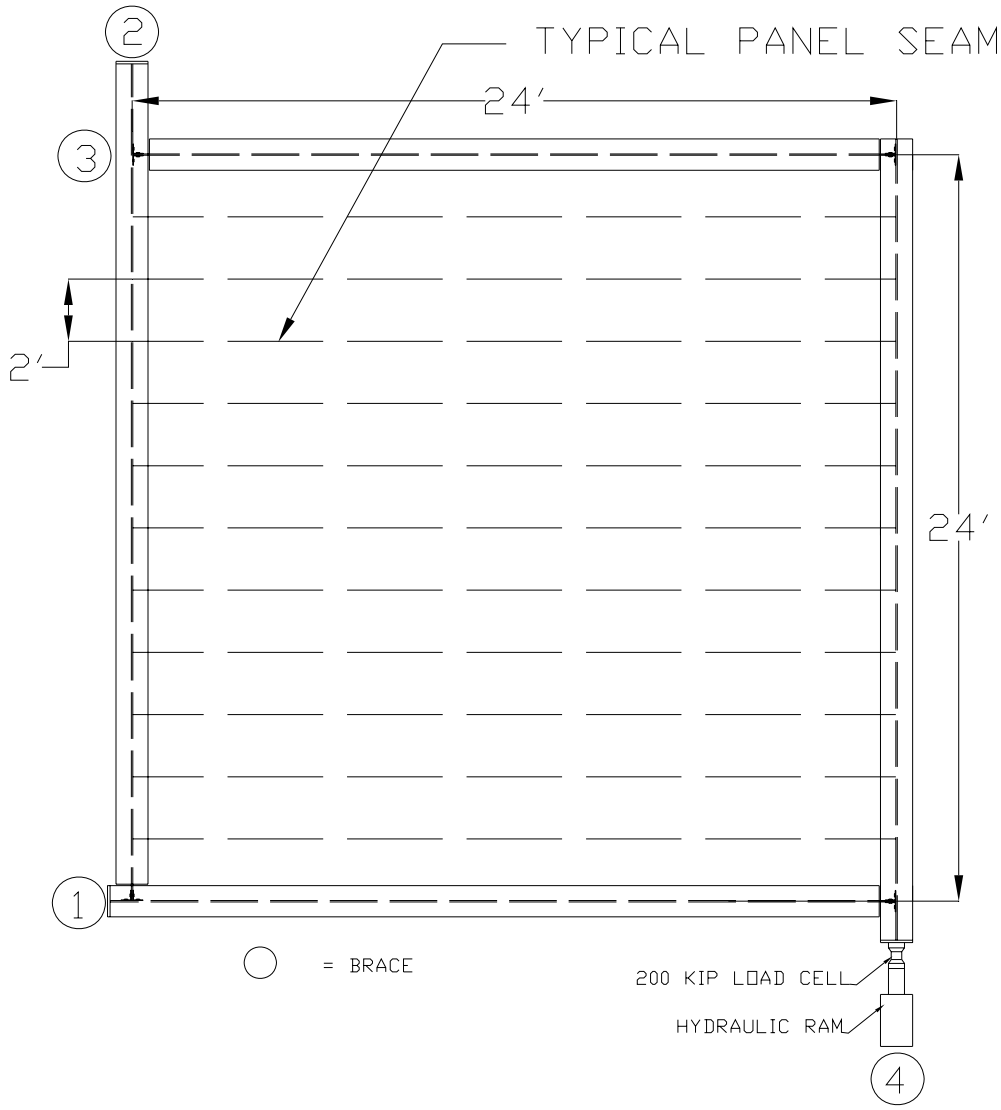

Figure 3-9: Typical Panel Layout

In this test program there were six different profiles that were produced by the four manufacturers that provided the test materials. The different profiles that were used in this test program are illustrated in Figure 3-10. Each specimen was connected with structural fasteners on each end in every valley. This resulted in either a 24/3 or 24/4 structural connection pattern depending on the pitch of the profile. Also along the outer

sides of the specimen a structural connection was made at 1 ft centers.

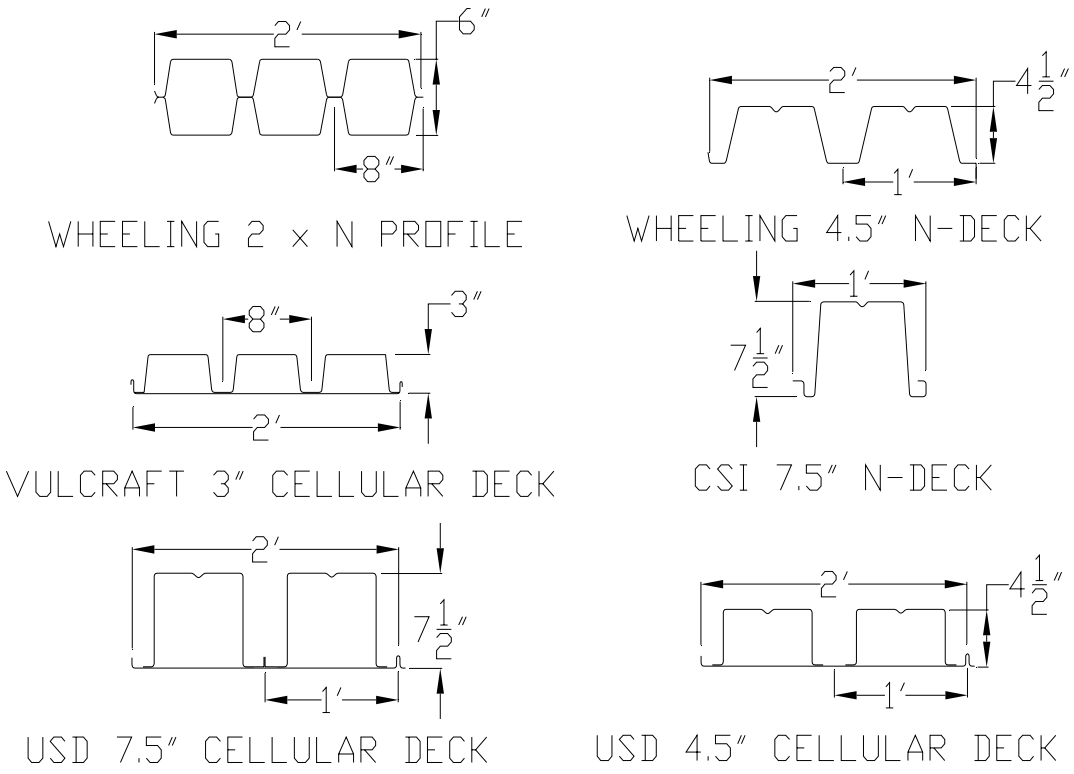

Figure 3-10: Test Program Deck Profiles

3.2.4 Test Loading and Measurements

As illustrated in Figure 3-1, load was applied to the test setup at Corner C. The load was applied with a 150 kip hydraulic ram that was attached to brace 4 and to the reaction floor as shown in Figure 3-8. The load was measured with a 200 kip load cell. The load cell was supported by an angle that was welded to the test frame until load was applied. The support angle was cut shorter than the total length of the load cell and the swivel head combined to avoid any load being transferred into the support angle.

The frame displacements were measured during each test by a minimum of nine displacement transducers. The transducer locations are shown in Figure 3-11, which are meant to match the designations used in the ICCES (2006) evaluation procedure. All of the load and displacement information was recorded for each test using a Vishay System

5000 Data Acquisition System. For the first thirteen diaphragms that were tested the System 5000 was set to record data points every three seconds. This was done to insure that no essential points of data were missed. It was found that this produced a very large amount of data and a decision was made to go to manual recordings after each small load increment. Therefore, for the remainder of tests a smaller amount of data was taken, which still exceeded the minimum amount of data required by the ICCES (2006) evaluation procedure.

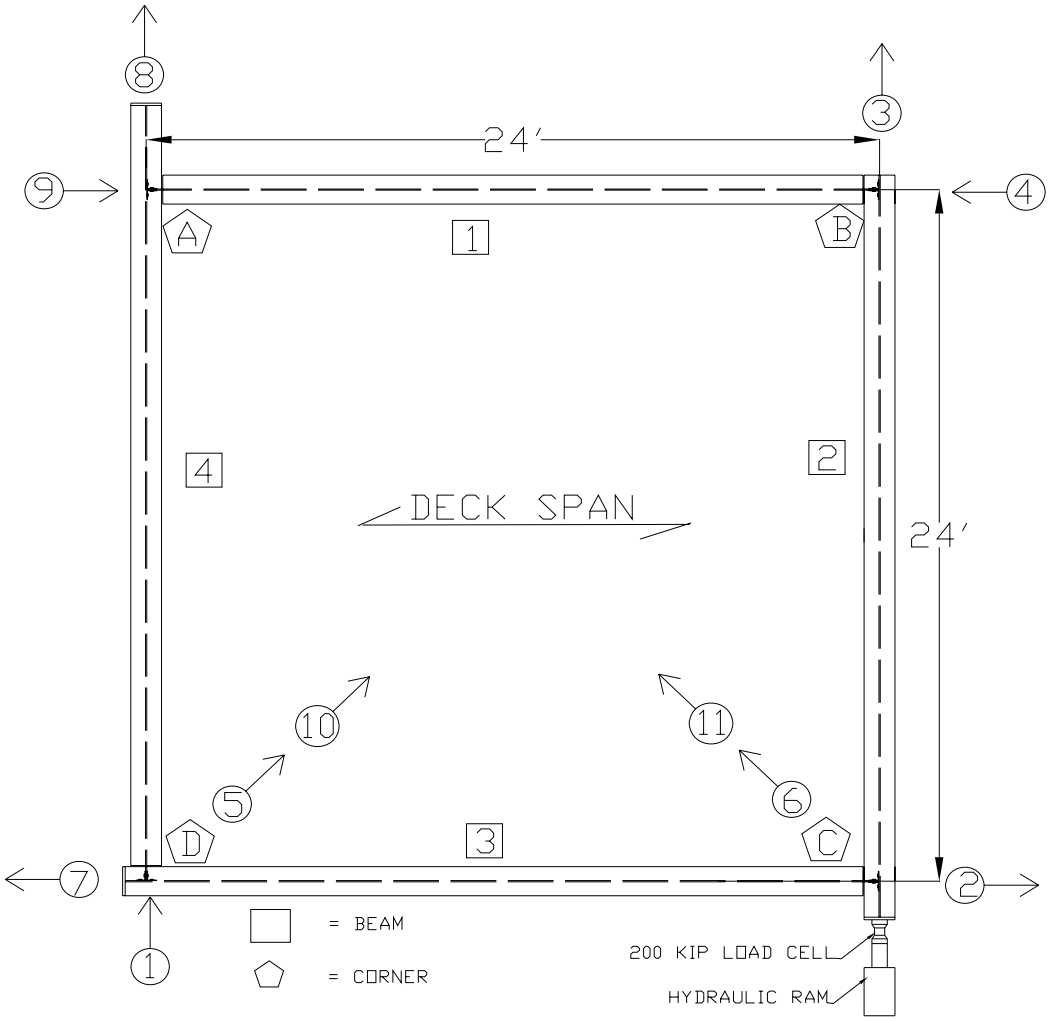

Figure 3-11: Displacement Transducer Configuration

In the ICCES evaluation procedure the transverse and parallel deflections of

displacement transducers 1 through 4 were combined to arrive at a net shear and corrected deflection. This combination is used to account for any rigid body motion in the frame assembly. In Figure 3-11 the direction of the arrows represents the positive direction of the deflections measured. These directions were chosen to correspond with the ICCES evaluation procedure. The corrected deflection, Δ_n, was computed by:

$$\Delta_n = \Delta_3 - \left[\Delta_1 + \frac{a}{b}\left(\Delta_2 + \Delta_4\right) \right] \tag{3.1}$$

Where, a and b are the dimensions of the diaphragm (24 ft and 24 ft respectively) given in Figure 3-11. In the ICCES evaluation procedure, the diagonal deflections of displacement transducers 5 and 6, as a pair, as well as 10 and 11 being a separate pair, were combined to arrive at a net shear and corrected deflection. Displacement transducers 5 and 6 were used for the first part of the experimental testing where their location was fixed no matter what depth of deck was being tested. Displacement transducers 10 and 11 were added for a few tests to check the flexibility of the supports on which the displacement transducers were mounted. Displacement transducers 10 and 11 were mounted such that the wire ran just barely above the top of the deck being tested. The corrected deflection, Δ_n, for the diagonals was computed by:

$$\Delta_n = \left(\left|\Delta_1\right| + \left|\Delta_2\right| \right) \cdot \frac{\sqrt{a^2 + b^2}}{2b} \tag{3.2}$$

According to the ICCES evaluation procedure the full frame test assembly is to be loaded to approximately one quarter and one half of the estimated maximum load. Once each one of these points is reached the load is to be removed and the recovery of the diaphragm recorded after five minutes. After these initial two loadings the full frame test assembly is loaded to failure making sure to record a minimum of 10 evenly spaced data points.

3.3 Coupon Tests

Tensile coupon tests were conducted on each of the diaphragm specimens tested. Two coupon tests were made from each different profile and thickness tested. This means that with a cellular profile four coupon tests were performed where two came from the flute and two came from the flat sheet. The tensile coupon tests were performed according to ASTM E8 specifications (ASTM 2004). A sample of the test setup is shown in Figure 3-12. The specimens were machined to the following nominal dimensions:

Length = 10 in. Width (C) = ¾ in. Milled Width (w) = ½ in.

Each specimen's dimensions as well as yield and ultimate strength are reported in Table 3-2. To properly measure the thickness of each sheet the protective coating, of either paint or galvanizing, had to be removed. To remove the coatings a solution of ten percent hydrochloric acid was used on a sample specimen. Once the oxidation in the solution was finished the thickness of the specimen was measured. The tension tests were conducted using a 10 kip load cell in an INSTRON Model 4468 screw operated testing machine. Tests were performed at a speed of 0.5 in./min until failure occurred.

Each coupon was instrumented with an MTS Model 632.25F-20 extensometer. This is a 50 percent extensometer that was left on each of the specimens until failure. Because the extensometer was left on the specimen until failure it was possible to develop a full stress strain curve for each coupon. Along with the extensometer changes, in percent, being monitored during each test, the cross-head displacements, in inches, were also measured.

Figure 3-12: Tensile Coupon Test Setup

Data was collected for each specimen at a rate of every 1.2 seconds during the linear portion of the test. This was done to attempt to get a clearer picture of the modulus of elasticity of the specimens. After the linear region of the response, the data acquisition was slowed down to once every 5 seconds to reduce the amount of data collected. Once the specimens failed, the two halves were pressed back together and the gage was measured. This was done to find the elongation of the specimen. This elongation measurement was then compared to the elongation reported by the extensometer. A summary of the tensile coupon test results is given in Table 3-2.

Table 3-2: Coupon Test Results

Test #	Test Designation	Coupon #	Average Yield Stress (ksi)	Average Ult. Stress (ksi)	Average % Elongation
1	WH-4.5-N-20-S-S	1,2	107	109	6
2	USD-4.5-C-20/20-S-S	3,4,5,6	48	58	40
3	CSI-7.5-N-18-S-S	7,8	50	61	39
4	USD-4.5-C-18/18-S-S	9,10,11,12	48	60	40
5	USD-7.5-C-18/20-S-S	13,14,15,16	48	59	39
6	CSI-7.5-N-16-S-S	17,18,19,20	44	60	40
7	WH-4.5-N-20-P-S	21,22	108	110	6
8	WH-4.5-N-16-P-S	23,24	91	92	8
9	CSI-7.5-N-18-P-S	25,26	50	61	38
10	USD-7.5-C-18/20-P-S	27,28,29,30	48	59	40
11	USD-7.5-C-16/18-P-S	31,32,33,34	48	59	41
12	WH-4.5-N-18-W-S	35,36	95	98	1
13	USD-4.5-C-20/20-W-S	37,38,39,40	48	58	40
14	WH-3-M-20/20-W-S	41,42,43,44	92	94	4
15	VC-3-C-16/16-P-BP	45,46	43	56	32
16	VC-3-C-20/20-P-BP	47,48	41	57	31
17	WH-3-M-16/16-P-S	49,50,51,52	86	89	7
18	VC-3-C-18/18-S-S	53,54	41	56	31
19	VC-3-C-20/20-S-S	55,56	41	56	31
20	WH-3-M-20/20-S-S	57,58,59,60	92	94	4

CHAPTER 4 – DIAPHRAGM STRENGTH AND STIFFNESS EVALUATION

4.1 Overview

This chapter shows the calculations involved for the shear strength and stiffness evaluation of the steel deck diaphragms in this project. The third edition of the Steel Deck Institute Diaphragm Design Manual was used to calculate the predicted strength and stiffness of each diaphragm. This method was used because of its simplicity which makes it much better for hand calculations without the use of any computer analysis. However, this manual is limited to thicknesses ranging from 0.014 in. to 0.064 in. and depths ranging from 9/16 in. to 3 in. because of the study parameters used to establish the manual (Luttrell, 2004). Luttrell (2005) proposed changes to the equations used in the SDIDDM03 to account for deep decks and cellular decks.

4.2 Diaphragm Shear Strength Calculations

The shear strength of a diaphragm, as opposed to the stiffness, is often the main focus in design. The diaphragm shear strength is mainly governed by the connection configuration that is used. The deck profile can also have a significant impact on the overall strength if buckling is the limiting factor; however, this case is more infrequent. Because the typical diaphragm has few connections at a large spacing the connection strength tends to govern.

4.2.1 SDIDDM03 Procedure

As shown previously in Chapter 2, the diaphragm shear strength is generally broken down to three limiting conditions: edge fasteners, interior panel fasteners, and corner fasteners. The edge fasteners are limited by the strength of the structural frame fastener as it relates to the end distribution factor as shown in Eq 2.1. The interior panel fasteners are limited by the strength of both the structural and side-lap connectors. The

interior panel fasteners limitation also is correlated to the edge flute's distortional tendency. The corner fasteners limitations are based on connector strength and distortion also but their forces are magnified because of their location as can be seen in Figure 4-2. If the example of an element that is put under a shear load, as in Figure 4-1, it can be see nhow there would be larger forces at the corner locations.

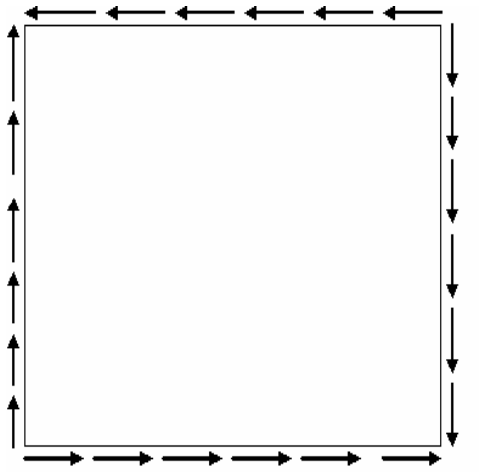

Figure 4-1: Element Shear Load

The force distribution assumes that there are both vertical and horizontal forces acting on the connector as in Figure 4-2. To get the actual force in the connector the resultant of these forces is taken, which is the reason for the square root term in the corner fastener limitation Eqn. 2.3.

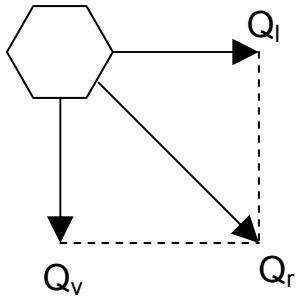

Figure 4-2: Corner Force Distribution

4.2.2 Connection Strength

The strength of fasteners are essential to diaphragm strength and stiffness. For structural connections, the main choices are self-drilling screws, powder actuated

fasteners and puddle welds. The side-lap connections typically used are self-drilling screws, button punch (crimps) and seam welds. Each connection has its own set of advantages and disadvantages which will be discussed in the upcoming sections. The connections that will be discussed in detail are the connections that pertain to this test program.

4.2.2.1 Screws

When it comes to construction practice the most user friendly connection is a screw connection. Some of the advantages to using screws are: consistent strength, no specialized equipment required and readily available. Because the screws are made using a strict manufacturing process their strengths are reliable. However, screws also have disadvantages as well which include: potential over tightening and labor intensity. The screws and equipment used in this study are shown in Fig. 4-3. The screws are classified as self drilling because of the drill bit located on the tip. The screws were installed with a Hilti TKT 1300 power clutch driven screw driver. Because the structural screws are driven through the deck and through a much thicker structural member it can be a labor intensive process with each structural screw taking approximately ten seconds to drive. With screws there is the risk of over tightening, which can cause a loss of strength in the fastener. If the screw is over tightened damage to the screw head can occur which can lead to premature screw failure. (Luttrell, 1981)

Figure 4-3: Screw Gun and Self-Drilling Screws

In diaphragm construction, screws can be used as both structural frame fasteners and side-lap fasteners. Because these two locations have different characteristics for the screw behavior, separate equations were developed for each case. With diaphragm connections strength and stiffness are major considerations therefore each topic has its own set of equations.

The most typical sizes of structural screws used in construction are No. 12 and No. 14. Because these are the most common sizes, the structural strength equation used in the SDIDDM03 is limited to those screw diameters. The strength equation for structural screws is:

$$Q_f = 1.25 \cdot F_y \cdot t\left(1 - 0.005 \cdot F_y\right), \text{kips} \tag{4.1}$$

Where:

F_y = yield stress of sheet steel, ksi

t = base sheet metal thickness, in

The flexibility equation is also limited to No. 12 and No. 14 screws. The flexibility equation is used to determine the stiffness of the diaphragm system. The flexibility equation for structural screws is:

$$S_f = \frac{1.30}{1000 \cdot \sqrt{t}}, \frac{\text{in}}{\text{kip}} \tag{4.2}$$

Where:

t = base sheet metal thickness, in.

For side-lap connections a different strength equation is used. Because side-lap screws tend to vary in size more than structural screws, the screw diameter is used in the equation. This makes the equation more of a universal fit to any configuration. The strength equation for side-lap screws is:

$$Q_s = 115 d \cdot t, \text{kips} \tag{4.3}$$

Where:

d = major diameter of the screw, in.

t = base sheet metal thickness, in.

The flexibility of a side-lap screw is considerably greater than a structural screw, as can be seen in the following equation.

$$S_s = \frac{3.0}{1000\sqrt{t}}, \frac{in}{kip} \quad (4.4)$$

4.2.2.2 Power Driven Pins

The power driven pins that were used for this test program were Hilti X-ENP-19 L15. These pins can be seen in Figure 4-4. These pins were designed to be used with support steel of ¼ in. and thicker. The use of power driven pins has many advantages for both construction and engineering. The advantages of power driven pins are consistent strength provided and easy installation.

Figure 4-4: Hilti X-ENP-19 L15 Powder Actuated Fastener

The most important advantage of power driven pins is their ease of installation. The pins and cartridges are loaded into the installation tool, which can be seen in Fig. 4-5, and the tool is operated like a gun. This installation tool had a specialized barrel that was used because of the narrow deep ribs present in the deep deck and cellular deck profiles. The time it takes for the installation of each pin can be around 2 seconds. Some

of the disadvantages of the power driven pin system are the specialized equipment required and the sensitivity of the pins to the base steel being used.

Figure 4-5: Hilti DX 76 Pin Installation Tool

The specialized equipment has to be either rented or purchased. Proper cleaning and maintenance is required. One of the other issues is the training and understanding of how the equipment works. The pins have a desired range of penetration that is required to obtain the maximum resistance. This means that the equipment has to be adjusted according to each different thickness of material the pins are being driven into. However, once the adjustment is complete for the base material the operation is just simply load the pin and fire into place.

Powder actuated fasteners can only be used as structural fasteners so they have to used in conjunction with other side-lap fastener types to complete the diaphragm system. As with all connections there are both strength and flexibility equations that have been developed for the Hilti X-ENP-19 L15 fasteners. These equations are different depending on the thickness of the base sheet metal being used for the connection. For thinner sheet metal the strength and flexibility equations are:

$$Q_f = 61.1 \cdot t \cdot (1 - 4 \cdot t), \text{kips} \tag{4.5}$$

$$S_f = \frac{1.25}{1000\sqrt{t}}, \frac{\text{in}}{\text{kip}} \tag{4.6}$$

Where:

t = base sheet metal thickness < 0.0280 in.

When the base sheet metal thickness is equal or higher than the above limit the equations change to:

$$Q_f = 56 \cdot t \cdot (1 - t), \text{kips} \tag{4.7}$$

$$S_f = \frac{0.75}{1000\sqrt{t}}, \frac{\text{in}}{\text{kip}} \tag{4.8}$$

Where:

0.028 in. ≤ t ≤ 0.060 in.

4.2.2.3 Puddle Welds

For construction purposes, welding the diaphragms to the structure has advantages and disadvantages. The biggest advantage of welding the diaphragms to the structure is that the strengths are typically higher than other connection methods. The disadvantages are the required specialized equipment, training and labor required. To properly weld light gage material a great deal of knowledge and experience is required. It is very common in the welding process to actually burn out the edges around the weld which means the steel sheet is not in contact with the weld and therefore not transferring the load properly. Another important factor in the welding is the penetration into the steel. If a weld goes through multiple layers of steel, the visible diameter to actual penetration diameter ratio of the weld greatly decrease and therefore decrease the capacity of the weld. Fig. 4-6 represents a typical puddle weld that was used in this test program.

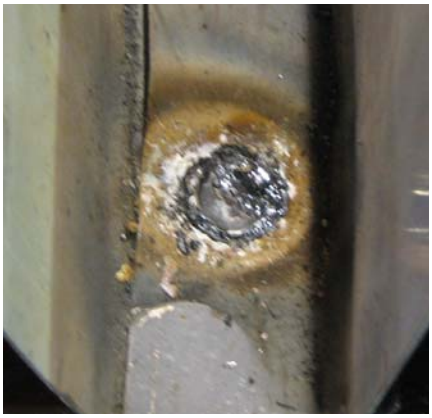

Figure 4-6: Puddle Weld

The welds that were used for this test program were ¾ in. visible diameter puddle welds. These welds were created by a Miller Dialarc 250 AC/DC constant current arc welder. The current that was used for the welds in this test program was 120 amps. The welding rods that were used were an E6010 material that has a 1/8 in. diameter. For both single thickness and double thickness welds several burn-off rate tests were performed. These tests were done to determine the amount of time it took to make a proper weld for each scenario. The SDIDDM03 arc-spot weld quality control requires that the burn-off rate for a 5/32 in. rod of either E60XX or E70XX be between 0.15in./sec and 0.25in./sec. As can be seen in Table 4-1 the burn-off rate for this test program was within this range. The arc spot welds were done by one of the lab technicians, Dennis Huffman, at the Structures and Materials Laboratory at Virginia Tech.

Table 4-1: Weld Burn-off Rate Data

Single Thickness (16 gage)				
Welding Rod (1/8 in. Diameter)				
Initial Length (in.)	Final Length (in.)	Burn-Off (in.)	Time (sec)	Burn-Off Rate (in./sec)
14	11.75	2.25	11.65	0.193
11.75	9	2.75	12.09	0.227
14	11.75	2.25	11.24	0.200
14	12	2	8.94	0.224
14	11.5	2.5	11.97	0.209
Double Thickness (16 gage)				
Welding Rod (1/8" Diameter)				
Initial Length (in.)	Final Length (in.)	Burn-Off (in.)	Time (sec)	Burn-Off Rate (in./sec)
14	11	3	14.97	0.200
14	10.25	3.75	17.23	0.218
14	11.125	2.875	14.41	0.200
14	10	4	18.4	0.217
14	11.375	2.625	13.2	0.199

Welding can be used for both structural fasteners and side-lap fasteners. In this program, puddle welds were only used to connect the diaphragm to the frame. As with other connections both strength and flexibility equations are available. The equations for strength and flexibility are:

$$Q_f = 2.2t \cdot F_u \cdot (d - t), \text{kips} \tag{4.9}$$

$$S_f = \frac{1.15}{1000\sqrt{t}}, \frac{\text{in}}{\text{kip}} \tag{4.10}$$

Where:

d = average visible diameter (limited to a minimum of ½ in.), in.

F_u = specified minimum steel strength, ksi

t = base sheet metal thickness, in.

4.2.2.4 Example Calculation

As can be seen from the previous sections the calculations required to determine the strength and stiffness of a diaphragm are not complicated. They do however need to take into account certain nuances that are present in each particular profile that can be used. In this section the calculation procedure for a cellular system will be shown.

The diaphragm calculations shown are for test 2, USD-4.5-C-20/20-S-S. This deck for this test is from USD and is 4.5 in. deep with a hat size of 20 ga and a bottom plate size of 20 ga. The connection configuration is a No. 12 Screw at 12 in. on center (one screw in every rib), and structural side screws also at 12 in. on center. The No. 12 side-lap screws are in a 36 in. on center pattern.

First an initial list of parameters for the problem must be established. These constants are:

$n = 1$	number of interior spans
$F_y = 48$ ksi	yield stress of sheet material
$F_u = 58$ ksi	ultimate stress of sheet material
$L = 24$ ft	total span of diaphragm
$w = 24$ in.	width of deck sheet
$h = 4.5$ in.	depth of deck profile
$t_{hat} = 0.0359$ in.	thickness of top hat
$t_{plate} = 0.0359$ in.	thickness of bottom plate
$w_{rib} = 12$ in.	width of a single rib (center to center)
$d = 0.2111$in.	major diameter of screw (in this case #12)
$n_s = 7$	number of intermediate side-lap in length per panel side-lap
$n_e = 23$	number of intermediate sheet-to-sheet connections per panel length and between purlin at edge
$n_p = 0$	number of purlins in length excluding ends

Once the initial parameters are defined the structural fasteners strength must be determined. In this case the No. 12 screws strength must be determined. As was shown before, Eq 4.1 is used for determining structural screw strength.

$$Q_f = 1.25(48\text{ksi})(0.0359\text{in})[1-0.005(48\text{ksi})](1000\text{ lb/kip})$$

$$Q_f = 1637\text{ lb}$$

Then the strength of the No. 12 side-lap screws must be determined. As was shown before, Eq 4.3 is used to determine the side-lap screw strength.

$$Q_s = 115(0.2111\text{in})(0.0359\text{in})(1000\text{ lb/kip})$$

$$Q_s = 872\text{ lb}$$

With a cellular profile there is a possibility that the profile will have two thicknesses at all of the structural connection locations. This means that the top hat and bottom plate thicknesses should be added together and used in the strength and stiffness equations. This example has a single thickness at connection locations as shown in Figure 3-10.

Once the connection strengths are determined the three diaphragm strength limitations are applied. There are a few constants to be determined that are used in the diaphragm strength calculations. These constants include the ratio of side-lap to structural fasteners, α_s, along with the edge flutes' flexibility, λ, and the fastener weighting factors, α_1 and α_2. The fastener weighting factors are based on the distance from the centerline of the deck to each connection.

$$\alpha_s = \frac{Q_s}{Q_f} = 872\text{lb}/1637\text{lb} = 0.521$$

$$\lambda = \max\left[1 - \frac{4.5\cdot\text{in}\cdot(24\cdot\text{ft})}{240\cdot\sqrt{0.0359\cdot\text{in}}}, 0.7\right] = 0.7$$

$x_1 = 12\text{in.}$ $x_2 = 12\text{in.}$

$$\alpha_1 = \frac{1}{w}\cdot\sum_{e=1}^{n} x_e$$

$\alpha_1 = 1$

$\alpha_2 = 1$ Equal because connection configuration is the same on the ends and purlins

Once these values are obtained the first strength limitation can be applied. The edge fastener limitation from Eq 2.1 is:

$$S_{ne} = (2\cdot 1 + 0\cdot 1 + 23)\cdot\frac{1637\text{lb}}{24\text{ft}}$$

$S_{ne} = 1705$ lb/ft

The next limitation is the strength of the interior fastener. This limitation is broken down

into two parts for simplicity. The limitation comes from Eq 2.2 which is:

$$B = 7\cdot(0.521) + \frac{1}{(24\text{in})^2}\cdot\left[(2)\cdot 0\cdot\sum_{p=1}^{4}\left(x_p\right)^2 + 4\cdot\sum_{e=1}^{4}\left(x_e\right)^2\right]$$

$$B = 5.727$$

$$S_{ni} = [\,2\cdot 1\cdot(0.7 - 1) + 5.727\,]\cdot\frac{1636\ \text{lb}}{24\ \text{ft}}$$

$$S_{ni} = 350\ \text{lb/ft}$$

The corner fastener strength is the final strength limitation. This limitation comes from Eq 2.3. The first portion of the corner fastener limitation is the average number of connectors per unit width.

$$N = \frac{\text{NumberEndFasteners}}{\text{width(ft)}}$$

$$N = \frac{3\text{Fasteners}}{2\text{ft}} = 1.5$$

$$S_{nc} = \left(1637\cdot\text{lb}\cdot\sqrt{\frac{1.5^2\cdot 5.727^2}{24\cdot\text{ft}^2\cdot 1.5^2 + 5.727^2}}\right) = 386\frac{\text{lb}}{\text{ft}}$$

As can be seen the minimum of the three fastener limitations the strength of the diaphragm is S_{ni} = 350 lb/ft. By inspection the stability check is neglected because of the low strength caused by the connection configuration being tested.

4.2.3 Comparison of SDIDDM03 Calculated Strength to Observed Strength

In this test program the SDIDDM03 (Luttrell 2004) and the white paper (Luttrell 2005) are being compared to the observed strength of each diaphragm configuration. Because the white paper only covers the equation modifications for diaphragm stiffness evaluation the SDIDDM03 was used for comparison purposes. In this section discussions are made first about the observed strength of each diaphragm followed by the original SDIDDM03 calculated strengths and finishing with a discussion on the areas of concern with the current equations. The order of the tests done in the test program is shown below

in Table 4-2. As can be seen in Table 4-2 the test number column has two numbers present per test. The first set of numbers represents the order of the tests as they were performed. The second set of numbers represents the test number from the original test program matrix. In the gage column there are either one or two numbers present. Two numbers are present if the profile is cellular, with the hat thickness being the first number and the bottom plate thickness being the second number.

Table 4-2: Test Matrix

Test	Manufacturer	Depth (in)	Gage	Structural Fastener	Stitch Fastener
1 (1)	Wheeling	4.5	20	#12 screws	#10, 36 in. o.c.
2 (6)	USD	4.5	20/20	#12 screws	#10, 36 in. o.c.
3 (4)	CSI	7.5	18	#12 screws	#10, 36 in. o.c.
4 (7)	USD	4.5	18/18	#12 screws	#10, 36 in. o.c.
5 (8)	USD	7.5	18/20	#12 screws	#10, 36 in. o.c.
6 (5)	CSI	7.5	16	#12 screws	#10, 36 in. o.c.
7 (11)	Wheeling	4.5	20	Hilti pins	#10, 36 in. o.c.
8 (10)	Wheeling	4.5	16	Hilti pins	#10, 36 in. o.c.
9 (13)	CSI	7.5	18	Hilti pins	#10, 36 in. o.c.
10 (15)	USD	7.5	18/20	Hilti pins	#10, 36 in. o.c.
11 (16)	USD	7.5	16/18	Hilti pins	#10, 36 in. o.c.
12 (18)	Wheeling	4.5	18	5/8 in. puddle welds	#10, 12 in. o.c.
13 (19)	USD	4.5	20/20	5/8 in. puddle welds	#10, 12 in. o.c.
14 (20)	Wheeling	6	20/20	5/8 in. puddle welds	#10, 12 in. o.c.
15 (12)	Vulcraft	3	16/16	Hilti pins	#10, 12 in. o.c.
16 (14)	Vulcraft	3	20/20	Hilti pins	#10, 12 in. o.c.
17 (17)	Wheeling	6	16/16	Hilti pins	#10, 12 in. o.c.
18 (3)	Vulcraft	3	18/18	#12 screws	#12, 12 in. o.c.
19 (2)	Vulcraft	3	20/20	#12 screws	#12, 12 in. o.c.
20 (9)	Wheeling	6	20/20	#12 screws	#12, 12 in. o.c.

Three different structural connections and two different side-lap connections were used in the test program. The first six tests had No. 12 screws in every valley for structural connections and No. 12 screws at 36 in. on center for side-lap connections. In these tests it was noticed that there was the same amount of structural connections and side-lap connections that would fail in either shear or bearing. Because the side-lap connections are so much more flexible than the structural connections it was also noticed that the side-laps could either fail by rolling over and pulling out of the bottom sheet,

bearing or shear. In the first six tests there was a variation in the thickness of the material at the side-lap locations. It was noted that the side-lap connections tended to have less roll over and pull out failures and more screw shear failures as the thickness increased. This trend lends itself to the current equations used in the SDIDDM03 because they are based on the thickness of the base sheet metal and the diameter of the connector.

With the USD cellular profiles used in this test program the side-lap configuration allows for the use of two different fasteners. A button punch fastener or a screw fastener can be used depending on the construction preference. In this test program, screws were the first choice for the diaphragm construction. However, with many of the samples provided it was noticed that the return flat on the stiffener was short. This issue can be better seen in Figure 4-7. Because of this piece being short it was difficult to make a proper screw connection. This improper screw connection lead to a failure mode of edge tear out which would not occur if all edge requirements could be satisfied. For a complete diagram of the different failure for each connector in the diaphragm tests refer to Tables C-1 through C-20 in Appendix C.

Figure 4-7: Side-lap Detail

Tests 7 through 11 were performed with Hilti pins as the structural connections in

every valley and No. 12 screws at 36 in. on center for the side-lap connections. It was noticed during these tests that the side-lap connections were failing at a much lower load than what would be required to fail the Hilti pins. Once this set of pin tests was completed it was decided that an increase in the side-lap connections should be made. For the remainder of the test performed the side-lap connection spacing was increased from 36 in. on center to 12 in. on center. During the pin tests it was noticed that certain pins would pull out of the base metal material. The cause for this was not easily determined. In all likelihood, the redistribution of forces once the side-lap connections failed caused the pins to be pulled out of the test frame.

After tests 7 through 11 were performed the next three tests, 12 through 14, were done with ¾ in. visible diameter puddle welds as the structural connections in every valley and No. 12 screws at 12 in. on center for the side-lap connections. As was expected the weld tests attained a much higher ultimate strength than the pin and screw tests. This was due in part to the increase of the number of side-lap connections and the higher strength of the puddle welds. It was noticed that the deck around the welded area was connected well and consequently would show signs of yielding even in the high strength steel specimens, i.e. greater than 80 ksi yield strength.

As can be seen in Table C-12 through C-14 there were several locations where the deck broke away from the puddle welds and these failures are indicated by the numbers in the connection locations. Also in several locations in Table C-12 a crack developed tangent to the puddle weld and parallel with the load being applied to the test setup as can be seen in Fig. 4-8. These cracks only developed on the welded tests that were made of high strength steel indicating some brittle behavior in the steel.

The failure locations tended to be adjacent connections which would show that as each connection fails the adjacent connections have an increase in their force because of redistribution. As each of these diaphragms passed their ultimate load the failure was progressive.

Figure 4-8: Weld Crack from Diaphragm Loading

Tests 15 through 17 used pins and tests 18 through 20 used screws as the structural fasteners. The first two pin tests were done with a pin in every valley for the structural connection and a button punch at 12 in. on center for the side-lap connections. The reason the button punch was used on these tests was because that is one of the recommended methods of connection. These tests had very low strengths in comparison to the predicted values. The reason for this was the button punch strength which will be discussed later. There were no structural connection failures and considerable slip occurred at each side-lap location. This indicates that the button punch connection was simply pushing apart the sheets that were clinched together.

The final pin test used the Wheeling 2 x N profile. This profile with the structural connections in every valley and No. 12 screws at 12 in. on center for the side-lap connections had a very high strength. This strength was due in part to the high strength steel from which the deck was made. The load developed with stiffness similar to a cellular profile however, once the diaphragm reached its ultimate load all of the pins that pulled out failed at once. As can be seen in Table C-17 this was the majority of the pins on the end of the diaphragm that the load was being applied. This Wheeling 2 x N test was performed with the two sections mirroring each other along with an added z-piece that was not present on the welded specimen. This z-piece was added to strengthen the end of each flute along with the full length of each end flute. A detail of the z-piece configuration is shown in Fig. 4-9.

Tests 18 and 19 used the Vulcraft cellular profile with No. 12 screws as the

structural fasteners and No. 12 screws as the side-lap fasteners. A hole was predrilled in the top sheet to facilitate screw installation. As can be seen in Tables C-18 through C-20 screw shear was the controlling limit state for tests 18 through 20. Once all of the coupons were milled and measured it was noticed that for two of the tests, test 16 and 18, the coupon thicknesses were different than the test designation. It was determined that the bundles that were used for these tests were mislabeled. These two tests were supposed to be cellular profiles with top and bottom thickness of 20 gage material. From inspection of the bundles used in each test it was determined that two thirds of each test was constructed with 20 gage material and the other third was constructed with 18 gage material. For the calculation purposes the thickness used for these tests was 20 gage since this would be the controlling configuration.

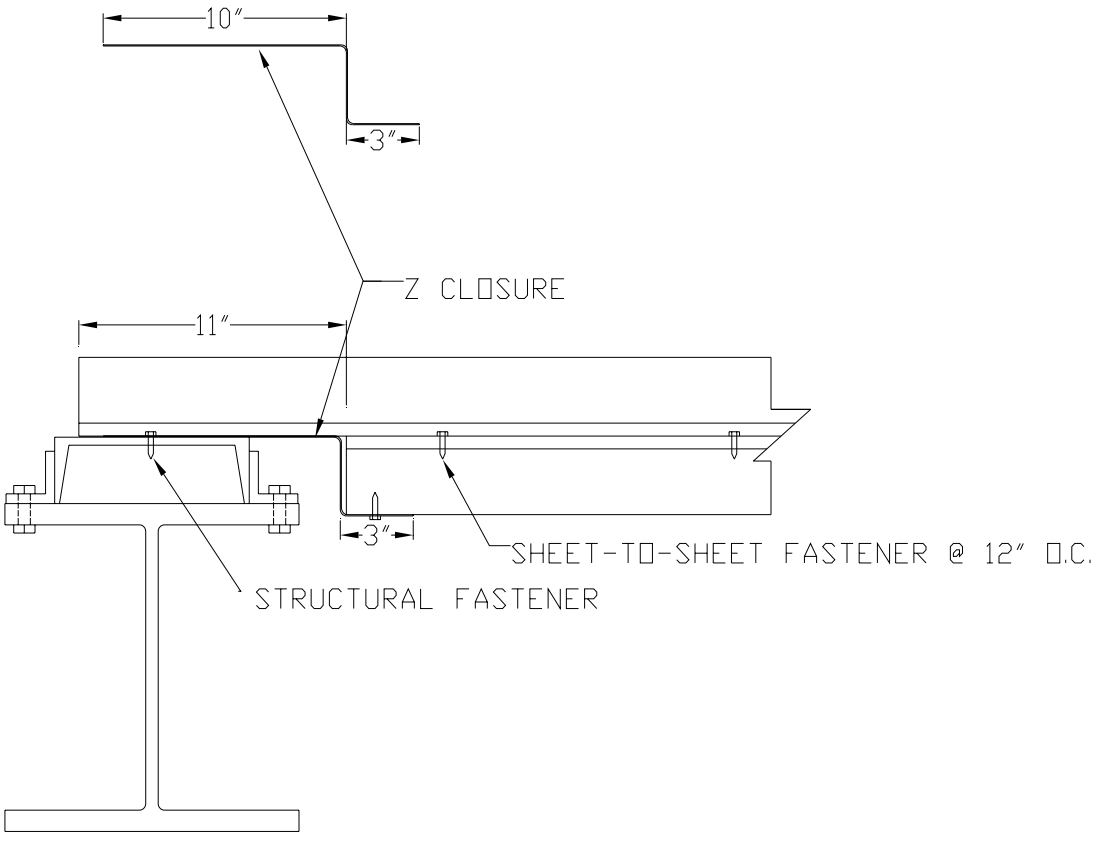

Figure 4-9: Z-Closure for 2 x N Deck

Now that the general findings from the tests have been discussed a comparison

between the observed strength and the SDIDDM03 calculated strength will be discussed. With the calculation procedure that SDI uses the material properties of the diaphragm sheet material such as yield stress and ultimate strength play an important role. For each diaphragm test a set of coupons were made to determine the actual yield stress and ultimate strength. The measured material properties were used for comparison of calculated to actual diaphragm response. For a comparison of the observed strengths with the SDIDDM03 calculated strengths refer to Figure 4-10. Upon first inspection it is clear that the SDIDDM03 is predicting strengths that are higher than most of the observed strengths from the diaphragm tests. For numerical data and the statistical data describing these results refer to Table 4-3. As can be seen in Table 4-3 the test to calculated ratio for the entire data set was less than 1.0 with a standard deviation that is approximately 0.240. Because the average of the comparison was less than 1.0 further investigation was done into the potential reason for this trend.

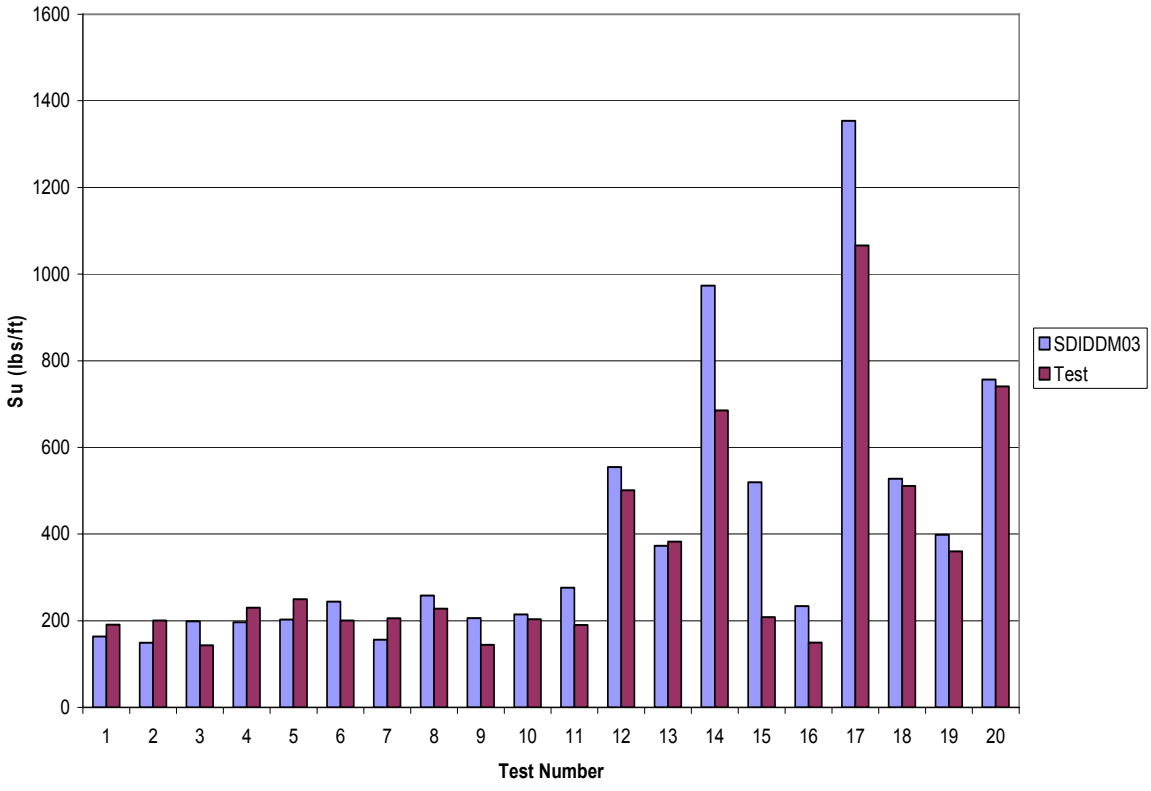

Figure 4-10: Strength Comparison, SDIDDM03 vs. Tested

Because of this conclusion a further look at the equations that were used to predict the diaphragm strength was necessary. The force distribution equations for the analysis of the diaphragms are dependent on the strength calculated for the different fasteners. A breakdown of the fastener strengths calculated by the SDIDDM03 is shown in Table 4-4. Upon inspecting each value, the first one that seems surprising is the nearly 3800 lb strength for the structural fastener used in test number five. The structural connector used in that test was a #12 screw.

Table 4-3: SDIDDM03 and Test Strength Results

Test No.	Test Designation	SDI S_u (lbs/ft)	Test Su (lbs/ft)	Ratio (Test/Calc)
1 (1)	WH-4.5-N-20-S-S	164	191	1.165
2 (6)	USD-4.5-C-20/20-S-S	149	201	1.348
3 (4)	CSI-7.5-N-18-S-S	198	143	0.723
4 (7)	USD-4.5-C-18/18-S-S	196	230	1.170
5 (8)	USD-7.5-C-18/20-S-S	202	250	1.234
6 (5)	CSI-7.5-N-16-S-S	244	201	0.822
7 (11)	WH-4.5-N-20-P-S	156	206	1.315
8 (10)	WH-4.5-N-16-P-S	258	228	0.881
9 (13)	CSI-7.5-N-18-P-S	206	144	0.700
10 (15)	USD-7.5-C-18/20-P-S	214	203	0.949
11 (16)	USD-7.5-C-16/18-P-S	276	190	0.689
12 (18)	WH-4.5-N-18-W-S	554	501	0.904
13 (19)	USD-4.5-C-20/20-W-S	373	383	1.026
14 (20)	WH-3-M-20/20-W-S	738	685	0.929
15 (12)	VC-3-C-16/16-P-BP	520	208	0.400
16 (14)	VC-3-C-20/20-P-BP	233	149	0.639
17 (17)	WH-3-M-16/16-P-S	1354	1066	0.788
18 (3)	VC-3-C-18/18-S-S	527	511	0.970
19 (2)	VC-3-C-20/20-S-S	398	360	0.903
20 (9)	WH-3-M-20/20-S-S	757	741	0.979
			Mean	0.927
			σ	0.240

The screw strength equation was based upon the total thickness of the sheet material penetrated and the yield stress of the sheet material. With cellular profiles the typical thickness that the structural connection will penetrate is a double thickness at all locations. This makes the typical bearing and tear out limit states not control as before. The shear strength of each type of fastener was determined by obtaining test data or information from the manufacturer.

Table 4-4: SDIDDM03 Fastener Strength

Test No.	Test Designation	SDIDDM03		SDIDDM03 w/ Shear Limitation	
		Q_f (lbs)	Q_s (lbs)	Qf (lbs)	Qs (lbs)
1 (1)	WH-4.5-N-20-S-S	2233	771	2000	771
2 (6)	USD-4.5-C-20/20-S-S	1637	771	1637	771
3 (4)	CSI-7.5-N-18-S-S	2227	1020	2000	1020
4 (7)	USD-4.5-C-18/18-S-S	2161	1018	2000	1018
5 (8)	USD-7.5-C-18/20-S-S	3798	771	2000	771
6 (5)	CSI-7.5-N-16-S-S	2565	1284	2000	1284
7 (11)	WH-4.5-N-20-P-S	1938	771	1938	771
8 (10)	WH-4.5-N-16-P-S	3149	1284	3149	1284
9 (13)	CSI-7.5-N-18-P-S	2534	1020	2534	1020
10 (15)	USD-7.5-C-18/20-P-S	4281	771	4281	771
11 (16)	USD-7.5-C-16/18-P-S	5364	1020	4500	1020
12 (18)	WH-4.5-N-18-W-S	7194	1020	6014	1020
13 (19)	USD-4.5-C-20/20-W-S	3271	771	3055	771
14 (20)	WH-3-M-20/20-W-S	5302	1743	4034	1743
15 (12)	VC-3-C-16/16-P-BP	5897	858	4500	858
16 (14)	VC-3-C-20/20-P-BP	3732	309	3732	309
17 (17)	WH-3-M-16/16-P-S	5897	2903	4500	2000
18 (3)	VC-3-C-18/18-S-S	3871	1020	2000	1020
19 (2)	VC-3-C-20/20-S-S	2925	771	2000	771
20 (9)	WH-3-M-20/20-S-S	4459	1542	2000	1542

It was determined that the shear strength of the No. 12 screws used was 2000 pounds and the Hilti X-ENP-19 L15 pins shear strength was 4500 pounds. It was also

important to determine the weld shear strength. The weld strength equation that is used in the SDIDDM03 (2004) is one of the equations that is used in AISI (2001). In this test program this weld strength equation was not found to control. If the other weld strength equations are used from AISI (2001) the calculated strength comes closer to the observed strength. Table 4-4 shows the fastener strengths where all limit states are considered. As can be seen there are many fastener strengths that are changed by this modification. This shows that not all of the limit states for each connector are being considered in the current SDIDDM03. Coverage of all limit states is essential for accurate design.

When checking all limit states in this test program it was found that limitations should be placed on the structural fastener, the side-lap fastener or both. The test to predicted ratios improved once the more complete evaluation of fastener strengths are included, as can be observed in Fig. 4-11 and Table 4-5.

If a comparison of the total data statistics in Table 4-5 for the diaphragm strength the mean is 0.994 and the standard deviation is 0.271. If tests 15 and 16 are eliminated from the data set, because of the use of button punch the statistics change to 1.045 and 0.231 respectively, which is an improvement in the right direction.

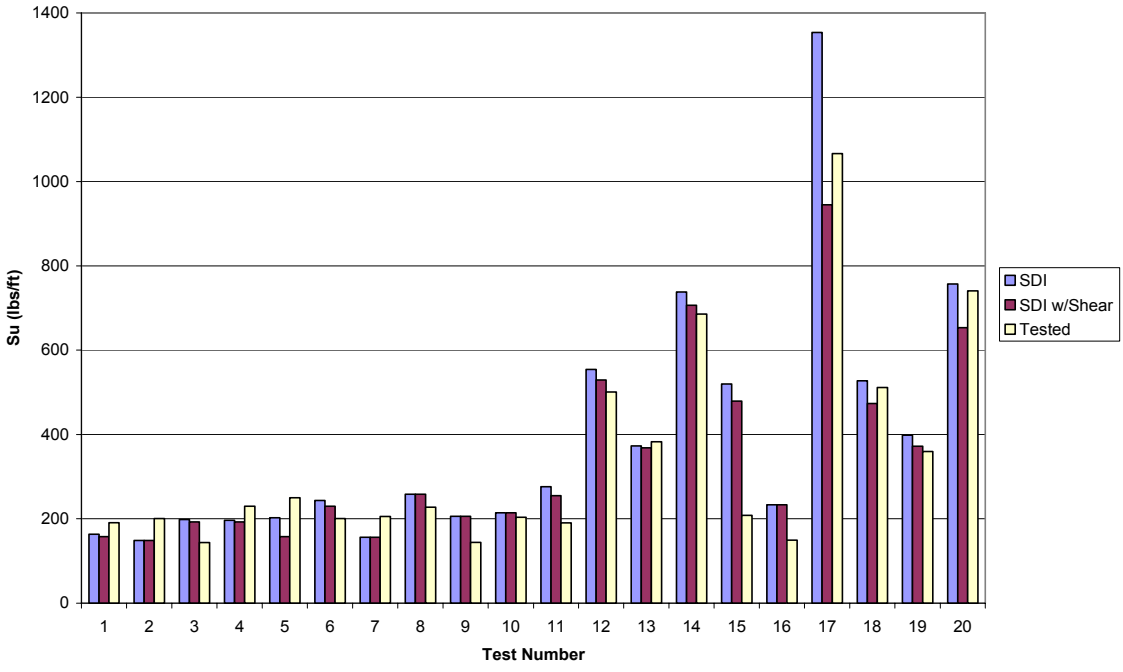

Figure 4-11: Strength Comparison with Shear Limitation

The fastener shear strength issue does not only occur in cellular profiles but also at side-lap locations where there are double thicknesses. It also occurs with high yield strength material and thick single sheet thickness. This can be shown in tests number 1, 3 and 5. Test 1 is made up of a high strength material, i.e. F_y = 107ksi. Tests 3 and 5 have a yield stress of 50 ksi and 48 ksi respectively and have the same shear limitation issues.

Table 4-5: SDIDDM03 with Shear Limitation and Test Strength Results

Test No.	Test Designation	SDI w/ Shear Su(lbs/ft)	Test Su (lbs/ft)	Ratio (Test/Calc)
1 (1)	WH-4.5-N-20-S-S	158	191	1.208
2 (6)	USD-4.5-C-20/20-S-S	149	201	1.348
3 (4)	CSI-7.5-N-18-S-S	193	143	0.744
4 (7)	USD-4.5-C-18/18-S-S	192	230	1.194
5 (8)	USD-7.5-C-18/20-S-S	158	250	1.583
6 (5)	CSI-7.5-N-16-S-S	230	201	0.873
7 (11)	WH-4.5-N-20-P-S	156	206	1.315
8 (10)	WH-4.5-N-16-P-S	258	228	0.881
9 (13)	CSI-7.5-N-18-P-S	206	144	0.700
10 (15)	USD-7.5-C-18/20-P-S	214	203	0.949
11 (16)	USD-7.5-C-16/18-P-S	255	190	0.747
12 (18)	WH-4.5-N-18-W-S	529	501	0.946
13 (19)	USD-4.5-C-20/20-W-S	369	383	1.039
14 (20)	WH-3-M-20/20-W-S	707	685	0.970
15 (12)	VC-3-C-16/16-P-BP	479	208	0.434
16 (14)	VC-3-C-20/20-P-BP	233	149	0.639
17 (17)	WH-3-M-16/16-P-S	945	1066	1.128
18 (3)	VC-3-C-18/18-S-S	473	511	1.080
19 (2)	VC-3-C-20/20-S-S	372	360	0.968
20 (9)	WH-3-M-20/20-S-S	653	741	1.134
			Mean	0.994
			σ	0.271

Even with the shear limitation applied to the calculations, tests 15 and 16 still show a considerably lower strength than the SDI prediction. This brings us back to the issue of the button punch strength. The current button punch equation is based upon the thickness of the material at the side-lap connection. As can be seen from Figure 4-7 the tested strengths for these two tests are considerably different than the calculated strengths. Test 15 was with a 16 gage sheet material and test 16 was with a 20 gage sheet material. The difference in the calculated strength and the observed strength seems to be greater as the thickness increases. This indicates a correlation between increasing material thickness and decreasing button punch strength. Wheeling provided a set of test data that was performed at an independent lab facility on button punch strength. The data that was provided is listed in Table 4-6.

Table 4-6: Wheeling Button Punch Data and SDI Test Comparison

	Wheeling Testing, lbs				SDI Tests, lbs	
	16 Gage	18 Gage	20 Gage	22 Gage	16 Gage	20 Gage
	112	120	265	275	94	103
	115	70	105	185		
	92	160	186	270		
	122	270	352			
	95	205				
		230				
Average	**107.2**	**176**	**227**	**243**		

The left portion of Table 4-6 is the Wheeling button punch test data. The right portion of Table 4-6 is the button punch strength back calculated from the SDIDDM03 calculations, assuming the Q_f term is correct, when the Q_s term is varied until the observed test strength and the calculated strengths are equal. As can be seen for the 16 gage material the test results fall within the lower range of the Wheeling results. The 20 gage material however only seems to match with the single outlying data point provided by Wheeling. This does give some validity to the notion that the button punch equation currently used in SDIDDM03 does not accurately predict the button punch strength.

4.2.4 Recommended Modifications to Strength Determination

Modifications to the SDI strength determination are recommended for all fastener types used in the test program. Each fastener type is discussed in detail with suggestions about the modification method given where needed.

A minor modification needs to be made for screw strength in the SDIDDM03. A limitation needs to be included that does not allow the fastener force to exceed the shear strength of the screw. In the AISI (2001) provisions, the different screw strength calculations are based on the physical dimensions of parameters like the screw head and the screw major diameter. These equations are checking for failures in the sheet metal and not the screw connector. Section E4.3.3 in AISI (2001) uses equation 4.11 which requires the nominal shear strengths are provided by the manufacturer.

$$P_{ns} = 0.8P_{ss} \tag{4.11}$$

Where:

P_{ss} = Nominal shear strength (resistance) of screw as reported by manufacturer or determined by independent laboratory testing

This implies that each manufacturer produces their screws from different grades of materials and could have variable shear strength. To place a shear limitation on the screw strength equation in the SDIDDM03 a provision similar to that in AISI (2001) is needed.

The pin strength equations in the SDIDDM03 are based on the sheet metal thickness alone. A shear limitation is also needed for these equations but a similar problem to the screw shear limitation exists. The problem here is more easily solved because there are many different equations for pin strength that are based on the model of pin being used. This would mean that the shear strength of each pin could easily be placed by the equation as an upper bound. This would eliminate the problem of designers using erroneously high strength values which would create more accurate diaphragm designs.

The weld strength equations in the SDIDDM03 are the same as one of the shear strength equations present in the AISI (2001). This equation does control the weld shear

strength as long as the following assumptions are made:

F_u = 55ksi

d_{weld} = 5/8 in.

These assumptions are the commonly used in the SDIDDM03. However, if different values than the aforementioned are assumed the shear strength is governed by a different equation. The AISI (2001) equations that are presented for weld shear are:

$$P_{na} = \frac{\pi \cdot d_e^{\,2}}{4} \cdot 0.75 \cdot F_{xx} \tag{4.12}$$

If:

$$\frac{d_a}{t} \le 0.815 \cdot \sqrt{\frac{E}{F_u}}$$

$$P_n = 2.20 \cdot t \cdot d_a \cdot F_u \tag{4.13}$$

$$0.815 \cdot \sqrt{\frac{E}{F_u}} < \frac{d_a}{t} < 1.397 \cdot \sqrt{\frac{E}{F_u}}$$

$$P_n = 0.280 \left(1 + 5.59 \cdot \frac{\sqrt{\frac{E}{F_u}}}{\frac{d_a}{t}} \right) \cdot t \cdot d_a \cdot F_u \tag{4.14}$$

$$\frac{d_a}{t} \ge 1.397 \cdot \sqrt{\frac{E}{F_u}}$$

$$P_n = 1.40 \cdot t \cdot d_a \cdot F_u \tag{4.15}$$

Where:

P_n = Nominal shear strength (resistance) of arc spot weld

d = Visible diameter of outer surface of arc spot weld

d_e = Effective diameter of arc spot weld

d_a = Average diameter of arc spot weld at mid-thickness of t where d_a = (d-t) for single sheet or multiple sheets not more than four lapped sheets over a supporting

member.

d_e = Effective diameter of fused area at plane of maximum shear transfer

$=0.7d - 1.5t \leq 0.55d$

t = Total combined base steel thickness (exclusive of coatings) of sheet involved in shear transfer above plane of maximum shear transfer.

F_{xx} = Tensile strength of electrode classification

F_u = Tensile strength of sheet material

The shear design of the arc spot weld is taken as the minimum of either Eq 4.12 or the equation that applies to the boundary conditions set in Eq 4.13 through 4.15. Equation 4.13 is the equation used in the SDIDDM03. For test number 12 the controlling equation was Eq 4.12, which is the shear strength of the weld material. For test numbers 13 and 14 the controlling equation was Eq 4.14. Tests 12 and 14 were done with high strength materials, which is the main reason for their different controlling equations. Test 13 and 14 were done with 20 gage material.

For making general assumptions about diaphragm design the current equation in the SDIDDM03 is adequate. However, if forensic analysis or research is being done, as in this project, the scope of the weld shear equations must be broadened. The AISI equations that applied to this project brought the predicted strengths closer to the observed strengths from the tests as can be seen in Figure 4-7.

The button punch strength equations in the SDIDDM03 need to be reinvestigated. The equation currently in the SDIDDM03 is:

$$Q_S = 240t^2 \tag{4.16}$$

This equation predicts that as the thickness of the sheet material increases there is a quadratic increase in strength. As can be shown, in a comparison of the Qs values predicted in Table 4-3 for tests 15 and 16 and the values shown in Table 4-5, there is a distinct difference in the actual strength. Observing the trend in Table 4-5 of the values found in the Wheeling testing, a different trend can be seen in Figure 4-12.

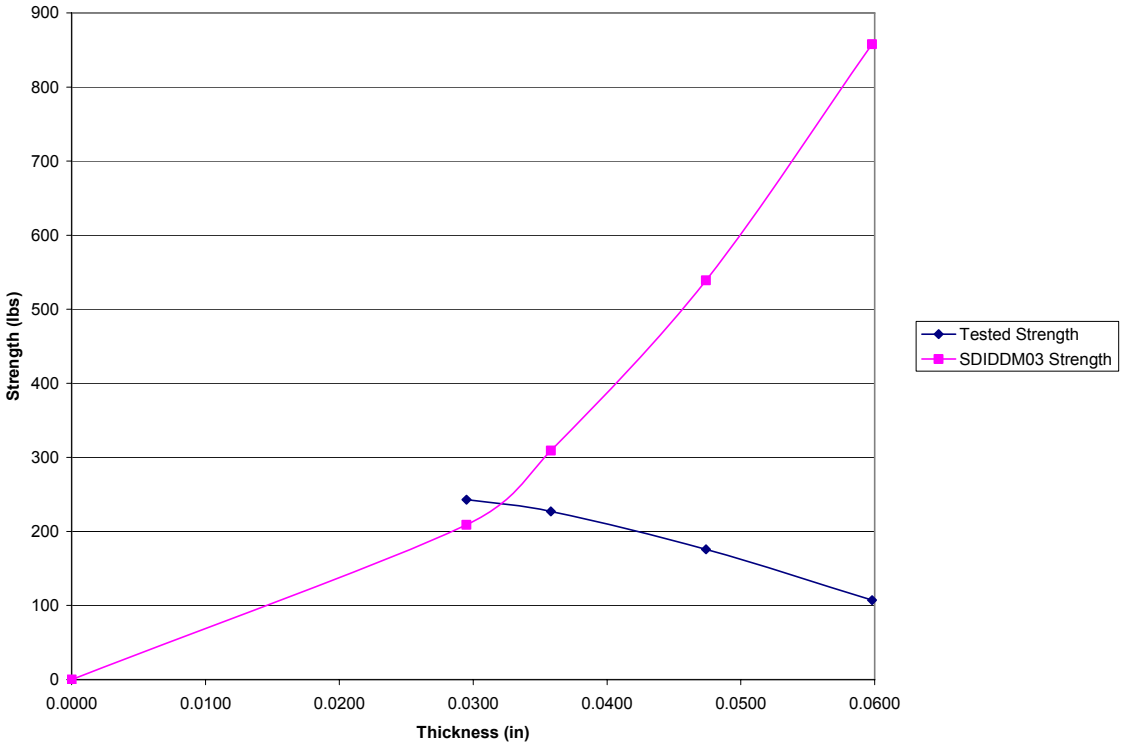

Figure 4-12: Button Punch Strength Trend

In the development of the SDI diaphragm design manuals the dominant materials used were light gage materials. With these materials the typical controlling limit states were bearing on the deck material. With the development of deep deck and cellular deck profiles, for spanning longer distances, the controlling limit states for light gage material do not apply. This is apparent with the typical shear limit state that controlled many of the diaphragms in this study. For the SDI diaphragm design manual to be a more complete document all applicable limit states must be considered. The equations for these limit states have already been developed in the AISI (2001) provisions and could easily be used in conjunction with the SDI diaphragm design manual.

4.3 Diaphragm Shear Stiffness Calculations

In some structures the stiffness of the diaphragm system is important. These are buildings that may have deflection limitations for drift from wind or seismic loading. In many cases an accurate calculation method to predict deflection is essential. Excessive

deflections can become serviceability issues in the life-cycle of a building and therefore must be predicted accurately. The SDIDDM03 contains a set of stiffness calculations that are designed to help predict the deflections of a building's diaphragm system. Luttrell (2005) addresses deep deck and cellular deck profiles that are not covered in the SDIDDM03.

4.3.1 SDIDDM03 Procedure

The stiffness calculations for a diaphragm in the SDIDDM03 are based upon several different factors. The main factors considered in the stiffness of a diaphragm system are shear, warping, and discrete connection displacements. The general equation that this forms is:

$$G' = \frac{\frac{P \cdot a}{L}}{\Delta_s + \Delta_d + \Delta_c} \tag{4.17}$$

Where:

$P = 0.4P_u$

a = dimension of diaphragm perpendicular to applied load, ft.

L = design length, ft.

Δ_s = displacement due to shear

Δ_d = displacement due to warping distortion

Δ_c = displacement due to discrete connections

This equation, with the in-depth evaluation of each displacement type, evolved into equation 2.5 as presented earlier. With the deep deck and cellular deck systems a few modifications were necessary to account for the changes in deck profile geometry. The cellular profile geometry affects the warping distortion and the shear deflections making for a more rigid system.

4.3.2 Example Calculation

This is a continuation of the problem that was begun in Section 4.2.2.4. The next diaphragm calculation process is the stiffness evaluation of the system. First the calculations were performed with the original SDI stiffness evaluation procedure. Then

the stiffness evaluations using the white paper presented by Luttrell were done so a comparison can be made between the two results.

Screws are used for both frame and side-lap fastening and the flexibility for each must be calculated. The flexibility for each is:

$$S_f = \frac{1.30}{1000 \cdot \sqrt{0.0359\,\text{in}}} = 0.006861\ \frac{\text{in}}{\text{k}}$$

$$S_s = \frac{3.0}{1000 \cdot \sqrt{0.0359\,\text{in}}} = 0.016\ \frac{\text{in}}{\text{k}}$$

The next thing that needed to be calculated was the stiffness coefficient. This stiffness coefficient comes from Eq 2.6.

$$C = \frac{2E \cdot t \cdot L}{w} \cdot S_f \left(\frac{1}{2 \cdot \alpha_1 + n_p \cdot \alpha_2 + 2 \cdot n_s \cdot \frac{S_f}{S_s}} \right) \tag{2.6}$$

$$C = \frac{2 \cdot 29500\,\text{ksi} \cdot 0.0359\,\text{in} \cdot 288\,\text{in}}{24\,\text{in}} \cdot 0.006861\,\frac{\text{in}}{\text{k}} \cdot \left(\frac{2}{2 \cdot 1 + 0 \cdot 1 + 2 \cdot 7 \cdot \frac{0.006861\,\frac{\text{in}}{\text{k}}}{0.016\,\frac{\text{in}}{\text{k}}}} \right)$$

$C = 21.619$

The warping constant D1 in the SDI manual that is required for this calculation is based on the connection configuration of one screw in every valley. The calculations to determine the warping constant are based upon the manufacturer's dimensions for the profile. The D1 value for this example is:

D1 = 1915ft.

The warping constant is multiplied by another constant that is configuration dependent. This constant, ρ, is based upon the number of spans for the diaphragm. For

single span diaphragms, as in this test program, ρ is equal to unity. Once all of these values are established the stiffness of the system can be evaluated. The stiffness that the current SDI manual uses is Eq 2.5.

$$G' = \frac{E \cdot t}{2 \cdot (1 + \nu) \cdot \frac{s}{d} + D_n + C} \tag{2.5}$$

$$G' = \frac{29500\ \text{ksi}\,(0.0359\ \text{in})}{2.6 \cdot \frac{21\,\text{in}}{12\,\text{in}} + \left(1.0 \cdot \frac{1915\,\text{ft}}{24\,\text{ft}}\right) + 21.619} = 9.995\ \frac{\text{k}}{\text{in}}$$

The white paper presented by Luttrell recommends a few changes to Eq 2.5. According to Luttrell, the first term in the denominator should be modified to better understand the shear path that is involved with a profile that has a bottom plate and a top flute. As this term decreases in value of the resultant stiffness increases. The second term in the denominator is also modified to account for the stiffness of the tubular section that is now present as opposed to the open corrugation. The first term in the denominator was modified as in Eq 2.10.

$$A_A = \frac{2.6 \cdot D_{DL}}{\left(1 + D_{DL} \cdot \frac{t_b}{t}\right)} \tag{2.10}$$

$$A_A = \frac{2.6\,(1.75)}{1 + (1.75)\frac{0.0359\ \text{in}}{0.0359\ \text{in}}} = 1.655$$

The second term in the denominator is modified and becomes:

$$\frac{\rho D_n}{3\cdot\frac{h}{in}\cdot\left(\frac{t_{bottom}}{t}\right)^3} = \frac{1.0(79.792)}{3\cdot 4.5\left(\frac{0.0359in}{0.0359in}\right)^3} = 5.91$$

The third term in the denominator is not modified at all because the stiffness coefficient remains the same if there is a bottom sheet or not. The final equation for the stiffness of the diaphragm system is Eq 2.9.

$$G' = \frac{E\cdot t}{A_A + \left(\frac{D_n}{3\cdot D_d\left(\frac{t_b}{t}\right)^3}\right) + C} \tag{2.9}$$

$$G' = \frac{29500ksi\cdot(0.0359in)}{1.655 + 5.91 + 21.619} = 36.289\frac{k}{in}$$

As can be seen from this result the new stiffness evaluation is more than three and a half times greater than the original SDI stiffness value.

4.3.3 Comparison of SDIDDM03 Calculated Stiffness to Observed Stiffness

In this study, the white paper (Luttrell, 2005) was compared to the stiffness results observed from tests of deep deck and cellular deck profiles. The observed stiffness of each diaphragm, the original SDIDDM03 calculated stiffness and the white paper stiffness are presented and discussed in this section. The section concludes with a discussion on the areas of concern with the current and proposed white paper equations.

Of the profiles tested, seven were deep N-deck profiles, ten were cellular profiles and three were the 2 x N profiles. It was easily seen that the cellular profiles produced a much greater stiffness than the N-deck profiles. The reason for the difference comes from the flat sheet attached to the hat section on the cellular profiles. As can be seen in Figure 4-13 under maximum load the N-deck profiles have a considerable amount of warping

distortion. This distortion is a major contribution to the deflection and consequentially the stiffness of the system. With the cellular profiles, as shown in Figure 4-14, the hat-section of the profile has relatively no distortion. This lack of distortion is due to the torsional rigidity of the closed section created by the flute and the pan.

Figure 4-13: Warping distortion of N-Deck

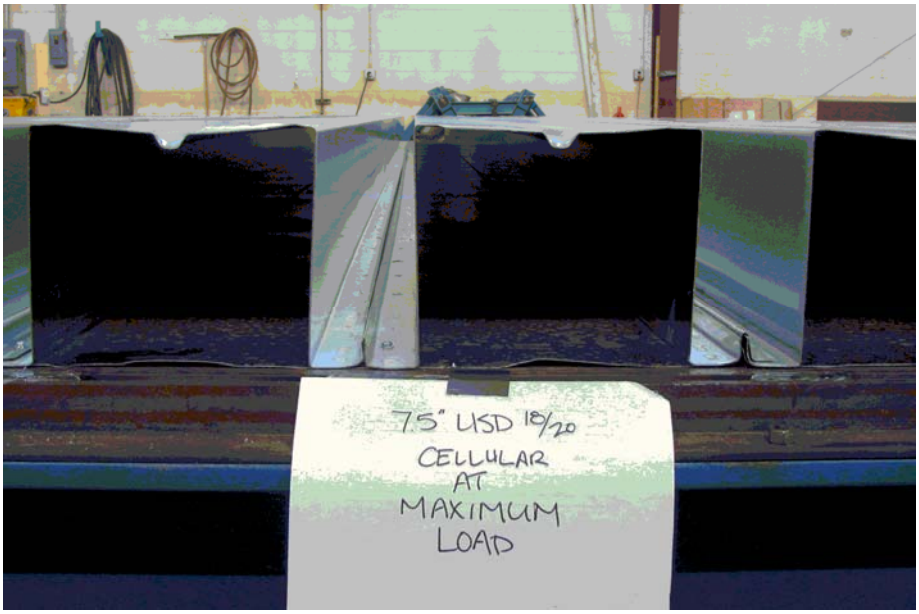

Figure 4-14: End view of Cellular Profile Test

The stiffness of the diaphragm was calculated at a load equal to forty percent of the maximum load attained in the test specimen. Adjustments were made to the maximum load and the stiffness according to the ICC (2006) evaluation procedure. In the ICC (2006) evaluation procedure the deflections of the system can be determined based on measurement of either specific corner displacements or by measuring the diagonal displacements. For this study both measurements were taken along with additional corner displacements so all the relevant displacement data was obtained. All of the load versus displacement plots for the diaphragms in this study are located in Figs. A-1 through A-20 in Appendix A. The maximum load and the stiffness of each diaphragm are shown in these figures. The stiffness shown represents the corrected corner displacements. Only this stiffness is shown because this is the typical stiffness that all the diaphragm equations have been based upon since the beginning of the SDI diaphragm design manuals.

In each of the tests, the diagonal displacements were smaller than the corner net displacement due to several factors. One of the most prevalent factors is the monitoring of many different corner displacement can be difficult. Many of the corner displacements, even under high loading, are small numbers. With such a high sensitivity the corrected deflection can be easily swayed. Also with measuring the corner displacements all the displacement transducers were located at the midpoint of the frames webs. Any type of distortion in the frame members could misrepresent the deflections the diaphragm is experiencing. Overall the typical difference between the corner and diagonal deflection numbers was approximately 0.2 in. A breakdown of the important displacements for each diaphragm is shown in Table 4-7.

The diagonal displacements only measure the shear displacement of the frame. Also the numbers for these displacements are not as small which requires a less sensitive instrument for measurement. This makes the measurements seem more representative of the true displacements being seen in the diaphragm.

Table 4-7: Diaphragm Displacements

Test No.	Test Designation	Δ At Max Load (in)		Δ At 0.4 Max Load (in)	
		Corner	Diagonal	Corner	Diagonal
1 (1)	WH-4.5-N-20-S-S	3.934	3.702	0.733	0.653
2 (6)	USD-4.5-C-20/20-S-S	2.831	2.758	0.067	0.020
3 (4)	CSI-7.5-N-18-S-S	5.119	4.956	0.575	0.405
4 (7)	USD-4.5-C-18/18-S-S	2.365	2.119	0.203	0.070
5 (8)	USD-7.5-C-18/20-S-S	3.287	3.043	0.095	0.037
6 (5)	CSI-7.5-N-16-S-S	3.830	3.628	0.591	0.373
7 (11)	WH-4.5-N-20-P-S	1.983	3.715	0.346	0.788
8 (10)	WH-4.5-N-16-P-S	1.277	1.078	0.391	0.240
9 (13)	CSI-7.5-N-18-P-S	6.604	6.426	1.340	1.200
10 (15)	USD-7.5-C-18/20-P-S	2.111	1.818	0.160	0.076
11 (16)	USD-7.5-C-16/18-P-S	1.490	1.216	0.150	0.034
12 (18)	WH-4.5-N-18-W-S	4.447	4.179	1.228	1.035
13 (19)	USD-4.5-C-20/20-W-S	1.704	1.464	0.205	0.052
14 (20)	WH-3-M-20/20-W-S	2.467	2.270	0.589	0.410
15 (12)	VC-3-C-16/16-P-BP	1.761	1.641	0.327	0.252
16 (14)	VC-3-C-20/20-P-BP	1.967	1.815	0.399	0.353
17 (17)	WH-3-M-16/16-P-S	1.138	0.832	0.291	0.111
18 (3)	VC-3-C-18/18-S-S	3.321	3.088	0.117	0.028
19 (2)	VC-3-C-20/20-S-S	4.222	4.060	0.194	0.122
20 (9)	WH-3-M-20/20-S-S	1.556	1.237	0.420	0.249

The magnitude of only 0.2 in. this does not sound like a major issue. However, if the 0.2 in. is consistent throughout the test then the small deflections used to calculate the stiffness, as shown in the last two columns of Table 4-7, can change the observed stiffness considerably. Table 4-8 shows the comparison of corner observed stiffness to diagonal observed stiffness.

Table 4-8: Corner and Diagonal Stiffness Comparison

Test No.	Test Designation	Stiffness (kips/in)		% Increase
		Corners	Diagonals	
1 (1)	WH-4.5-N-20-S-S	4.92	5.94	21
2 (6)	USD-4.5-C-20/20-S-S	62.58	205.88	229
3 (4)	CSI-7.5-N-18-S-S	4.38	6.01	37
4 (7)	USD-4.5-C-18/18-S-S	24.20	70.38	191
5 (8)	USD-7.5-C-18/20-S-S	55.09	143.76	161
6 (5)	CSI-7.5-N-16-S-S	6.72	10.65	58
7 (11)	WH-4.5-N-20-P-S	12.73	4.97	-61
8 (10)	WH-4.5-N-16-P-S	13.13	21.42	63
9 (13)	CSI-7.5-N-18-P-S	1.80	2.01	12
10 (15)	USD-7.5-C-18/20-P-S	27.19	62.43	130
11 (16)	USD-7.5-C-16/18-P-S	28.61	126.81	343
12 (18)	WH-4.5-N-18-W-S	10.27	12.14	18
13 (19)	USD-4.5-C-20/20-W-S	49.35	194.76	295
14 (20)	WH-3-M-20/20-W-S	29.60	42.52	44
15 (12)	VC-3-C-16/16-P-BP	14.37	18.62	30
16 (14)	VC-3-C-20/20-P-BP	8.44	10.78	28
17 (17)	WH-3-M-16/16-P-S	82.54	217.08	163
18 (3)	VC-3-C-18/18-S-S	94.59	392.50	315
19 (2)	VC-3-C-20/20-S-S	39.16	62.39	59
20 (9)	WH-3-M-20/20-S-S	39.78	67.02	68

In tests 7, 11 and 13 there were slight malfunctions that affected the data collected. Test 7 there was a short found in one of the wires connecting a diagonal displacement transducer and displacement transducer two, a corner measurement, to the data acquisition system. This gave erroneous values of displacement and changed the diagonal stiffness to less than the corner stiffness. However, only one of the diagonal displacement transducers was shorting out. When calculating the deflection of the diaphragm only one of the diagonals is required. If the single diagonal is analyzed, the deflection can be calculated with the following equation.

$$\Delta_{diag} = \frac{a^2 + b^2 - d^2}{2 \cdot b} \tag{4.18}$$

Where:

a & b are defined in Eq 3.1

d = length of the diagonal

It was also found that in test 11 and 13 one of the diagonal displacement transducer supports was loose. This caused a false stiffness because of the added flexibility in the displacement transducer support. Using Eq 4.18 with the diagonal displacement transducer that was not loose a better graph of the load versus displacement was obtained. Because of this observed flexibility, a second set of displacement transducers were added to the system. These displacement transducers were added, at the level of the diaphragm being tested, to see if there was any flexibility in the supports that should be addressed. As can be seen in Fig A-14 the new diagonal displacement transducer data almost overlaps the previously used displacement transducer data indicating little to no flexibility in the system.

Observing the percentage of increase in stiffness based on corner displacements versus stiffness based on diagonal displacements, the average increase is 110 percent and the standard deviation is 113 percent. If the true stiffness of the diaphragm is more accurate from measuring the diagonal displacements then the current modeling equations need modification.

The ICC (2006) evaluation procedure requires that the loading sequence up to the maximum applied load shall be done at a load rate taking no less than ten minutes. This is a requirement because if the loading is done too quickly a false strengthening of the system will occur because of dynamic load effects. During the first eleven tests of this study the load rate was done so that the *total* loading time was not less than ten minutes. This made the final loading cycle in many of these tests less than ten minutes. A summary of the final loading cycle's times are given in Table 4-9.

Table 4-9: Final Loading Time of Diaphragms

Test	Test Designation	Final Loading Time (min)
1 (1)	WH-4.5-N-20-S-S	7.4
2 (6)	USD-4.5-C-20/20-S-S	6.1
3 (4)	CSI-7.5-N-18-S-S	7.5
4 (7)	USD-4.5-C-18/18-S-S	6
5 (8)	USD-7.5-C-18/20-S-S	9.4
6 (5)	CSI-7.5-N-16-S-S	6.5
7 (11)	WH-4.5-N-20-P-S	6.8
8 (10)	WH-4.5-N-16-P-S	3.6
9 (13)	CSI-7.5-N-18-P-S	5.6
10 (15)	USD-7.5-C-18/20-P-S	4.3
11 (16)	USD-7.5-C-16/18-P-S	4.6
12 (18)	WH-4.5-N-18-W-S	42
13 (19)	USD-4.5-C-20/20-W-S	42.95
14 (20)	WH-3-M-20/20-W-S	76.6
15 (12)	VC-3-C-16/16-P-BP	28.8
16 (14)	VC-3-C-20/20-P-BP	22
17 (17)	WH-3-M-16/16-P-S	66.47
18 (3)	VC-3-C-18/18-S-S	56.7
19 (2)	VC-3-C-20/20-S-S	35.28
20 (9)	WH-3-M-20/20-S-S	40.8

Once this mistake was realized the final loading cycle was slowed down as noted. If a comparison of the results shown in Fig 4-11 for strength are done it can be stated that the strength relationship varied, either higher or lower than calculated, throughout the entire test program. This shows that the loading rates for the tests in this program had no adverse affect on the test results. Also if a comparison of the load rate for the tests with the stiffness of the diaphragms shown in Fig 4-15 and 4-16 no direct correlation can be seen.

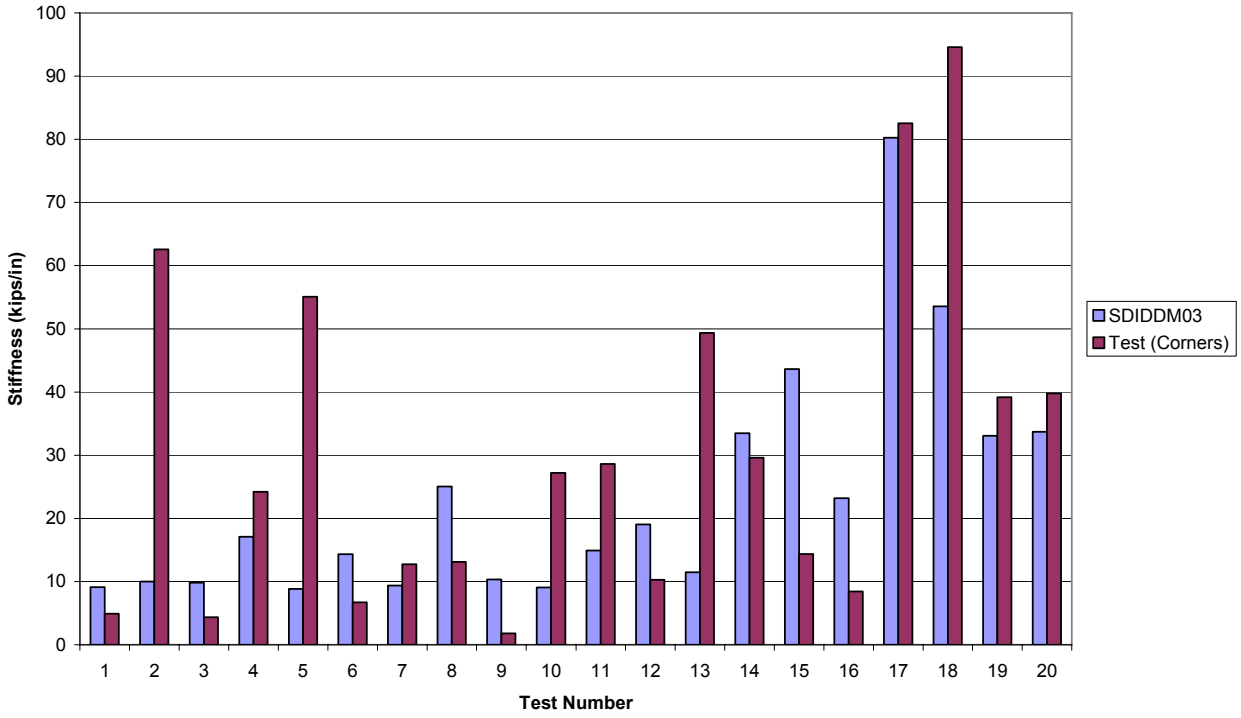

Figure 4-15: Stiffness Comparison, SDIDDM03 versus Test (Corners)

In looking at the results found from the stiffness portion of this study it can be seen that the CSI profiles tested (Tests 3, 6 and 9) below expectations. Also the button punch side-lap used in tests 15 and 16 have shown to fall below stiffness predictions as well. In comparing the stiffness from the corner measurements with the original SDIDDM03 (2004), Fig. 4-15, stiffness a more stable relationship can be seen excluding the previously mentioned tests. If a comparison is made between the original SDIDDM03 (2004) stiffness and the observed stiffness from diagonal measurements, Fig. 4-16, it is easily seen that there is no correlation between these results. The statistics for these comparisons can be seen in Table 4-10. With these statistical results consideration must be made for tests 15 and 16 which have been conclusively seen as outlying results. When comparing the statistical results of the SDIDDM03 in comparison with the stiffness derived from the corner and diagonal displacements respectively an unusual trend can be seen. The stiffness from the corner displacements seems to have a much better correlation than the stiffness from the diagonal displacements. This is intuitive because the

SDIDDM03 was developed from testing based on the stiffness derived from the corner displacements. However, neither comparison yields a consistent correlation with the diagonal displacement stiffness having a more scattered result than the corner displacement stiffness.

Table 4-10: SDIDDM03 Stiffness Comparison with Statistics

Test	Stiffness (kips/in)			Ratio	Ratio
	Corners	Diagonals	SDIDDM03	(Corner/SDIDDM03)	(Diagonals/SDIDDM03)
1 (1)	4.92	5.94	9.11	0.540	0.652
2 (6)	62.58	205.88	10.00	6.261	20.598
3 (4)	4.38	6.01	9.81	0.446	0.613
4 (7)	24.20	70.38	17.10	1.415	4.115
5 (8)	55.09	143.76	8.84	6.233	16.266
6 (5)	6.72	10.65	14.31	0.470	0.745
7 (11)	12.73	4.97	9.38	1.357	0.530
8 (10)	13.13	21.42	25.08	0.524	0.854
9 (13)	1.80	2.01	10.37	0.174	0.194
10 (15)	27.19	62.43	9.10	2.989	6.863
11 (16)	28.61	126.81	14.93	1.917	8.496
12 (18)	10.27	12.14	19.06	0.539	0.637
13 (19)	49.35	194.76	11.49	4.297	16.954
14 (20)	29.60	42.52	33.46	0.885	1.271
15 (12)	14.37	18.62	43.66	0.329	0.427
16 (14)	8.44	10.78	23.19	0.364	0.465
17 (17)	82.54	217.08	80.25	1.029	2.705
18 (3)	94.59	392.50	53.59	1.765	7.324
19 (2)	39.16	62.39	33.09	1.183	1.885
20 (9)	39.78	67.02	33.72	1.180	1.988
			Mean	1.695	4.679
			σ	1.847	6.274

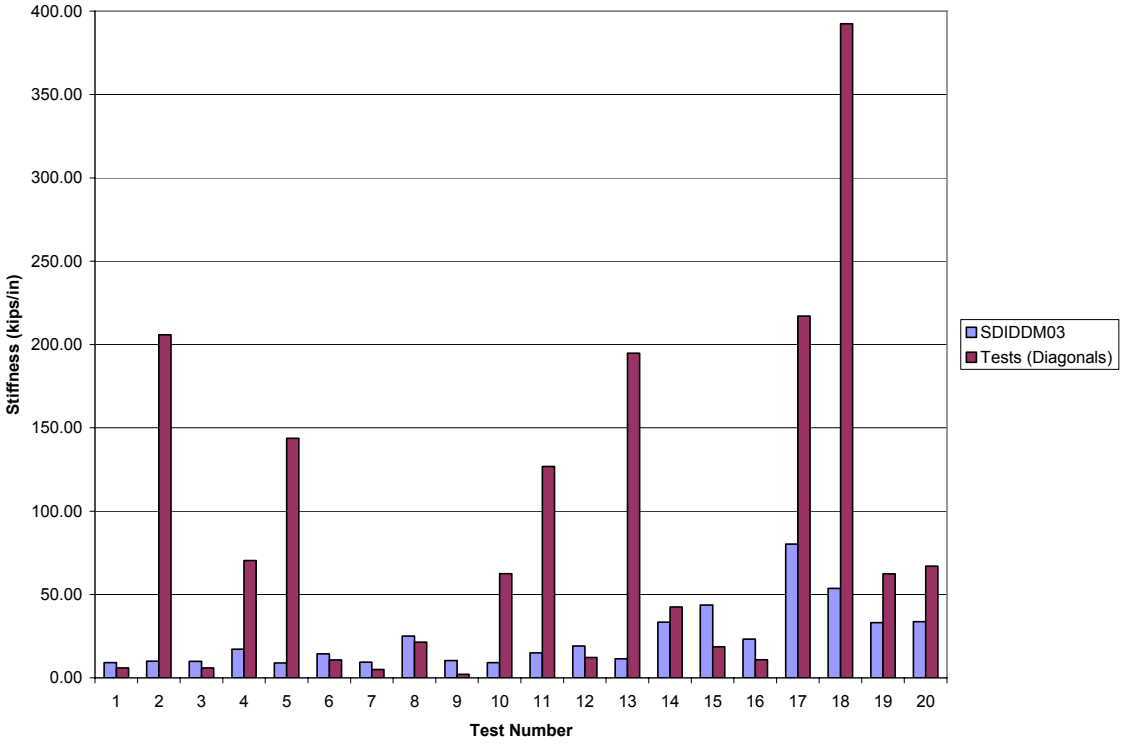

Figure 4-16: Stiffness Comparison, SDIDDM03 versus Test (Diagonals)

4.3.4 Comparison of White Paper Calculated Stiffness to Observed Stiffness

If one observes the comparison of the white paper (Luttrell, 2005) with the observed stiffness based on the diagonal measurements in Fig 4-17 it is evident that there is a high variability in the results. As can be seen in Fig 4-17 the observed stiffness, based on diagonal measurements, has a tendency to dramatically exceed the calculated values based on the white paper (Luttrell, 2005). For the statistical comparison of the white paper stiffness to both stiffness observed from the corner displacements and the diagonal displacements refer to Table 4-11.

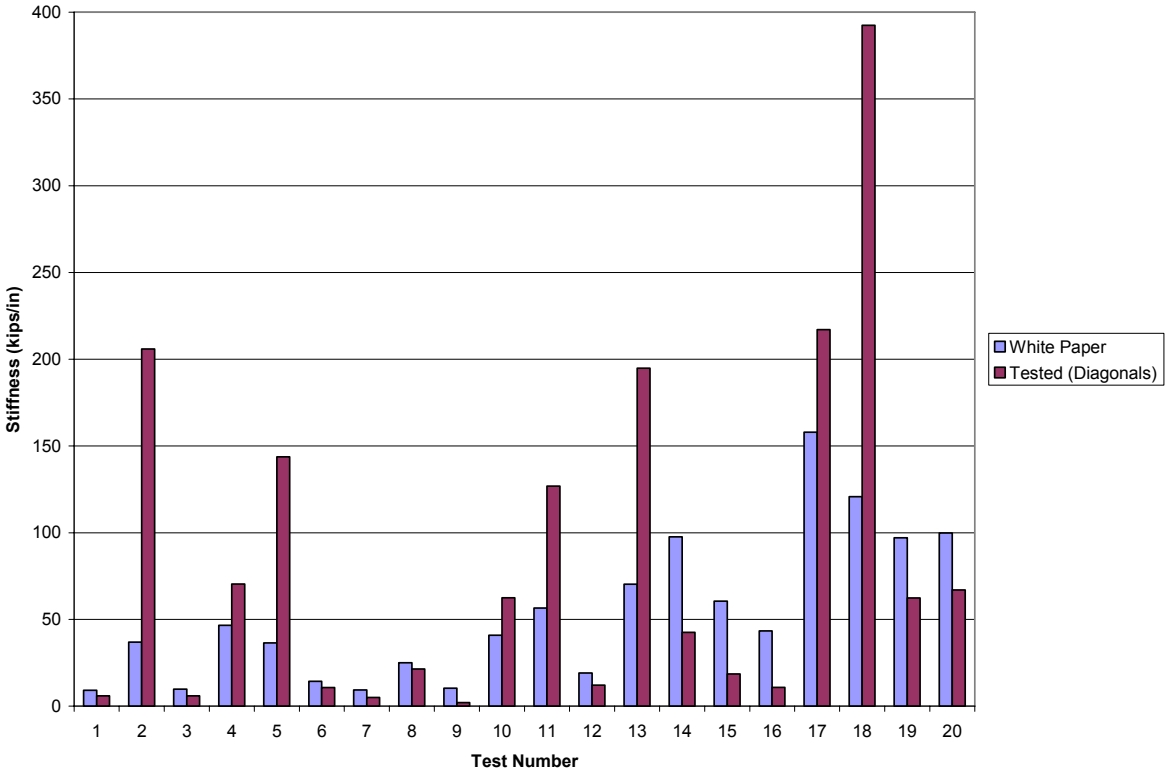

Figure 4-17: Stiffness Comparison, White Paper versus Test (Diagonals)

If now comparison of the statistical results of the white paper to the diagonal observed stiffness is done it is seen that there is a mean ratio greater than 1.0. This shows a better trend however, the standard deviation is almost exactly the same as the mean which shows large variation in the test results. If the same comparison is done with the white paper and the observed stiffness from corner displacements it can be seen that there is a mean less than 1.0 indicating an trend of results less than the calculated results. Also with this comparison the standard deviation shows a large variation in the results. The current SDI calculation procedure was developed based upon the use of a corner observed stiffness. This should make the results for the corner observed stiffness match better with the tested results. Even with this data that is inconsistent for the diaphragm stiffness it can be seen that calculated stiffness from the observed diagonal displacements is valid and could potentially be a better alternative to measuring corner displacements.

Table 4-11: White Paper Stiffness Comparison with Statistics

Test No.	Stiffness (kips/in)			Ratio Test (Diag)/White Paper	Ratio Test (Corner)/White Paper
	Diagonals	Corner	White Paper		
1 (1)	5.94	4.92	9.11	0.652	0.540
2 (6)	205.88	62.58	36.97	5.569	1.693
3 (4)	6.01	4.38	9.81	0.613	0.446
4 (7)	70.38	24.20	46.58	1.511	0.520
5 (8)	143.76	55.09	36.43	3.946	1.512
6 (5)	10.65	6.72	14.31	0.745	0.470
7 (11)	4.97	12.73	9.38	0.530	1.357
8 (10)	21.42	13.13	25.08	0.854	0.523
9 (13)	2.01	1.80	10.37	0.194	0.174
10 (15)	62.43	27.19	40.85	1.528	0.666
11 (16)	126.81	28.61	56.52	2.244	0.506
12 (18)	12.14	10.27	19.06	0.637	0.539
13 (19)	194.76	49.35	70.29	2.771	0.702
14 (20)	42.52	29.60	97.58	0.436	0.303
15 (12)	18.62	14.37	60.58	0.307	0.237
16 (14)	10.78	8.44	43.36	0.249	0.195
17 (17)	217.08	82.54	157.95	1.374	0.523
18 (3)	392.50	94.59	120.77	3.250	0.783
19 (2)	62.39	39.16	97.02	0.643	0.404
20 (9)	67.02	39.78	99.86	0.671	0.398
			Mean	1.436	0.625
			σ	1.435	0.420

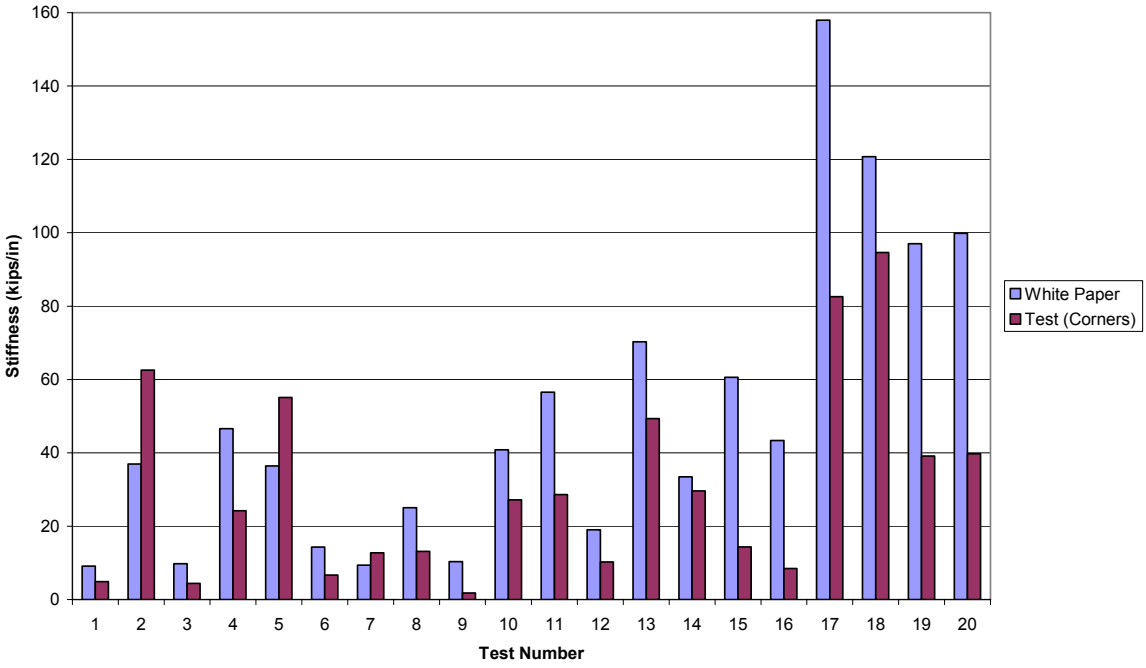

Figure 4-18: Stiffness Comparison, White Paper versus Test (Corners)

If the button punch stiffness equation is found to not be an accurate prediction of the true stiffness the statistical data for all of these comparison will be affected. Since tests 15 and 16 had a button punch side-lap connection each test was seen to be a statistical outlier. The mean for each comparison with tests 15 and 16 excluded will generally increase and the standard deviation will decrease

4.3.5 Recommended Modifications to Stiffness Evaluation

The shear stiffness of the diaphragm configurations tested in this study were calculated using the SDIDDM03 (Luttrell, 2004) and the white paper (Luttrell, 2005). As can be seen from the comparison results there is a correlation between the white paper results and the tested results from diagonal observed stiffness. The original SDIDDM03 comparison with the tested results from the corner observed stiffness seems to have close to the same correlation as the diagonal observed stiffness with the white paper. The

deflection numbers being used to determine the diaphragm stiffness, based on the corner displacements, are small numbers. This causes the stiffness measurements to be very sensitive and consequentially difficult to ascertain their true value. Measuring the diagonal displacements of a diaphragm is much easier and is not nearly as sensitive as measuring the corner displacements. More testing needs to be done to find a correct correlation between tested stiffness and predicted stiffness.

CHAPTER 5 – SUMMMARY, CONCLUSIONS, AND RECOMMENDATIONS

5.1 Summary

The purpose of this study was to compare the tested strength and stiffness of deep deck and cellular deck profiles to the modifications of the SDIDDM03 as proposed by Luttrell (2005). In this test program a total of 20 diaphragms were constructed and loaded to failure. Seven of the tests were performed on N-deck profiles, ten tests were performed on cellular profiles and three tests were performed on 2 x N deck profiles. The fastener types and configurations were varied between the tests. These variations were done to check the side-lap fastener strength and the structural fastener strength. Because of the strength of the diaphragms being tested no attempts were made to check the stability portion of the SDIDDM03 (Luttrell, 2004).

The stiffness of the diaphragms was also examined to determine their relationship with the SDI white paper (Luttrell, 2005). Measurements of both the corner and the diagonal displacements of the diaphragm were taken. These measurements were used with the ICC evaluation procedure to determine the diaphragm stiffness. A comparison was made between the corner and diagonal displacements as well as the SDIDDM03 (Lutttrell, 2004) and the white paper (Luttrell, 2005) to show the different stiffness reported for each diaphragm.

5.2 Conclusions

Concerning diaphragm strength the experimental results indicate that the SDIDDM03 (Luttrell, 2004) calculation procedure produces lower results than the testing indicated. With the current connection strength equations the typical controlling limit state was bearing. This is indicated by the focus on the sheet material properties as opposed to the connector properties. By adding a shear limitation onto the connection strength equations the predicted results were changed in some cases dramatically. The calculations in many cases were changed to values much more representative of the

tested values. For each of the connections tested in this study the shear limitation was obtained from the manufacturer of the respective connector.

With displacements of a diaphragm there are many factors to take into consideration. Some of the major contributors that can skew data are frame distortions, connection quality and data acquisition sensitivity. Frame distortions can occur from the loading of the diaphragm system. Any movement or buckling of the web, since all measurements for the corners are taken at the midpoint of the web, can cause slight changes in the deflection readings. Also with the corner measurements many of the readings are going to be small even under large loads. With such small numbers accurate data acquisition can be more difficult.

After comparing the stiffness calculated for both the corner and diagonal displacements a comparison was made. When a comparison was made with the SDIDDM03 (Luttrell, 2004) and the tested corner observed stiffness a relatively good trend was seen. Approximately the same statistical correlation was found with the white paper (Luttrell, 2005) and the diagonal observed stiffness. Neither comparison was completely conclusive but this could have come from the many variables involved in determining the diaphragm stiffness.

5.3 Recommendations

When it comes to strength modifications there are some for each type of fastener that were used in this test program. The fasteners that modifications are recommended for are: screws, pins, welds and button punch. Each fastener type is discussed with suggestions about the modification method given where needed.

With the screw fasteners a minor modification needs to done. A limitation needs to be placed on the screw strength equation that does not allow the force in the connection to exceed the shear strength of the connector. This however could potentially be a tricky task for one reason. In the AISI (2001) the different screw strength calculations are based on the physical dimensions of things like the screw head and the screw major diameter. These equations are checking for failures in the sheet metal and not the screw connector. However, for the screw shear strength it is recommended that either the manufacturer be contacted or independent testing be done. This implies that

each manufacturer produces their screws from different grades of materials and could have variable shear strength.

The pin strength equations in the SDIDDM03 (Luttrell, 2004) are based on the sheet metal thickness alone. A shear limitation is also needed for these equations but a similar problem to the screw shear limitation exists. The problem here is easily solved because there are many different equations for pin strength that are based on the model of pin being used. This means that the shear strength of each pin could easily be placed by the equation as an upper bound. This would eliminate the problem of designers using erroneously high strength values which would create more accurate diaphragm designs.

The weld strength equations in the SDIDDM03 (Luttrell, 2004) are the same as one of the shear strength equations present in the AISI (2001). This equation does control diaphragm design as long as certain assumptions are made. However, if there are different values than the typical assumptions then there is the potential for other limit states to control. There are dimensional limits that control shear related to the diaphragm material and there are also shear limitations related to the weld material only. For the three tests performed in this study the equation currently present in the SDIDDM03 (Luttrell, 2004) did not control.

For making general assumptions about diaphragm design the current equation in the SDIDDM03 is not bad. However, if forensic analysis or research is being done as in this study the scope of the weld shear equations must be broadened. The AISI equations that applied to this project brought the predicted strengths closer to the observed strengths from the tests as can be seen in Figure 4-4.

The button punch strength equations in the SDIDDM03 need to be reinvestigated. The current equation predicts that as the thickness of the sheet material increases there is a quadratic increase in strength. As was shown, there is a distinct difference in the calculated strength and stiffness of the button punch and the tested strength and stiffness.

When it comes to stiffness evaluation, a modification to the white paper is difficult to make. With the limited number of tests performed, a true trend is difficult to ascertain. As can be seen from the comparison results there is not a good correlation between the white paper results and the tested results. The SDIDDM03 comparison with the tests seems to have approximately the same correlation. The deflection numbers being

used to determine the diaphragm stiffness, based on the corner displacements, are small numbers. This causes the stiffness measurements to be very sensitive and consequentially difficult to ascertain their true value. More testing needs to be done to find a correct correlation between tested stiffness and predicted stiffness.

REFERENCES

Ameen, A. (1990) "Cold-Formed Steel Diaphragms with End Closures," Department of Civil Engineering, West Virginia University

AISI (1967), Design of Light Gage Steel Diaphragms , Washington, DC.

AISI (2002),"Cantilever Test Method for Cold-Formed Steel Diaphragms," TS-7-02, Washington, DC.

AISI (2001),"North American Specification for the Design of Cold-Formed Steel Structural Members," Washington, DC.

ASTM (2004), "ASTM E8-04: Standard Test Method for Tension Testing of Metallic Materials", Annual Book of ASTM Standards, 03.01, 62-85.

Apparao, T. V. S. R. (1966) "Tests on Light Gage Steel Diaphragms", Report No. 328, Department of Structural Engineering, Cornell University, Ithaca, NY

Bryan, E. R. (1972) "The Stressed Skin Design of Steel Buildings." Crosby Lockwood Staples, London, England, 159.

Davies, J.M. (1974) "The Design of Shear Diaphragms of Corrugated Steel Sheeting." Department of Civil Engineering, University of Salford, Salford, England, Report No. 74/50.

Ellifritt, D.S. and Luttrell L.D. (1970), "Strength and Stiffness of Steel Deck Subjected to In-plane Loading," Report No. 2011, Department of Civil Engineering, West Virginia University, Morgantown, WV

Fazio, P. Ha K. and Chockalingam, S. (1979) Strength of cold-formed steel shear diaphragms, Canadian Journal of Civil Engineering. 6(1), 5-17.

Glatt, C. (1990) "A Comparison of Steel Deck Diaphragm Design Methods: Tri-Services Manual vs. Steel Deck Institute Manual," Report, Civil Engineering Department, University of Kansas, Lawrence, KS.

ICC Evaluation Service (2006) "Acceptance Criteria for Steel Deck Roof and Floor Systems," AC43, Whittier, California.

Luttrell, L.D.,(1965a) "Structural Performance of Light Gage Steel Diaphragms", Report No. 319, Department of Structural Engineering, Cornell University, Ithaca, NY.

Luttrell, L.D.,(1965b) Light Gage Steel Shear Diaphragms, Civil Engineering Department Publication, West Virginia University, Morgantown, WV.

Luttrell, L.D., (1967) "Strength and Behavior of Light Gage Steel Shear Diaphragms", Report No. 67-1, Department of Structural Engineering, Cornell University, Ithaca, NY.

Luttrell, L.D., (1981) "Steel Deck Institute Diaphragm Design Manual", First Edition, Steel Deck Institute.

Luttrell, L.D., (1987) "Steel Deck Institute Diaphragm Design Manual", Second Edition, Steel Deck Institute.

Luttrell, L.D., (2004) "Steel Deck Institute Diaphragm Design Manual", Third Edition, Steel Deck Institute.

Luttrell, L.D.,(2005) "Deeper Steel Deck and Cellular Diaphragms", Steel Deck Institute white paper.

Nilson, A.H., (1956), Deflection of Light Gage Steel Floor Systems Under Action of Horizontal Loads, Thesis, Cornell University, Ithaca, NY.

Nilson, A.H., (1960a) "Shear Diaphragms of Light Gage Steel", Journal of the Structural Division, ASCE, 86(11), 111-139.

Nilson, A.H.,(1960b) "Diaphragm Action in Light Gage Steel Construction," American Iron and Steel Institute.

Nilson, A.H., (1969a) "H.H. Robertson DC Deck Used in Shear Diaphragms," Test 69-1, Cornell University, Ithaca, NY.

Nilson, A.H., (1969b) "H.H. Robertson DC Deck Used in Shear Diaphragms," Test 69-2, Cornell University, Ithaca, NY.

Seismic Design for Buildings, Tri-Services Manual,(1982) (TM 5-809-10; NAVFAC P-355; AFM 88-3, Chapter 13), U.S. Government Printing Office, Philadelphia, PA.

S.B. Barnes Associates for R.C. Mahon, (1959) "Test Program on Mahon Steel Decks…Used as Diaphragms,", Detroit, 34, Michigan.

APPENDIX A – DIAPHRAGM TEST RESULTS

In the following section a presentation of the test results that were observed is given. Each of the diaphragm test specimens were subjected to a single load at Corner C. This load was meant to represent a static load that causes shear forces on the diaphragm. All together 20 different diaphragm tests were performed. These tests had variations in profile, thickness, material strength, and connection configuration.

For each test a summary of the section properties and configurations are included. The tabulated data that the graphs are derived from is included on a CD located at the back of this document. The data for each of the diaphragm tests will include the deflections read by the displacement transducers and the load readings from the load cell. For each of the displacement transducers the positive direction sign convention can be found in Figure 3-11. Also included in each of these tabulated values are the corrected deflections for both the corner displacement transducers and the diagonal displacement transducers. Also a list of the corresponding values for the bare frame at the appropriate deflections for each test is present to determine the maximum load resisted by the diaphragm itself.

Test 1:

Wheeling 4.5 in 20 Ga. – Screw Test

Diaphragm Setup:

Width:	24 ft
Span:	24 ft
No. of Panels	12
Structural Connection	#12 TEK Screw/rib at ends #12 TEK Screw/ft at sides
Side-lap Fastener	#12 TEK Screw @ 36 in o/c

Steel Deck:

Measured Thickness:	0.0365 in
Deck Height:	4.5 in
F_y = 107 ksi	F_u = 109 ksi

Results

Maximum Applied Load:		11905 lbs
Deflection at Max. Load:	Corners	3.934 in
	Diagonals	3.702 in
Design Load:	Corners	10749 lbs
	Diagonals	11019 lbs
Stiffness Evaluation:	Corners	4.919 kips/in
	Diagonals	5.939 kips/in
Deflection for Stiffness Determination:		
	Corners	0.733 in
	Diagonals	0.653 in
Observed Failure Limit State:	Side Lap Fastener	

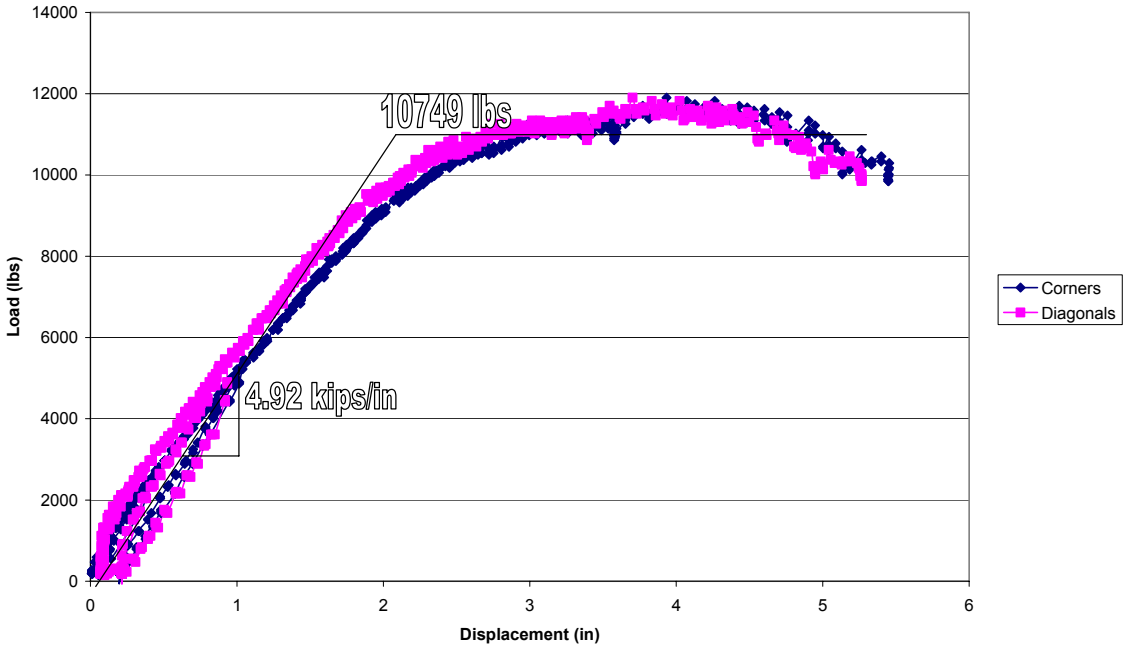

Figure A-1: Load vs. Displacement
Wheeling 4.5 in 20 Ga.

Test 2:

United Steel Deck 4.5 in 20/20 Ga. – Screw Test

Diaphragm Setup:

Width:	24 ft
Span:	24 ft
No. of Panels	12
Structural Connection	#12 TEK Screw/rib at ends #12 TEK Screw/ft at sides
Side-lap Fastener	#12 TEK Screw @ 36 in o/c

Steel Deck:

Measured Thickness:	0.0359 in
Deck Height:	4.5 in
F_y = 48 ksi	F_u = 58 ksi

Results

Maximum Applied Load:		11865 lbs
Deflection at Max. Load:	Corners	2.831 in
	Diagonals	2.758 in
Design Load:	Corners	11311 lbs
	Diagonals	11311 lbs
Stiffness Evaluation:	Corners	62.58 kips/in
	Diagonals	205.88 kips/in
Deflection for Stiffness Determination:		
	Corners	0.067 in
	Diagonals	0.020 in
Observed Failure Limit State:	Side Lap Fastener	

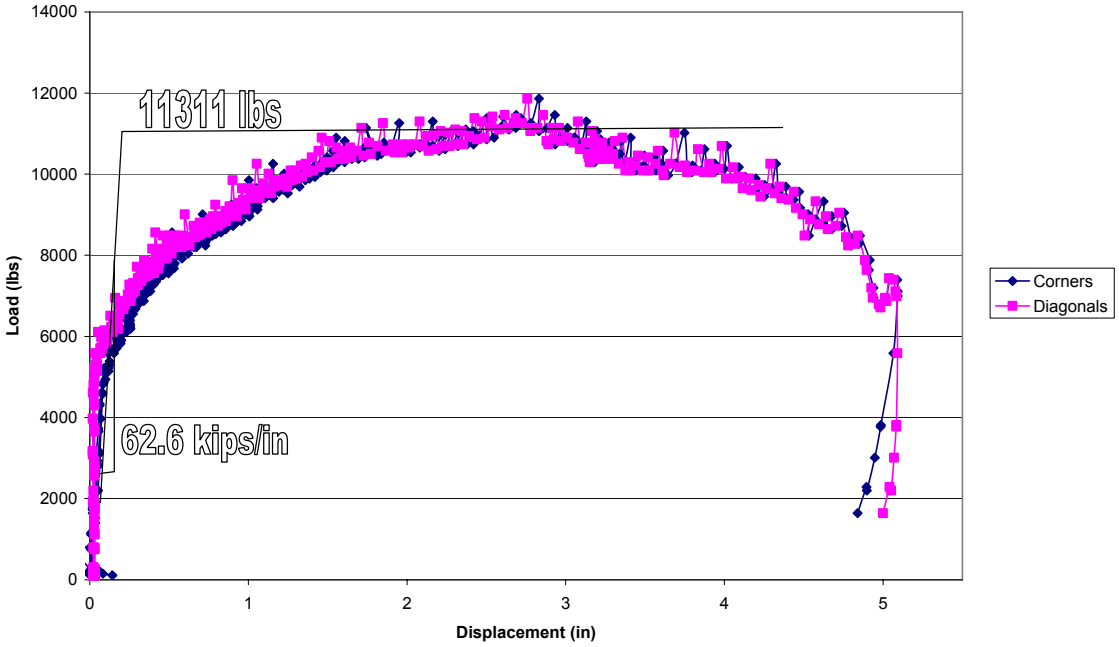

Figure A-2: Load vs. Displacement
United Steel Deck 4.5 in 20/20 Ga.

Test 3:

Consolidated Systems 7.5 in 18 Ga. – Screw Test

Diaphragm Setup:

Width:	24 ft
Span:	24 ft
No. of Panels	24
Structural Connection	#12 TEK Screw/rib at ends #12 TEK Screw/ft at sides
Side-lap Fastener	#12 TEK Screw @ 36 in o/c

Steel Deck:

Measured Thickness:	0.0465 in
Deck Height:	7.5 in
F_y = 50 ksi	F_u = 61 ksi

Results

Maximum Applied Load:		9288 lbs
Deflection at Max. Load:	Corners	5.119 in
	Diagonals	4.956 in
Design Load:	Corners	8091 lbs
	Diagonals	8011 lbs
Stiffness Evaluation:	Corners	4.38 kips/in
	Diagonals	6.01 kips/in
Deflection for Stiffness Determination:		
	Corners	0.575 in
	Diagonals	0.405 in
Observed Failure Limit State:	Side Lap Fastener	

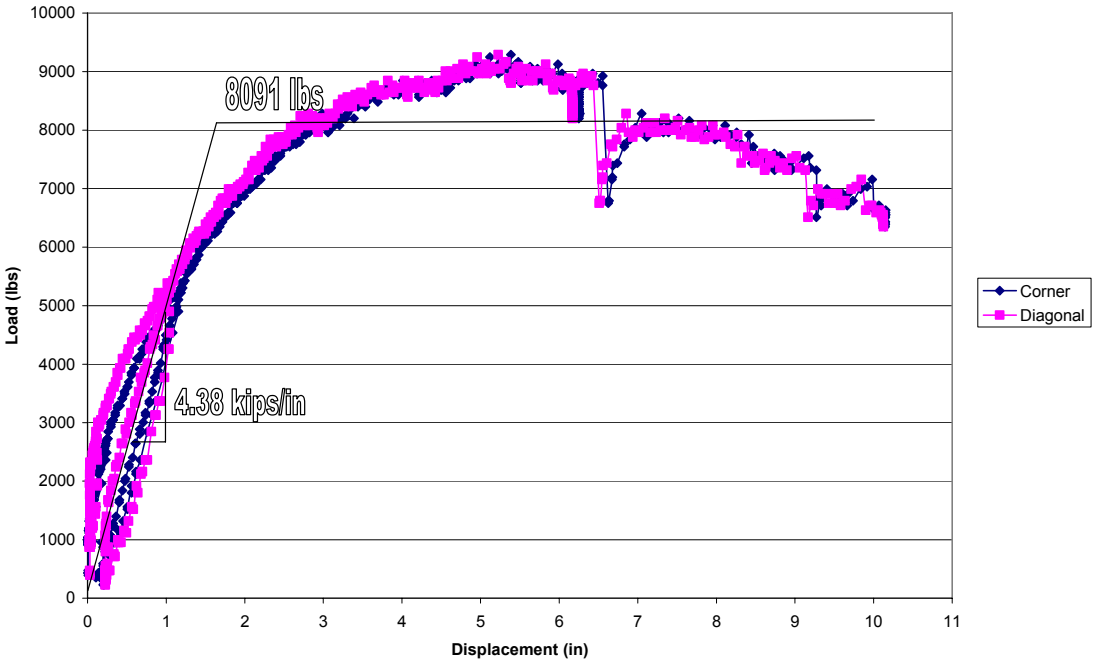

Figure A-3: Load vs. Displacement
Consolidated Systems 7.5 in 18 Ga.

Test 4:

United Steel Deck 4.5 in 18/18 Ga. – Screw Test

Diaphragm Setup:

Width:	24 ft
Span:	24 ft
No. of Panels	12
Structural Connection	#12 TEK Screw/rib at ends #12 TEK Screw/ft at sides
Side-lap Fastener	#12 TEK Screw @ 36 in o/c

Steel Deck:

Measured Thickness:	0.0472 in
Deck Height:	4.5 in
F_y = 48 ksi	F_u = 60 ksi

Results

Maximum Applied Load:		13434 lbs
Deflection at Max. Load:	Corners	2.365 in
	Diagonals	2.119 in
Design Load:	Corners	12962 lbs
	Diagonals	13002 lbs
Stiffness Evaluation:	Corners	24.20 kips/in
	Diagonals	70.38 kips/in
Deflection for Stiffness Determination:		
	Corners	0.203 in
	Diagonals	0.070 in
Observed Failure Limit State:	Side Lap Fastener	

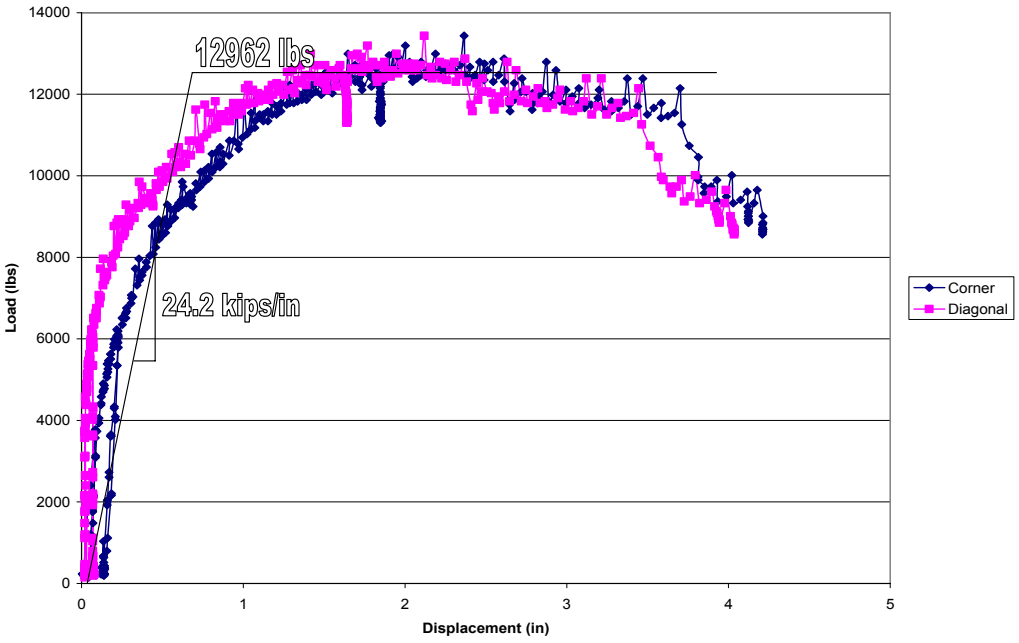

Figure A-4: Load vs. Displacement
United Steel Deck 4.5 in 18/18 Ga.

Test 5:

United Steel Deck 7.5 in 18/20 Ga. – Screw Test

Diaphragm Setup:

Width:	24 ft
Span:	24 ft
No. of Panels	12
Structural Connection	#12 TEK Screw/rib at ends #12 TEK Screw/ft at sides
Side-lap Fastener	#12 TEK Screw @ 36 in o/c

Steel Deck:

Measured Thickness:	0.0475 in/ 0.0358 in
Deck Height:	7.5 in
F_y = 48 ksi	F_u = 59 ksi

Results

Maximum Applied Load:		14723 lbs
Deflection at Max. Load:	Corners	3.190 in
	Diagonals	3.043 in
Design Load:	Corners	14089 lbs
	Diagonals	14089 lbs
Stiffness Evaluation:	Corners	55.09 kips/in
	Diagonals	143.76 kips/in
Deflection for Stiffness Determination:		
	Corners	0.095 in
	Diagonals	0.037 in
Observed Failure Limit State:	Side Lap Fastener	

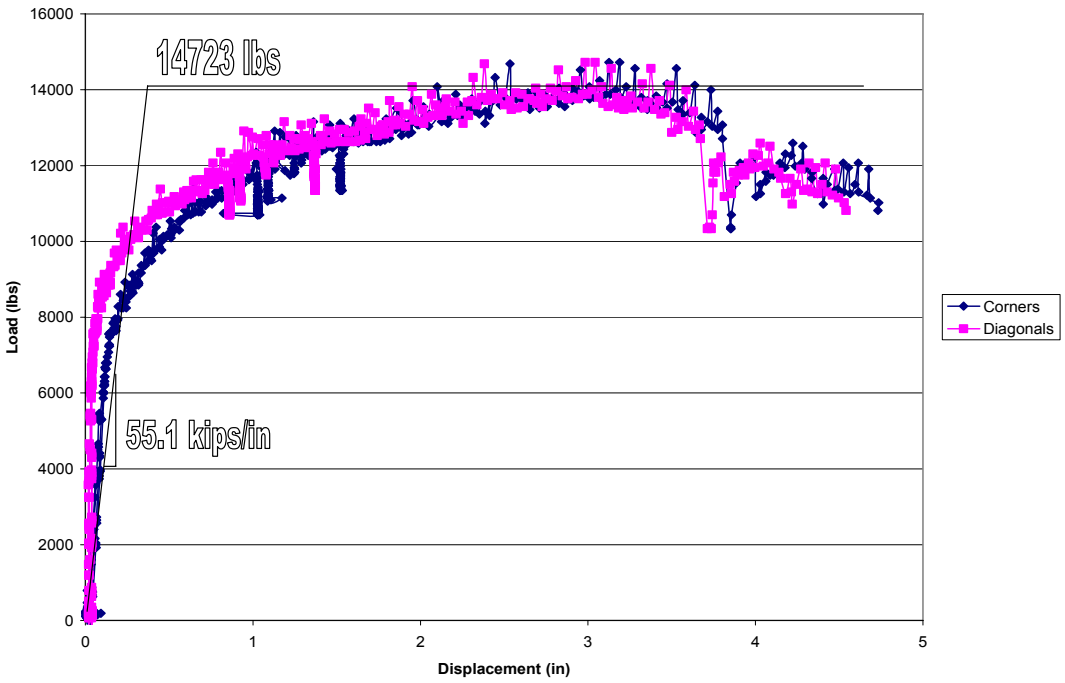

Figure A-5: Load vs. Displacement
United Steel Deck 7.5 in 18/20 Ga.

Test 6:

Consolidated Systems 7.5 in 16 Ga. – Screw Test

Diaphragm Setup:

Width:	24 ft
Span:	24 ft
No. of Panels	24
Structural Connection	#12 TEK Screw /rib at ends #12 TEK Screw /ft at sides
Side-lap Fastener	#12 TEK Screw @ 36 in o/c

Steel Deck:

Measured Thickness:	0.0595 in
Deck Height:	7.5 in
F_y = 44 ksi	F_u = 60 ksi

Results

Maximum Applied Load:		12227 lbs
Deflection at Max. Load:	Corners	3.830 in
	Diagonals	3.628 in
Design Load:	Corners	11311 lbs
	Diagonals	11311 lbs
Stiffness Evaluation:	Corners	6.72 kips/in
	Diagonals	10.65 kips/in
Deflection for Stiffness Determination:		
	Corners	0.591 in
	Diagonals	0.373 in
Observed Failure Limit State:	Side Lap Fastener	

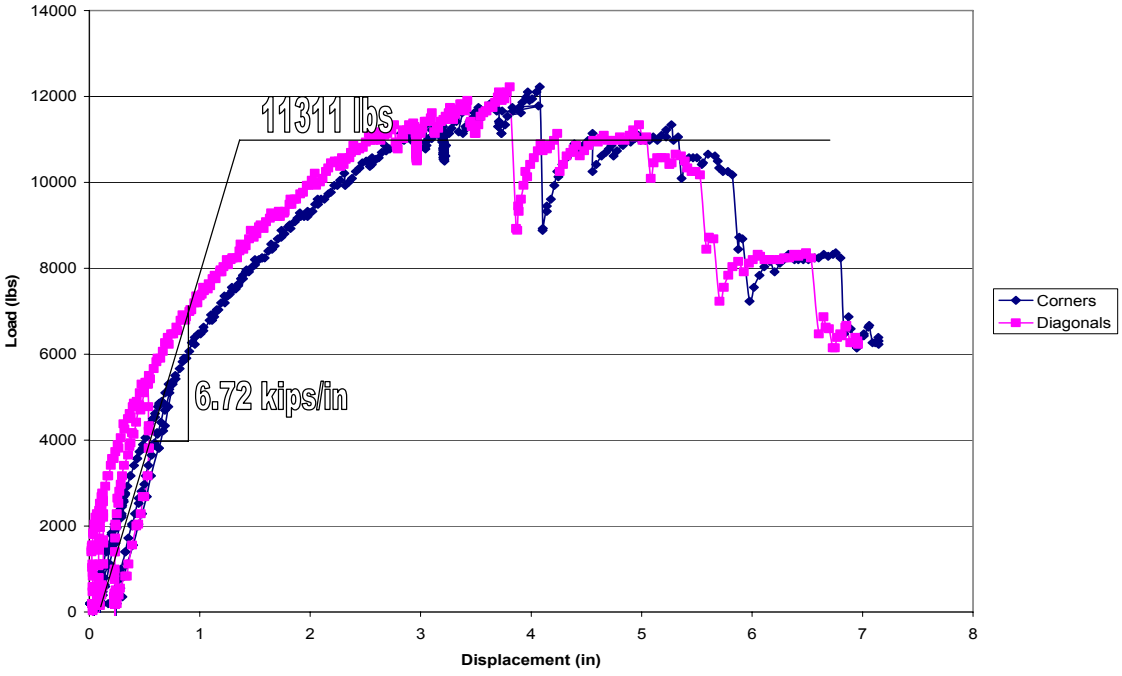

Figure A-6: Load vs. Displacement
Consolidated Systems 7.5 in 16 Ga.

Test 7:

Wheeling 4.5 in 20 Ga. – Pin Test

Diaphragm Setup:

Width:	24 ft
Span:	24 ft
No. of Panels	12
Structural Connection	Hilti Pin X-ENP-19 L15/rib at ends Hilti Pin X-ENP-19 L15/ft at sides
Side-lap Fastener	#12 TEK Screw @ 36 in o/c

Steel Deck:

Measured Thickness:	0.0360 in
Deck Height:	4.5 in
F_y = 108 ksi	F_u = 110 ksi

Results

Maximum Applied Load:		11985 lbs
Deflection at Max. Load:	Corners	1.983 in
	Diagonals	3.715 in
Design Load:	Corners	11593 lbs
	Diagonals	11110 lbs
Stiffness Evaluation:	Corners	12.73 kips/in
	Diagonals	4.97 kips/in
Deflection for Stiffness Determination:		
	Corners	0.346 in
	Diagonals	0.788 in
Observed Failure Limit State:	Side Lap Fastener	

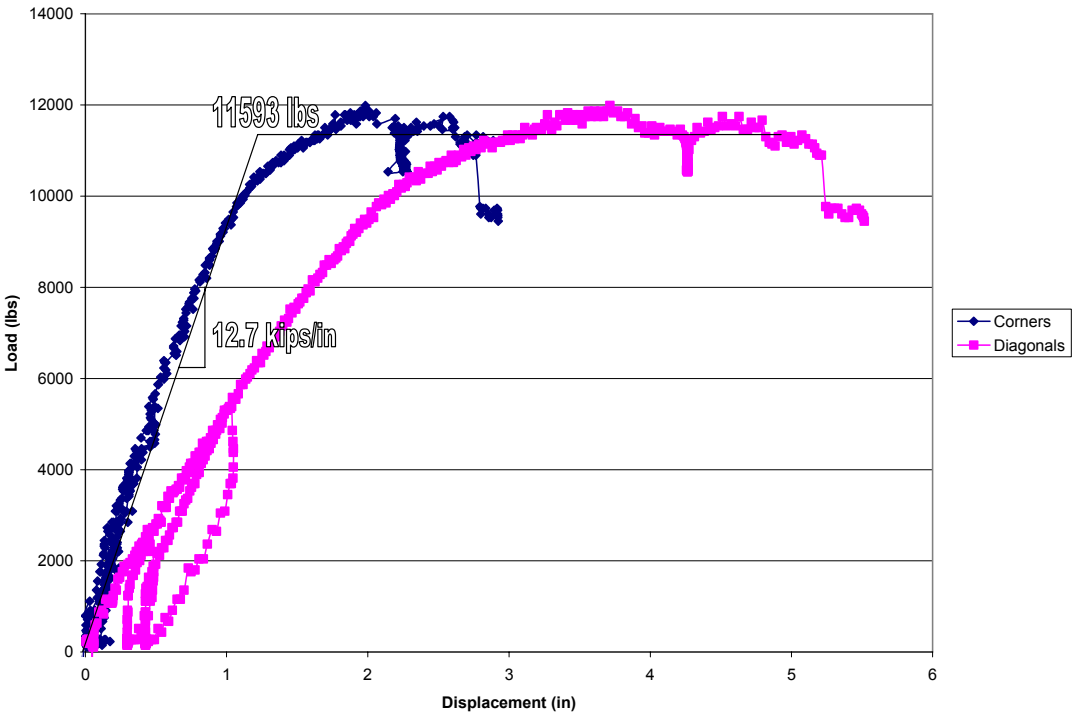

Figure A-7: Load vs. Displacement
Wheeling 4.5 in 20 Ga.

Test 8:

Wheeling 4.5 in 16 Ga. – Pin Test

Diaphragm Setup:

Width:	24 ft
Span:	24 ft
No. of Panels	12
Structural Connection	Hilti Pin X-ENP-19 L15/rib at ends Hilti Pin X-ENP-19 L15/ft at sides
Side-lap Fastener	#12 TEK Screw @ 36 in o/c

Steel Deck:

Measured Thickness:	0.0590 in
Deck Height:	4.5 in
F_y = 91 ksi	F_u = 92 ksi

Results

Maximum Applied Load:		12831 lbs
Deflection at Max. Load:	Corners	1.277 in
	Diagonals	1.077 in
Design Load:	Corners	12831 lbs
	Diagonals	12831 lbs
Stiffness Evaluation:	Corners	13.13 kips/in
	Diagonals	21.42 kips/in
Deflection for Stiffness Determination:		
	Corners	0.391 in
	Diagonals	0.240 in
Observed Failure Limit State:	Side Lap Fastener	

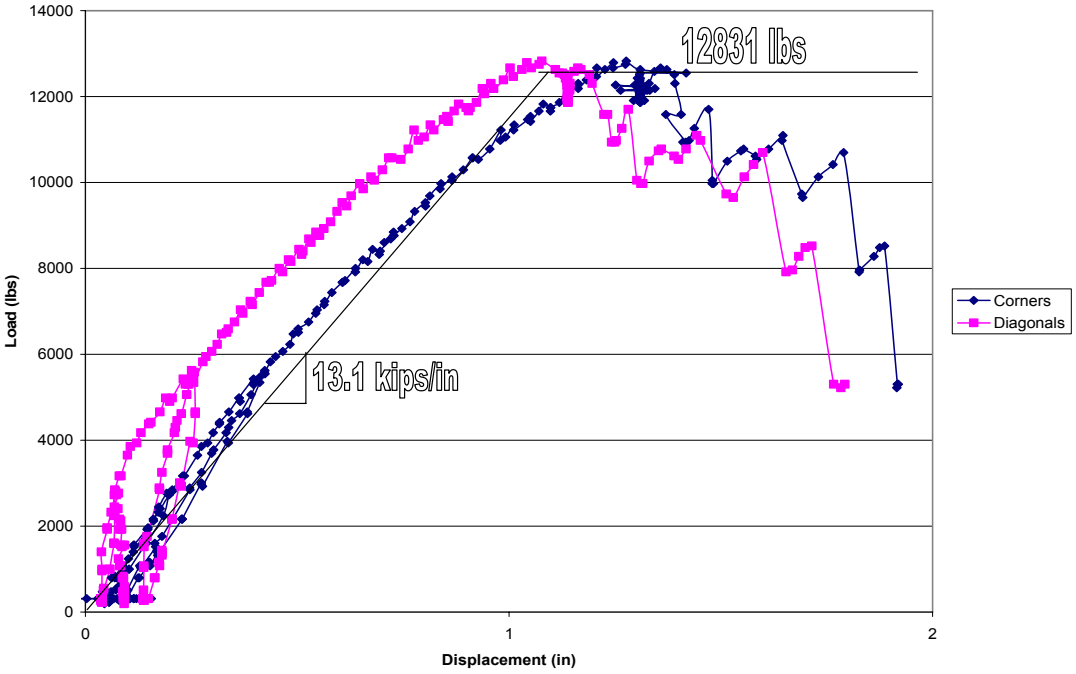

Figure A-8: Load vs. Displacement
Wheeling 4.5 in 16 Ga.

Test 9:

Consolidated Systems 7.5 in 18 Ga. – Pin Test

Diaphragm Setup:

Width:	24 ft
Span:	24 ft
No. of Panels	24
Structural Connection	Hilti Pin X-ENP-19 L15/rib at ends Hilti Pin X-ENP-19 L15/ft at sides
Side-lap Fastener	#12 TEK Screw @ 36 in o/c

Steel Deck:

Measured Thickness:	0.0460 in
Deck Height:	7.5 in
F_y = 50 ksi	F_u = 61 ksi

Results

Maximum Applied Load:		9530 lbs
Deflection at Max. Load:	Corners	6.604 in
	Diagonals	6.426 in
Design Load:	Corners	8131 lbs
	Diagonals	8131 lbs
Stiffness Evaluation:	Corners	1.80 kips/in
	Diagonals	2.01 kips/in
Deflection for Stiffness Determination:		
	Corners	1.340 in
	Diagonals	1.200 in
Observed Failure Limit State:	Side Lap Fastener	

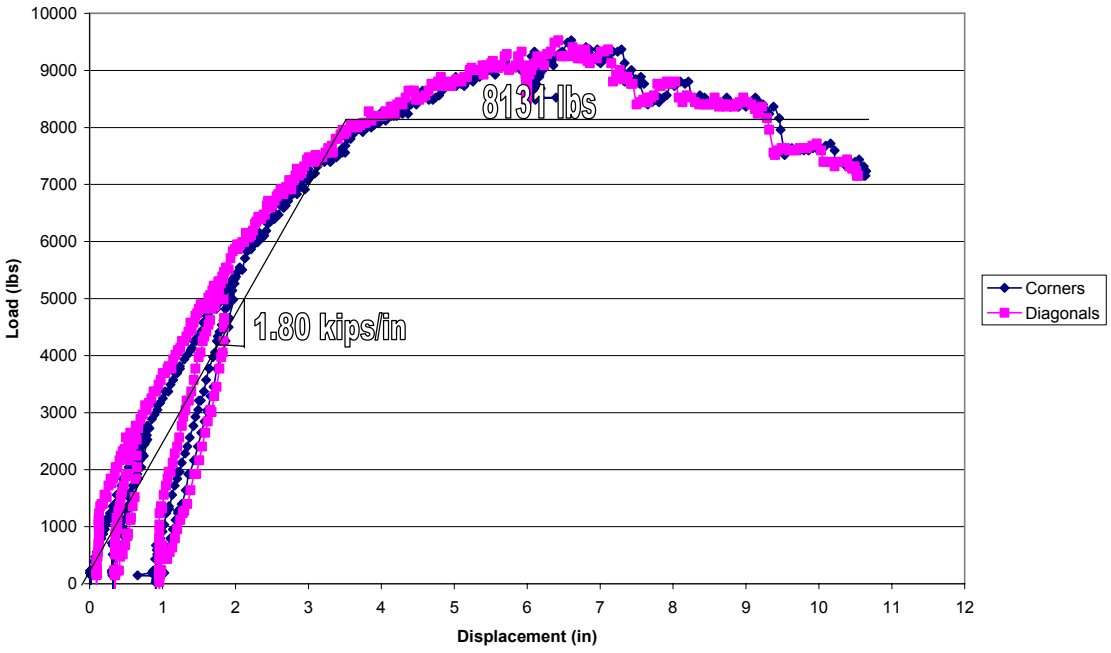

Figure A-9: Load vs. Displacement
Consolidated Systems 7.5 in 18 Ga.

Test 10:

United Steel Deck 7.5 in 18/20 Ga. – Pin Test

Diaphragm Setup:

Width:	24 ft
Span:	24 ft
No. of Panels	12
Structural Connection	Hilti Pin X-ENP-19 L15/rib at ends Hilti Pin X-ENP-19 L15/ft at sides
Side-lap Fastener	#12 TEK Screw @ 36 in o/c

Steel Deck:

Measured Thickness:	0.0474 in/ 0.0358 in
Deck Height:	7.5 in
F_y = 48 ksi	F_u = 59 ksi

Results

Maximum Applied Load:		11865 lbs
Deflection at Max. Load:	Corners	2.111 in
	Diagonals	1.818 in
Design Load:	Corners	11472 lbs
	Diagonals	11865 lbs
Stiffness Evaluation:	Corners	27.19 kips/in
	Diagonals	62.43 kips/in
Deflection for Stiffness Determination:		
	Corners	0.160 in
	Diagonals	0.076 in
Observed Failure Limit State:	Side Lap Fastener	

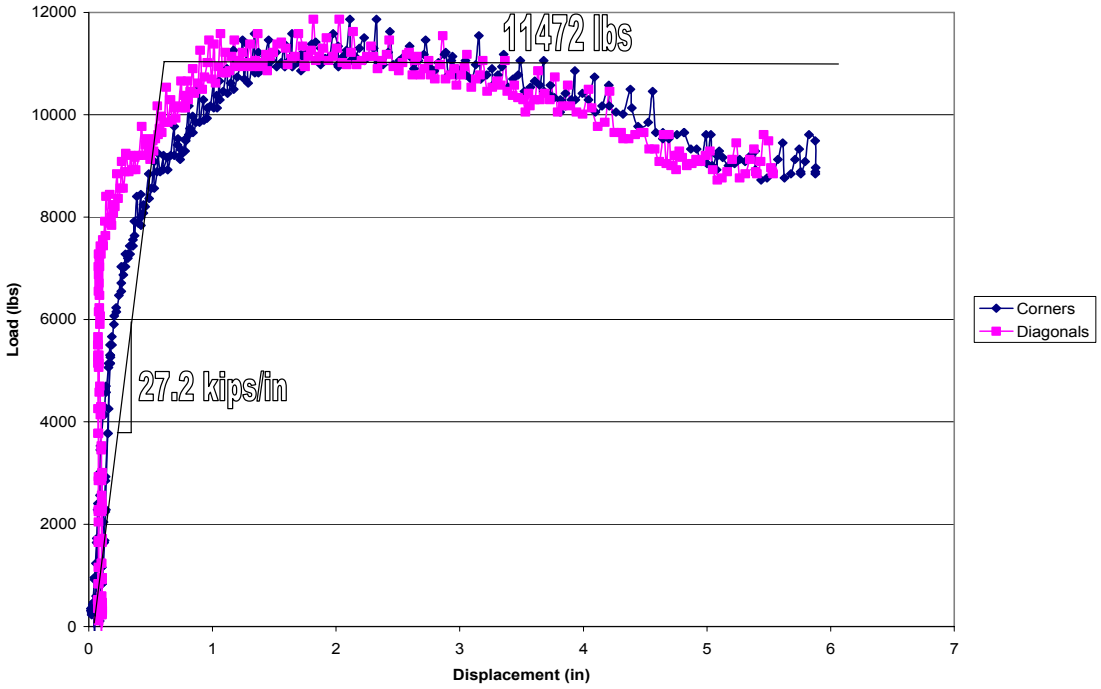

Figure A-10: Load vs. Displacement
United Steel Deck 7.5 in 18/20 Ga.

Test 11:

United Steel Deck 7.5 in 16/18 Ga. – Pin Test

Diaphragm Setup:

Width:	24 ft
Span:	24 ft
No. of Panels	12
Structural Connection	Hilti Pin X-ENP-19 L15/rib at ends Hilti Pin X-ENP-19 L15/ft at sides
Side-lap Fastener	#12 TEK Screw @ 36 in o/c

Steel Deck:

Measured Thickness:	0.0597 in/ 0.0471 in
Deck Height:	7.5 in
F_y = 48 ksi	F_u = 59 ksi

Results

Maximum Applied Load:		10737 lbs
Deflection at Max. Load:	Corners	1.490 in
	Diagonals	1.216 in
Design Load:	Corners	10737 lbs
	Diagonals	10737 lbs
Stiffness Evaluation:	Corners	28.61 kips/in
	Diagonals	126.81 kips/in
Deflection for Stiffness Determination:		
	Corners	0.150 in
	Diagonals	0.034 in
Observed Failure Limit State:	Side Lap Fastener	

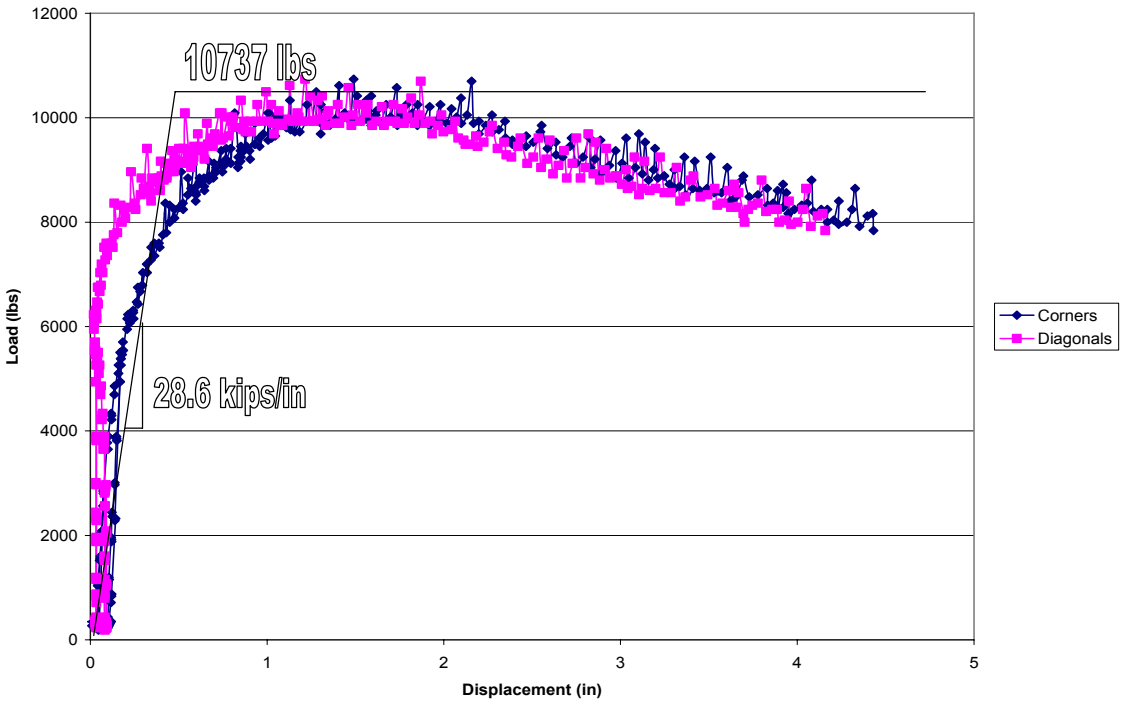

Figure A-11: Load vs. Displacement
United Steel Deck 7.5 in 16/18 Ga.

Test 12:

Wheeling 4.5 in 18 Ga. – Weld Test

Diaphragm Setup:

Width:	24 ft
Span:	24 ft
No. of Panels	12
Structural Connection	¾" Diameter Weld/rib at ends ¾" Diameter Weld/ft at sides
Side-lap Fastener	#12 TEK Screw @ 12 in o/c

Steel Deck:

Measured Thickness:	0.0462 in
Deck Height:	4.5 in
F_y = 95 ksi	F_u = 98 ksi

Results

Maximum Applied Load:		34085 lbs
Deflection at Max. Load:	Corners	4.447 in
	Diagonals	4.179 in
Design Load:	Corners	33064 lbs
	Diagonals	33019 lbs
Stiffness Evaluation:	Corners	10.27 kips/in
	Diagonals	12.14 kips/in
Deflection for Stiffness Determination:		
	Corners	1.228 in
	Diagonals	1.035 in
Observed Failure Limit State:	Structural Fastener	

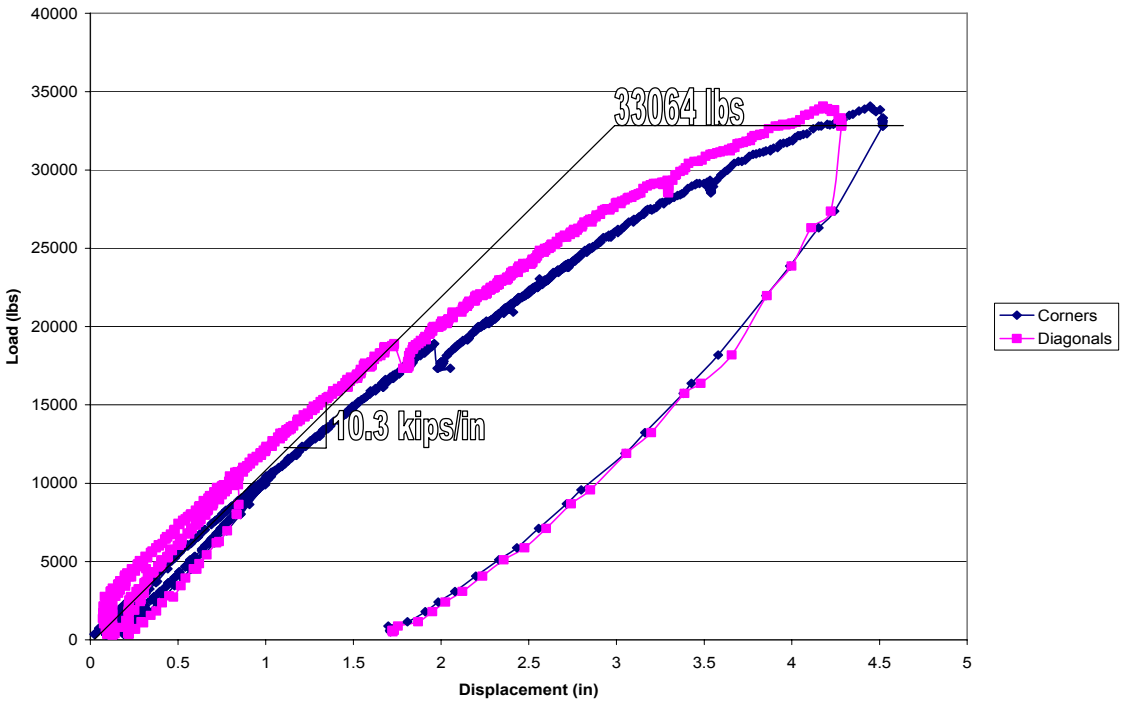

Figure A-12: Load vs. Displacement
Wheeling 4.5 in 18 Ga.

Test 13:

United Steel Deck 4.5 in 20/20 Ga. – Weld Test

Diaphragm Setup:

Width:	24 ft
Span:	24 ft
No. of Panels	12
Structural Connection	¾" Diameter Weld/rib at ends ¾" Diameter Weld/ft at sides
Side-lap Fastener	#12 TEK Screw @ 12 in o/c

Steel Deck:

Measured Thickness:	0.0358 in
Deck Height:	4.5 in
F_y = 48 ksi	F_u = 58 ksi

Results

Maximum Applied Load:		25269 lbs
Deflection at Max. Load:	Corners	1.704 in
	Diagonals	1.464 in
Design Load:	Corners	25269 lbs
	Diagonals	25269 lbs
Stiffness Evaluation:	Corners	49.35 kips/in
	Diagonals	194.76 kips/in
Deflection for Stiffness Determination:		
	Corners	0.205 in
	Diagonals	0.052 in
Observed Failure Limit State:	Structural Fastener	

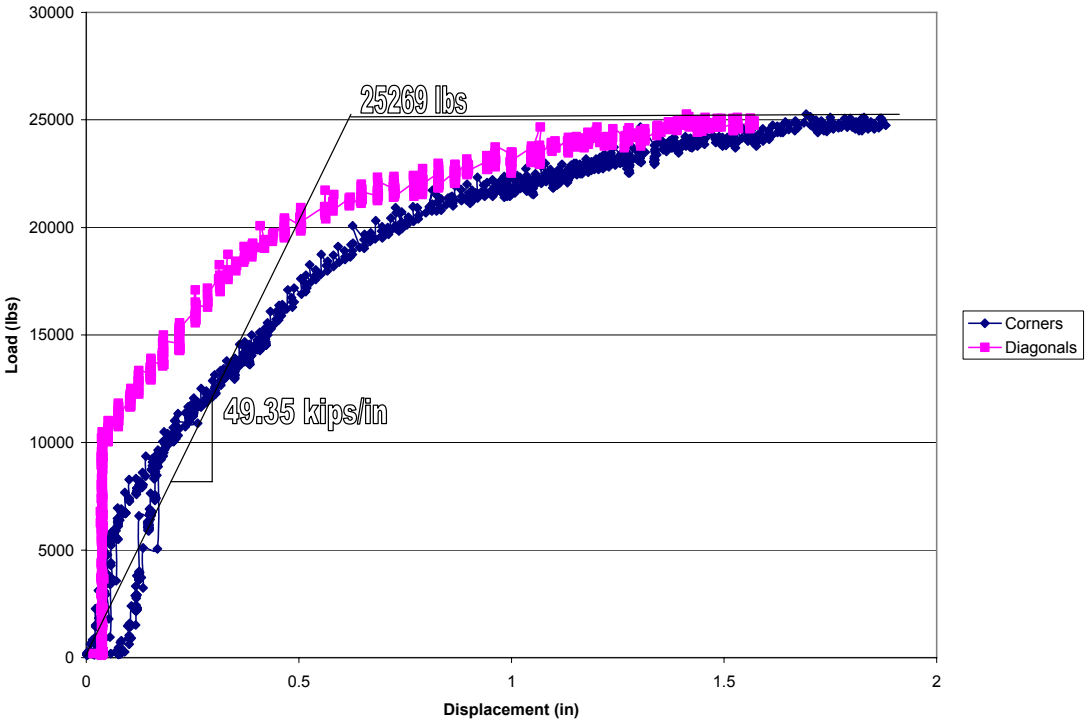

Figure A-13: Load vs. Displacement
United Steel Deck 4.5 in 20/20 Ga.

Test 14:

Wheeling 6 in 20/20 Ga. – Weld Test

Diaphragm Setup:

Width:	24 ft
Span:	24 ft
No. of Panels	12
Structural Connection	¾" Diameter Weld/rib at ends ¾" Diameter Weld/ft at sides
Side-lap Fastener	#12 TEK Screw @ 12 in o/c

Steel Deck:

Measured Thickness:	0.0359 in
Deck Height:	6 in
F_y = 92 ksi	F_u = 94 ksi

Results

Maximum Applied Load:		45235 lbs
Deflection at Max. Load:	Corners	2.467 in
	Diagonals	2.270 in
Design Load:	Corners	45235 lbs
	Diagonals	45235 lbs
Stiffness Evaluation:	Corners	29.60 kips/in
	Diagonals	42.52 kips/in
Deflection for Stiffness Determination:		
	Corners	0.589 in
	Diagonals	0.410 in
Observed Failure Limit State:	Structural Fastener	

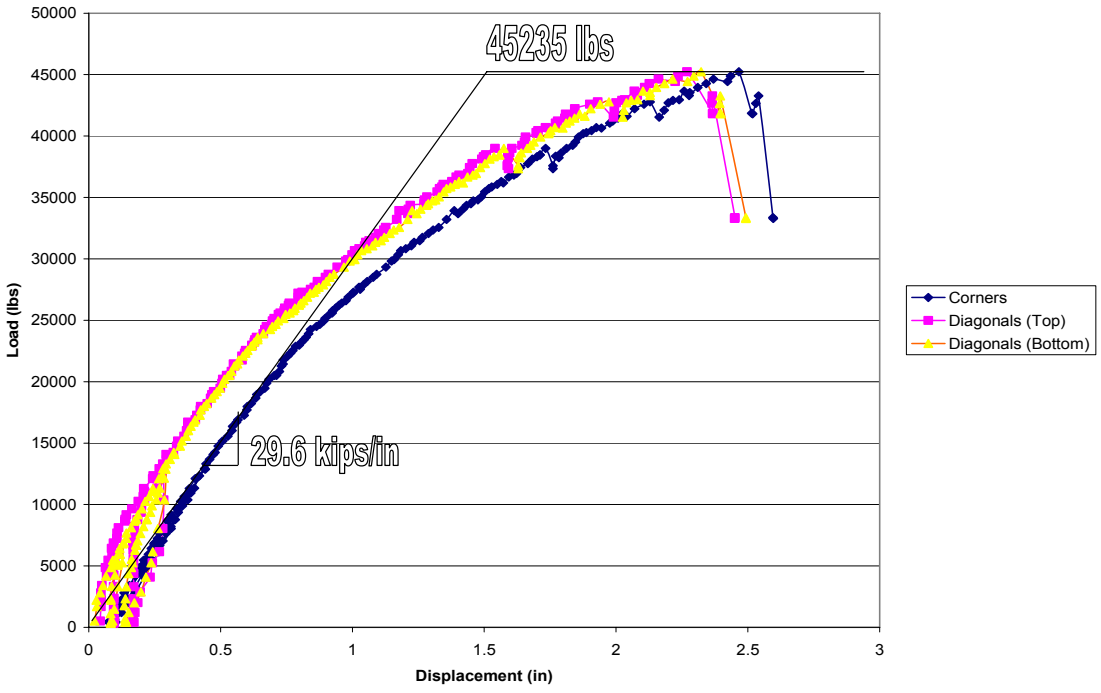

Figure A-14: Load vs. Displacement
Wheeling 6 in 20/20 Ga.

Test 15:

Vulcraft 3 in 16/16 Ga. – Pin Test

Diaphragm Setup:

Width:	24 ft
Span:	24 ft
No. of Panels	12
Structural Connection	Hilti Pin X-ENP-19 L15/rib at ends Hilti Pin X-ENP-19 L15/ft at sides
Side-lap Fastener	Button Punch @ 12 in o/c

Steel Deck:

Measured Thickness:	0.0592 in
Deck Height:	3 in
F_y = 43 ksi	F_u = 56 ksi

Results

Maximum Applied Load:		11733 lbs
Deflection at Max. Load:	Corners	1.761 in
	Diagonals	1.641 in
Design Load:	Corners	11733 lbs
	Diagonals	11733 lbs
Stiffness Evaluation:	Corners	14.37 kips/in
	Diagonals	18.62 kips/in
Deflection for Stiffness Determination:		
	Corners	0.327 in
	Diagonals	0.252 in
Observed Failure Limit State:	Structural Fastener	

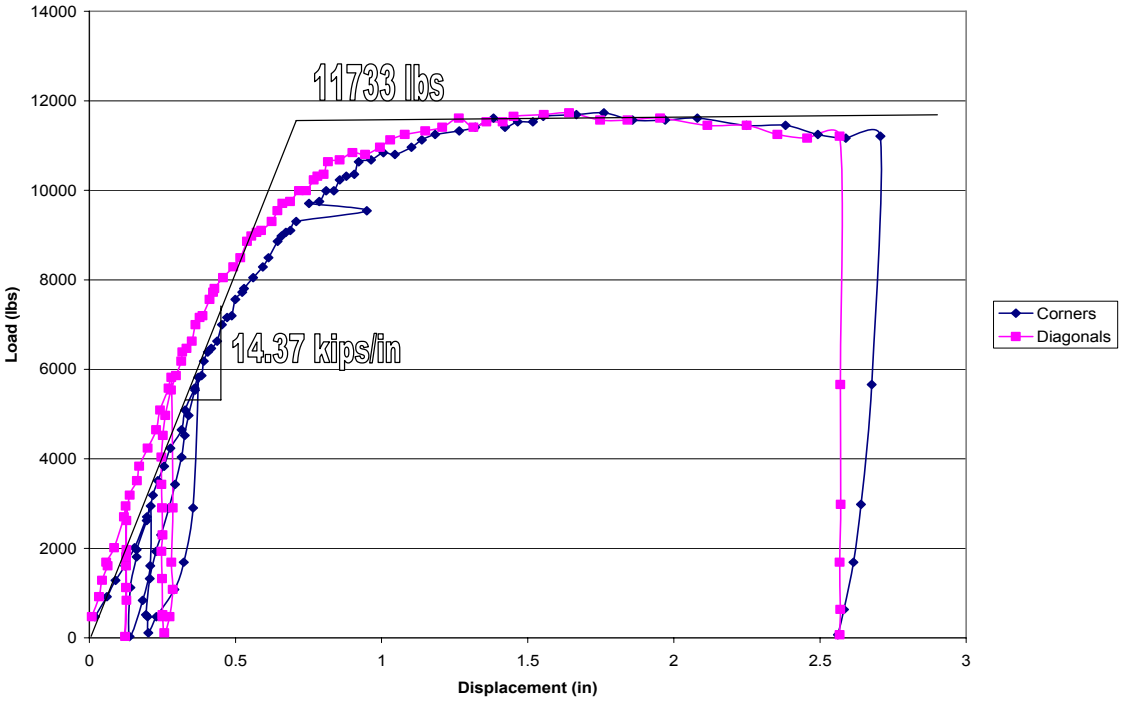

Figure A-15: Load vs. Displacement
Vulcraft 3 in 16/16 Ga.

Test 16:

Vulcraft 3 in 20/20 Ga. – Pin Test

Diaphragm Setup:

Width:	24 ft
Span:	24 ft
No. of Panels	12
Structural Connection	Hilti Pin X-ENP-19 L15/rib at ends Hilti Pin X-ENP-19 L15/ft at sides
Side-lap Fastener	Button Punch @ 12 in o/c

Steel Deck:

Measured Thickness:	0.0461 in
Deck Height:	3 in
F_y = 41 ksi	F_u = 57 ksi

Results

Maximum Applied Load:		8898 lbs
Deflection at Max. Load:	Corners	1.924 in
	Diagonals	1.781 in
Design Load:	Corners	8416 lbs
	Diagonals	8898 lbs
Stiffness Evaluation:	Corners	7.72 kips/in
	Diagonals	10.09 kips/in
Deflection for Stiffness Determination:		
	Corners	0.399 in
	Diagonals	0.353 in
Observed Failure Limit State:	Structural Fastener	

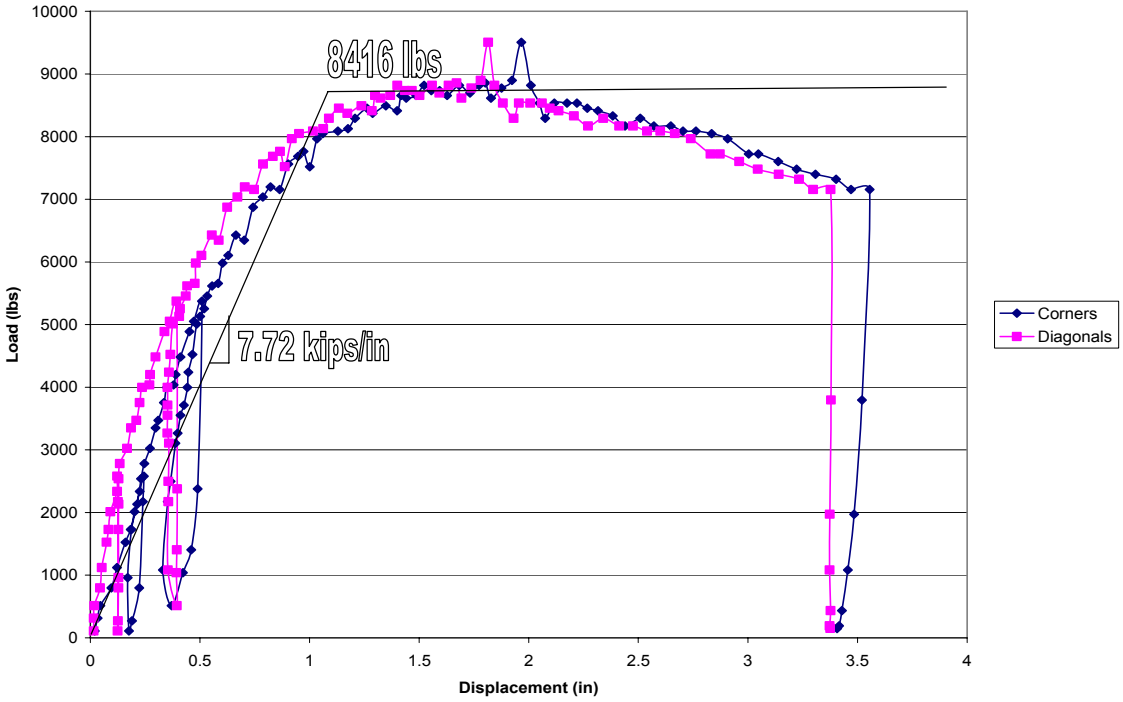

Figure A-16: Load vs. Displacement
Vulcraft 3 in 20/20 Ga.

Test 17:

Wheeling 6 in 16/16 Ga. – Pin Test

Diaphragm Setup:

Width:	24 ft
Span:	24 ft
No. of Panels	12
Structural Connection	Hilti Pin X-ENP-19 L15/rib at ends Hilti Pin X-ENP-19 L15/ft at sides
Side-lap Fastener	#12 TEK Screw @ 12 in o/c

Steel Deck:

Measured Thickness:	0.0576 in
Deck Height:	6 in
F_y = 86 ksi	F_u = 89 ksi

Results

Maximum Applied Load:		60133 lbs
Deflection at Max. Load:	Corners	1.138 in
	Diagonals	0.832 in
Design Load:	Corners	60133 lbs
	Diagonals	60133 lbs
Stiffness Evaluation:	Corners	82.54 kips/in
	Diagonals	217.08 kips/in
Deflection for Stiffness Determination:		
	Corners	0.291 in
	Diagonals	0.111 in
Observed Failure Limit State:	Structural Fastener	

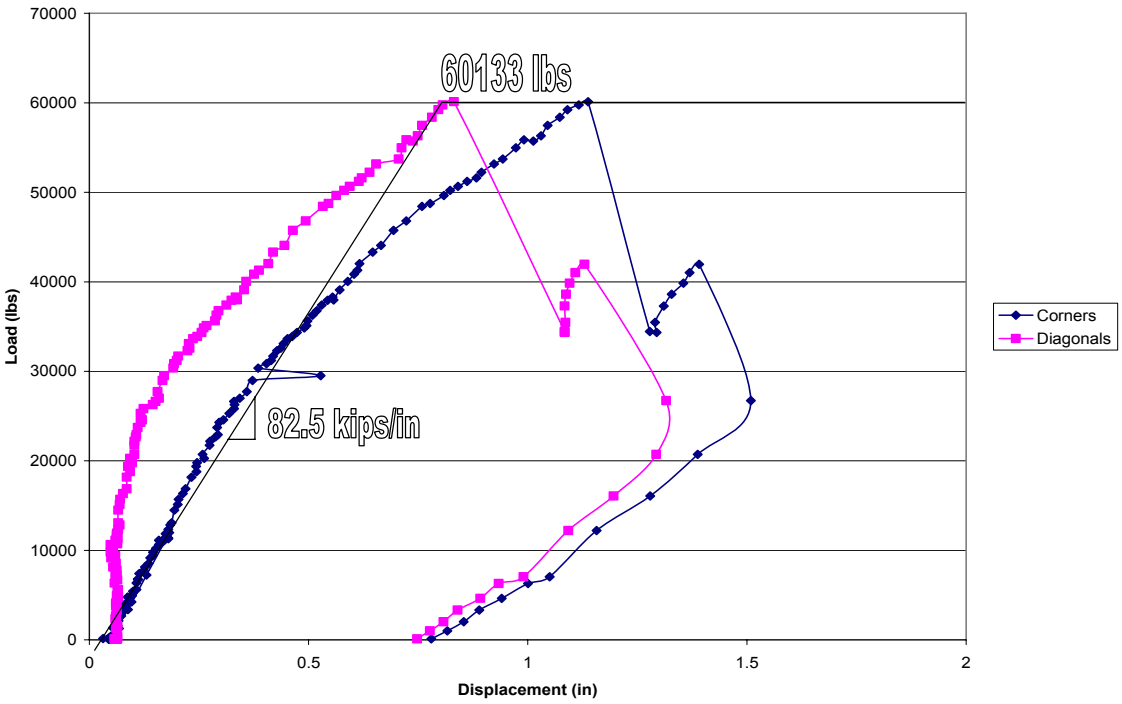

Figure A-17: Load vs. Displacement
Wheeling 6 in 16/16 Ga.

Test 18:

Vulcraft 3 in 18/18 Ga. – Screw Test

Diaphragm Setup:

Width:	24 ft
Span:	24 ft
No. of Panels	12
Structural Connection	#12 TEK Screw /rib at ends #12 TEK Screw /ft at sides
Side-lap Fastener	#10 TEK Screw @ 12 in o/c

Steel Deck:

Measured Thickness:	0.0464 in
Deck Height:	3 in
F_y = 41 ksi	F_u = 56 ksi

Results

Maximum Applied Load:		29675 lbs
Deflection at Max. Load:	Corners	3.321 in
	Diagonals	3.088 in
Design Load:	Corners	28834 lbs
	Diagonals	28879 lbs
Stiffness Evaluation:	Corners	94.59 kips/in
	Diagonals	392.50 kips/in
Deflection for Stiffness Determination:		
	Corners	0.117 in
	Diagonals	0.028 in
Observed Failure Limit State:	Structural Fastener	

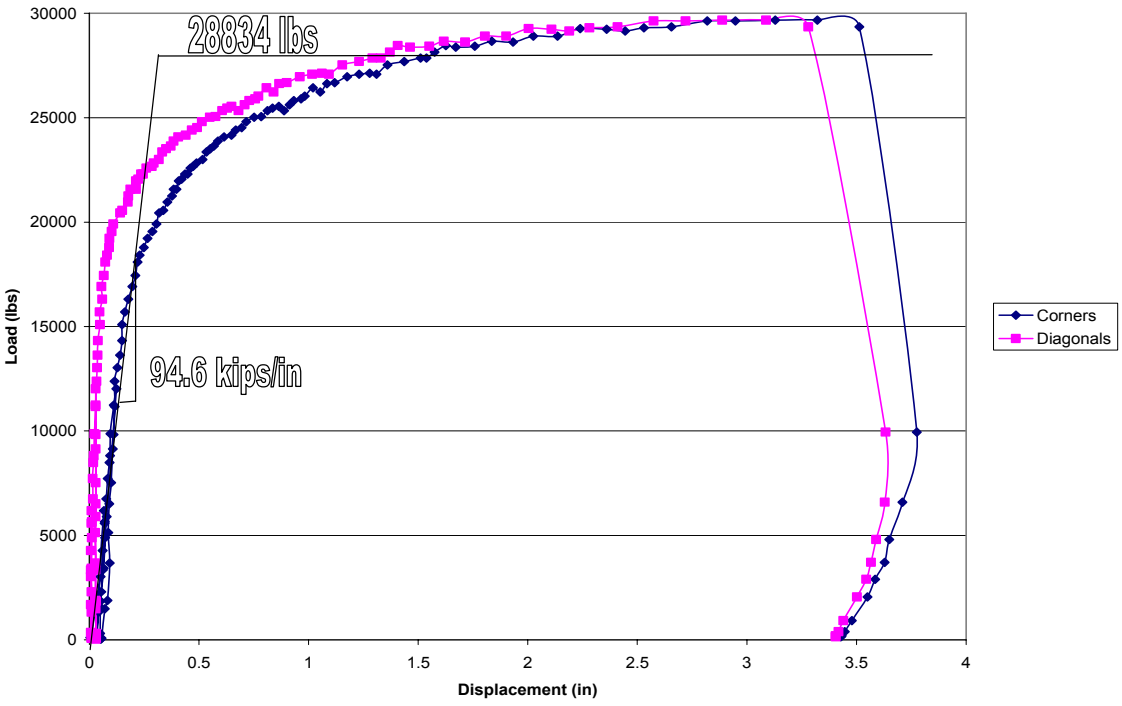

Figure A-18: Load vs. Displacement
Vulcraft 3 in 18/18 Ga.

Test 19:

Vulcraft 3 in 20/20 Ga. – Screw Test

Diaphragm Setup:

Width:	24 ft
Span:	24 ft
No. of Panels	12
Structural Connection	#12 TEK Screw /rib at ends #12 TEK Screw /ft at sides
Side-lap Fastener	#10 TEK Screw @ 12 in o/c

Steel Deck:

Measured Thickness:	0.0460 in
Deck Height:	3 in
$F_y = 41$ ksi	$F_u = 56$ ksi

Results

Maximum Applied Load:		21170 lbs
Deflection at Max. Load:	Corners	4.222 in
	Diagonals	4.060 in
Design Load:	Corners	20295 lbs
	Diagonals	20295 lbs
Stiffness Evaluation:	Corners	39.16 kips/in
	Diagonals	62.39 kips/in
Deflection for Stiffness Determination:		
	Corners	0.194 in
	Diagonals	0.122 in
Observed Failure Limit State:	Structural Fastener	

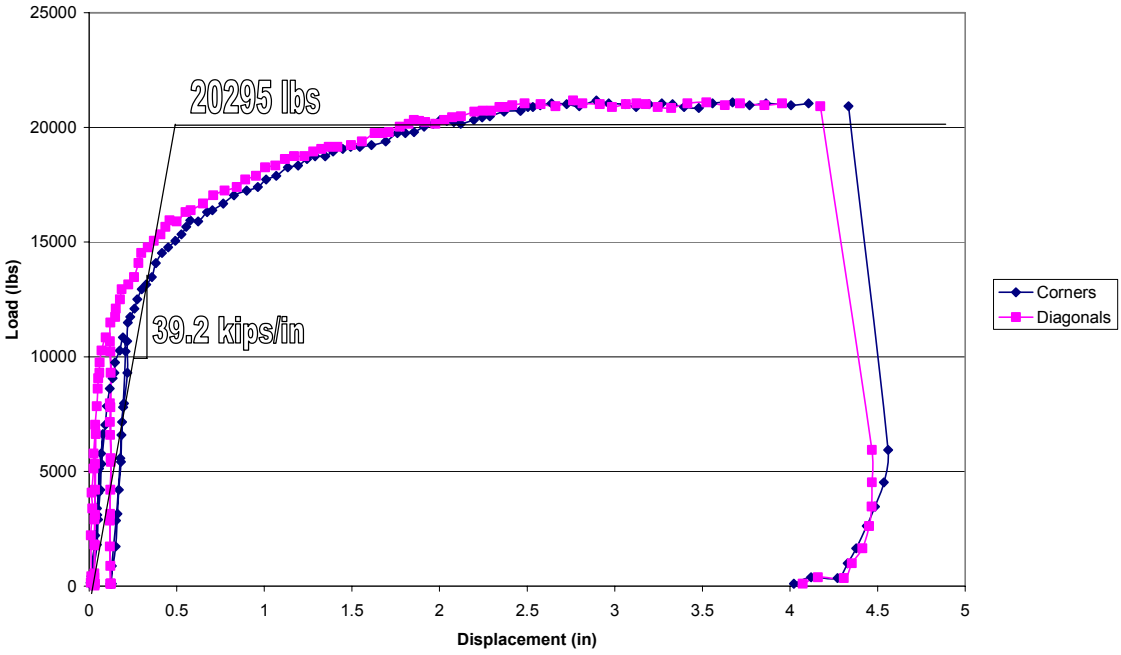

Figure A-19: Load vs. Displacement
Vulcraft 3 in 18/18 Ga.

Test 20:

Wheeling 6 in 20/20 Ga. – Screw Test

Diaphragm Setup:

Width:	24 ft
Span:	24 ft
No. of Panels	12
Structural Connection	#12 TEK Screw /rib at ends #12 TEK Screw /ft at sides
Side-lap Fastener	#10 TEK Screw @ 12 in o/c

Steel Deck:

Measured Thickness:	0.0358 in
Deck Height:	6 in
F_y = 92 ksi	F_u = 94 ksi

Results

Maximum Applied Load:		41786 lbs
Deflection at Max. Load:	Corners	1.556 in
	Diagonals	1.237 in
Design Load:	Corners	41786 lbs
	Diagonals	41786 lbs
Stiffness Evaluation:	Corners	39.78 kips/in
	Diagonals	67.02 kips/in
Deflection for Stiffness Determination:		
	Corners	0.420 in
	Diagonals	0.249 in
Observed Failure Limit State:	Structural Fastener	

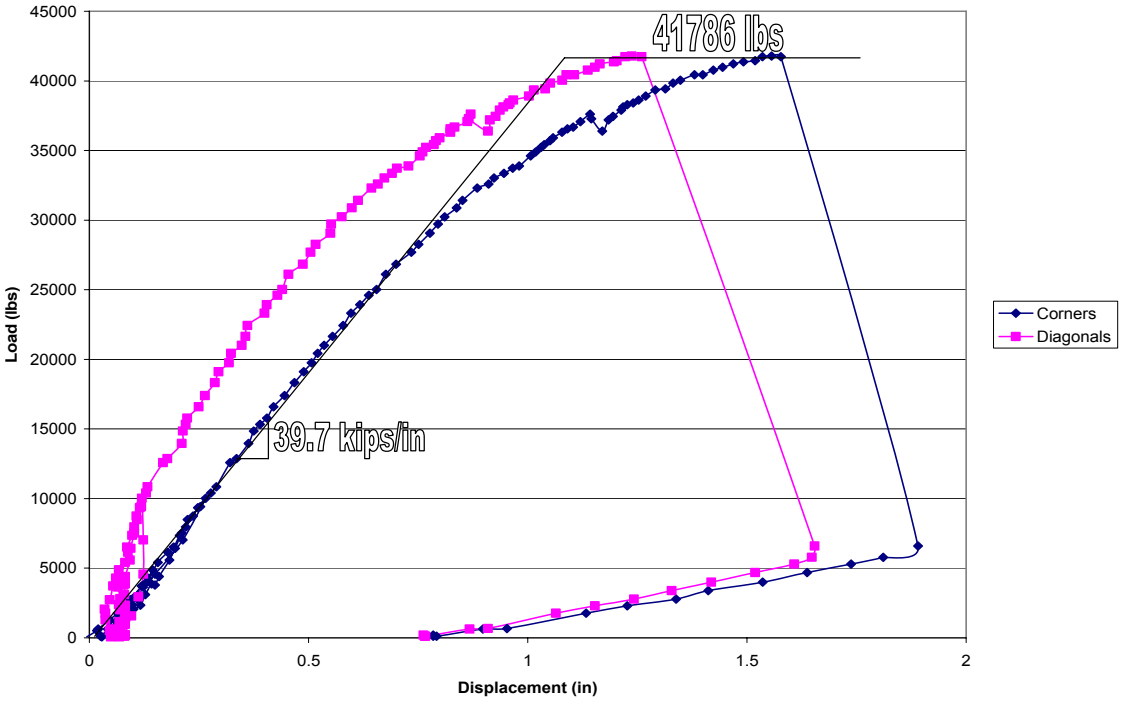

Figure A-20: Load vs. Displacement
Wheeling 6 in 20/20 Ga.

APPENDIX B – REDUCED COUPON AND DIAPHRAGM DATA

Table B-1: Measured Coupon Data

Test #	Coupon #	Measure Width (in)	Measured Thickness (in)	Yield Stress (ksi)	Ultimate Stress (ksi)	% Elongation
1	1	0.4720	0.4735	107.73	108.95	6.7
	2	0.4720	0.4735	107.09	108.25	6.1
2	3	0.4710	0.4725	46.37	56.66	40.5
	4	0.5160	0.5175	46.10	56.90	41.0
	5	0.5160	0.5175	48.83	58.30	38.6
	6	0.5150	0.5165	48.92	58.42	40.7
3	7	0.5160	0.5175	50.18	60.85	39.1
	8	0.5140	0.5155	49.20	60.79	39.2
4	9	0.5050	0.5065	46.36	59.15	39.8
	10	0.5060	0.5075	46.81	59.12	40.9
	11	0.5040	0.5055	50.08	60.23	40.1
	12	0.5060	0.5075	49.26	60.04	39.9
5	13	0.5040	0.5055	47.37	59.27	38.6
	14	0.5050	0.5065	47.07	58.82	41.6
	15	0.5140	0.5155	49.24	59.40	39.7
	16	0.5030	0.5045	49.20	59.20	37.8
6	17	0.5020	0.5035	43.39	59.33	41.3
	18	0.5150	0.5165	42.59	59.46	39.3
	19	0.5030	0.5045	45.76	59.74	39.6
	20	0.5020	0.5035	45.51	59.96	39.4
7	21	0.5060	0.5075	108.26	109.74	5.0
	22	0.5040	0.5055	108.58	109.62	7.0
8	23	0.5040	0.5055	90.73	92.08	8.2
	24	0.5010	0.5025	91.38	92.43	8.5
9	25	0.4610	0.4625	50.17	61.02	36.7
	26	0.4620	0.4635	50.07	60.70	38.8

Table B-1: Continued

10	27	0.4610	0.4625	46.77	58.71	40.5
	28	0.4720	0.4735	46.62	58.91	42.3
	29	0.4620	0.4635	49.46	59.67	39.9
	30	0.4620	0.4635	49.22	59.74	38.1
11	31	0.5040	0.5055	46.03	58.49	42.4
	32	0.5030	0.5045	46.42	58.91	41.7
	33	0.4620	0.4635	48.85	58.91	40.1
	34	0.4630	0.4645	48.75	58.83	40.8
12	35	0.5020	0.5035	94.64	97.96	0.6
	36	0.5030	0.5045	94.89	97.17	1.4
13	37	0.5020	0.5035	46.30	56.59	41.8
	38	0.5010	0.5025	44.49	56.09	41.2
	39	0.5020	0.5035	49.72	59.26	39.0
	40	0.5040	0.5055	49.80	59.64	37.2
14	41	0.4710	0.4725	92.73	94.03	3.0
	42	0.4600	0.4615	91.38	93.56	7.0
	43	0.4720	0.4735	92.51	94.22	4.2
	44	0.4710	0.4725	92.89	94.01	2.8
15	45	0.5020	0.5035	43.14	56.46	32.1
	46	0.5030	0.5045	42.85	56.42	31.9
16	47	0.5060	0.5075	41.54	56.54	29.9
	48	0.5020	0.5035	41.27	56.65	31.2
17	49	0.5080	0.5095	85.37	87.66	6.7
	50	0.5150	0.5165	85.79	88.59	6.9
	51	0.4620	0.4635	85.87	88.37	4.6
	52	0.4710	0.4725	86.10	89.91	8.3

Table B-1: Continued

18	53	0.5150	0.5165	41.18	55.87	32.5
	54	0.5170	0.5185	41.69	56.03	29.3
19	55	0.4620	0.4635	40.94	55.85	31.1
	56	0.4630	0.4645	42.02	56.48	31.7
20	57	0.4910	0.4925	90.91	92.84	3.9
	58	0.4720	0.4735	91.31	93.33	4.8
	59	0.4720	0.4735	92.90	94.68	3.9
	60	0.4720	0.4735	92.78	94.27	4.0

Table B-2: Corrected Deflection at Maximum Load

Test	Deflection At Max Load (in)	
	Corner	Diag
1 (1)	3.934	3.702
2 (6)	2.831	2.758
3 (4)	5.119	4.956
4 (7)	2.365	2.119
5 (8)	3.287	3.043
6 (5)	3.83	3.628
7 (11)	1.983	3.7148
8 (10)	1.277	1.078
9 (13)	6.604	6.426
10 (15)	2.111	1.818
11 (16)	1.49	1.216
12 (18)	4.447	4.179
13 (19)	1.704	1.464
14 (20)	2.467	2.27
15 (12)	1.761	1.641
16 (14)	1.967	1.815
17 (17)	1.1378	0.83184
18 (3)	3.3209	3.0876
19 (2)	4.2219	4.06
20 (9)	1.5564	1.2372

Figure B-1: Deflection at Maximum Load Comparison, Corner vs. Diagonals

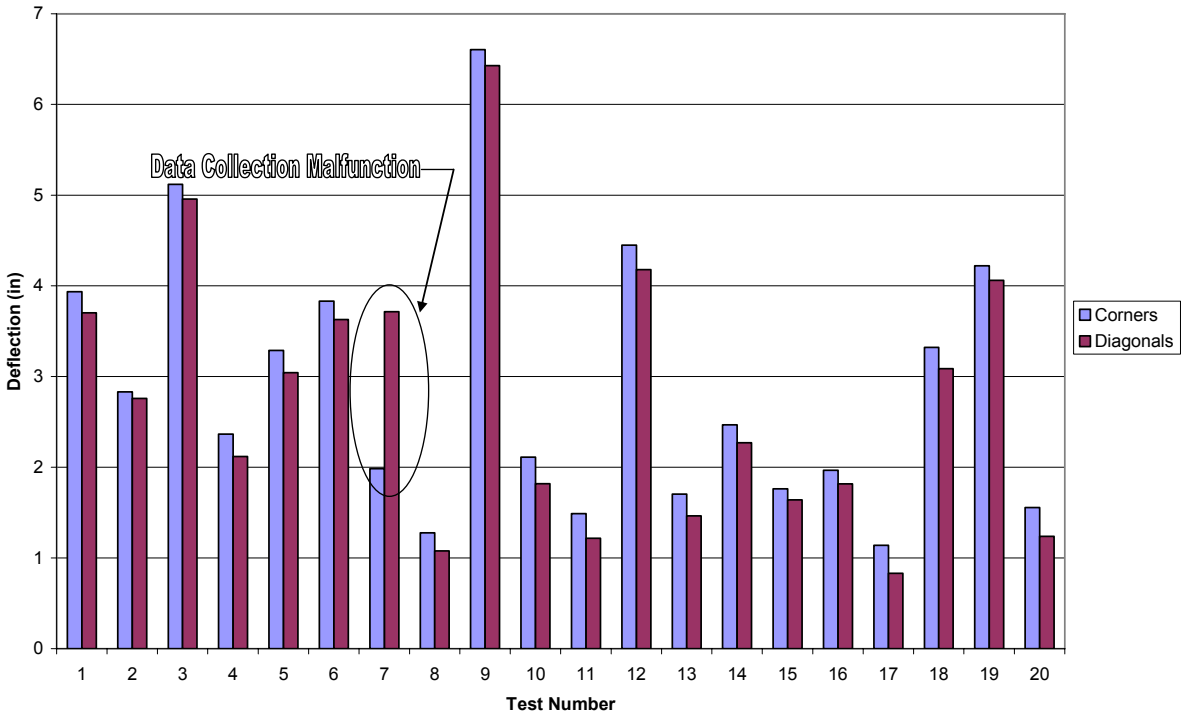

Table B-3: SDIDDM03 Strength

Test No.	SDI			Test Su	%
	Q_f (lbs)	Q_s (lbs)	S_u (lbs/ft)	(lbs/ft)	Difference
1 (1)	2233	771	164	191	17
2 (6)	1637	771	149	201	35
3 (4)	2227	1020	198	143	-28
4 (7)	2161	1018	196	230	17
5 (8)	3798	771	202	250	23
6 (5)	2565	1284	244	201	-18
7 (11)	1938	771	156	206	32
8 (10)	3149	1284	258	228	-12
9 (13)	2534	1020	206	144	-30
10 (15)	4281	771	214	203	-5
11 (16)	5364	1020	276	190	-31
12 (18)	7194	1020	554	501	-10
13 (19)	3271	771	373	383	3
14 (20)	5320	1743	738	685	-7
15 (12)	5897	858	520	208	-60
16 (14)	3732	309	233	149	-36
17 (17)	5897	2903	1354	1066	-21
18 (3)	3871	1020	527	511	-3
19 (2)	2925	771	398	360	-10
20 (9)	4459	1542	757	741	-2
				Average	-7

Table B-4 SDIDDM03 Strength with Shear Limitation

Test No.	SDI w/ Shear Limitation			Test Su (lbs/ft)	% Difference
	Qf (lbs)	Qs (lbs)	Su(lbs/ft)		
1 (1)	2000	771	158	191	21
2 (6)	1637	771	149	201	35
3 (4)	2000	1020	193	143	-26
4 (7)	2000	1018	192	230	19
5 (8)	2000	771	158	250	58
6 (5)	2000	1284	230	201	-13
7 (11)	1938	771	156	206	32
8 (10)	3149	1284	258	228	-12
9 (13)	2534	1020	206	144	-30
10 (15)	4281	771	214	203	-5
11 (16)	4500	1020	255	190	-25
12 (18)	7194	1020	529	501	-5
13 (19)	3271	771	369	383	4
14 (20)	4034	1743	707	685	-3
15 (12)	4500	858	479	208	-57
16 (14)	3732	309	233	149	-36
17 (17)	4500	2000	945	1066	13
18 (3)	2000	1020	473	511	8
19 (2)	2000	771	372	360	-3
20 (9)	2000	1542	653	741	13
				Average	-1

APPENDIX C - DIAPHRAGM TEST CONNECTION FAILURE MATRIX

In the following section a table is presented that shows the connection failures that were present in each diaphragm test. There are many different failure modes that were observed and each one was given a symbol to organize the tables more efficiently. The typical failure modes present for the pin and screw tests are:

N – Nothing

NA – No Attachment (Top sheet had no edge distance therefore not considered to be attached)

S – Shear

P – Pull Over or Pull Out (Pull out applies to the pins only)

L – Local Buckling

R – Roll

B – Bearing

T – Edge Tear Out

D – Displacement from button punch failure

For a welded test the same designations apply but a few additional ones were added. These additions were done to explain the structural welds and their separation from the sheet material.

NP – No Penetration

1 – 25 % Release

2 – 50 % Release

3 – 75 % Release

4 – 100 % Release

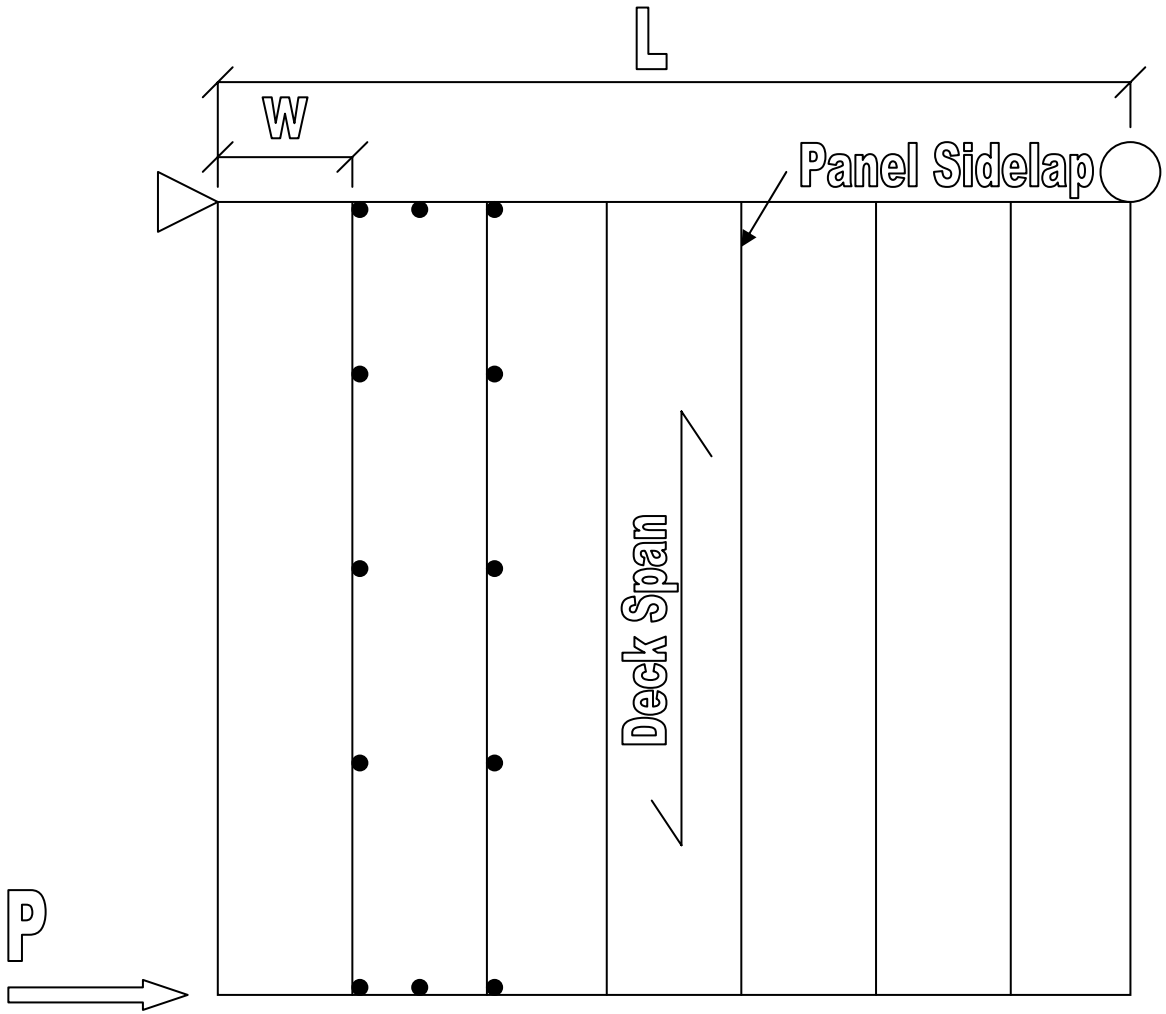
L
W
Panel Sidelap
Deck Span
P

Table C-1: Connection Failure Matrix for Test #1

N	B	L	N	L	N	L	B	L	N	L	N	L	B	L	N	L	B	L	N	L	S	L	B	N
N																								N
N																								N
N		R		R		R		R		R		R		R		R		R		R		R		N
N																								N
N																								N
N		R		R		R		R		S		R		S		R		R		R		R		N
N																								N
N																								N
N		R		R		R		R		R		R		R		R		R		R		R		N
N																								N
N																								N
N		R		R		R		R		R		R		R		R		R		R		R		N
N																								N
N																								N
N		R		R		R		S		R		R		R		R		R		R		R		N
N																								N
N																								N
N		S		S		R		R		R		R		S		R		S		R		R		N
N																								N
N																								N
N		S		S		R		S		S		R		S		R		S		R		R		N
N																								N
N																								N
N	B	P	N	B	N	B	B	P	N	B	N	B	B	P	N	B	N	P	N	B	B	P	B	N

Table C-2: Connection Failure Matrix for Test #2

N	B	B	N	B	N	B	N	B	B	L	N	L	N	L	N	L	N	L	N	L	B	L	B	N
N																								N
N																								N
N		S		R		S		R		S		R		R		R		R		R		R		N
N																								N
N																								N
N		R		R		S		R		S		R		R		R		R		R		R		N
N																								N
N																								N
N		R		R		B		R		R		R		R		R		R		R		R		N
N																								N
N																								N
N		R		R		B		R		S		B		R		R		R		R		R		N
N																								N
N																								N
N		R		R		R		R		R		R		R		R		R		R		R		N
N																								N
N																								N
N		R		R		R		R		S		R		R		R		R		R		R		N
N																								N
N																								N
N		R		S		B		R		R		R		R		R		R		R		R		N
N																								N
N																								N
N	B	B	N	B	N	B	N	B	B	B	N	B	N	B	N	B	N	B	N	B	B	B	B	N

Table C-3: Connection Failure Matrix for Test #3

N	B	B	B	B	B	B	B	N	B	B	B	N	N	B	B	N	N	N	B	N	N	N	B	N
N																								N
N																								N
N	R	R	R	R	R	R	R	R	R	R	R	R	R	R	R	R	R	R	R	R	R	R	R	N
N																								N
N																								N
N	S	R	R	R	R	R	R	R	S	R	R	R	R	R	R	R	R	R	R	R	R	R	R	N
N																								N
N																								N
N	S	R	R	R	R	R	R	R	S	R	S	R	S	R	R	R	R	R	R	R	R	R	R	N
N																								N
N																								N
N	S	R	R	R	R	R	R	R	S	R	R	R	R	R	R	R	S	R	R	R	R	R	R	N
N																								N
N																								N
N	S	R	R	R	R	R	R	R	R	R	R	R	S	R	R	R	R	R	R	R	R	R	R	N
N																								N
N																								N
N	S	R	R	R	R	R	R	R	S	R	R	R	R	R	R	R	S	R	R	R	R	R	R	N
N																								N
N																								N
N	S	R	R	R	R	R	R	R	S	R	S	R	R	R	R	R	R	R	R	R	R	R	R	N
N																								N
N																								N
N	P	B	B	N	B	N	N	N	B	B	N	N	B	B	N	N	N	N	N	N	N	B	B	N

Table C-4: Connection Failure Matrix for Test #4

N	B	B	B	B	N	B	N	B	N	B	B	S	N	B	N	L	N	B	B	S	B	S	N	N
N																								N
N																								N
N		T		B		R		R		B		T		B		R		R		R		S		N
N																								N
N																								N
N		T		R		T		R		B		T		R		R		R		R		S		N
N																								N
N																								N
N		T		R		B		R		R		R		R		R		R		R		T		N
N																								N
N																								N
N		T		R		R		R		R		S		B		T		R		R		S		N
N																								N
N																								N
N		T		B		B		R		R		R		B		R		R		R		S		N
N																								N
N																								N
N		B		B		R		R		R		T		R		S		R		R		S		N
N																								N
N																								N
N		B		B		R		R		R		B		B		T		R		R		S		N
N																								N
N																								N
N	B	B	B	B	N	B	N	B	N	B	B	L	N	B	N	B	N	S	S	S	S	B	N	N

Table C-5: Connection Failure Matrix for Test #5

N	N	L	N	S	N	B	S	L	N	L	N	B	N	B	S	B	N	B	N	B	S	S	S	N
N																								N
N																								N
N		R		R		R		B		R		R		R		B		R		R		B		N
N																								N
N																								N
N		R		R		R		B		R		R		R		B		R		R		B		N
N																								N
N																								N
N		R		R		R		B		R		R		R		B		R		R		B		N
N																								N
N																								N
N		R		R		R		B		R		R		R		B		B		R		R		N
N																								N
N																								N
N		R		R		R		B		R		R		R		B		R		R		B		N
N																								N
N																								N
N		R		R		R		B		R		R		R		B		R		R		B		N
N																								N
N																								N
N		R		R		R		B		R		R		R		B		R		R		R		N
N																								N
N																								N
N	S	B	N	B	N	B	S	B	N	B	N	B	N	B	S	B	N	B	N	B	S	P	S	N

Table C-6: Connection Failure Matrix for Test #6

N	B	B	B	B	B	B	B	B	B	S	S	S	B	N	N	N	N	N	N		N	N	N	N
N																								N
N																								N
N	S	R	R	S	R	R	S	R	R	S	R	R	R	S	R	S	R	R	R	R	R	R	R	N
N																								N
N																								N
N	S	R	R	S	R	R	S	R	R	S	R	R	R	R	R	R	R	R	R	S	R	R	R	N
N																								N
N																								N
N	S	R	R	S	R	R	S	R	R	S	R	R	R	R	R	R	R	R	R	S	R	R	R	N
N																								N
N																								N
N	S	R	R	S	R	R	S	R	R	S	R	R	R	R	R	R	R	R	R	S	R	R	R	N
N																								N
N																								N
N	S	R	R	S	R	R	S	R	R	S	R	R	R	R	R	R	R	R	R	S	R	R	R	N
N																								N
N																								N
N	S	R	R	S	R	R	S	R	R	S	R	R	R	R	R	R	R	R	R	S	R	R	R	N
N																								N
N																								N
N	S	R	R	S	R	R	S	R	R	S	R	R	R	R	R	R	R	R	R	S	R	R	R	N
N																								N
N																								N
N	S	B	B	B	N	N	B	N	N	S	S	S	B	S	N	N	N	N	N	N	N	N	N	N

Table C-7: Connection Failure Matrix for Test #7

N	N	L	N	L	N	L	N	L	N	L	N	L	N	L	N	L	N	L	N	L	N	L	N	N
N																								N
N																								N
N		R		R		R		R		R		R		R		R		R		R		R		N
N																								N
N																								N
N		R		S		R		R		R		R		R		R		S		R		R		N
N																								N
N																								N
N		R		S		R		R		R		R		R		R		R		R		S		N
N																								N
N																								N
N		R		R		R		R		R		R		R		R		R		R		R		N
N																								N
N																								N
N		R		R		R		R		R		R		R		R		R		R		R		N
N																								N
N																								N
N		R		R		R		R		R		R		R		R		S		R		R		N
N																								N
N																								N
N		R		R		R		R		R		R		R		R		R		R		S		N
N																								N
N																								N
N	N	N	N	N	N	N	N	N	N	N	N	N	N	N	N	N	N	N	N	N	N	N	N	N

Table C-8: Connection Failure Matrix for Test #8

N	N	N	N	N	N	N	N	N	N	N	N	N	N	P	N	N	N	N	N	N	N	N	N	N
N																								N
N																								N
N		N		S		N		S		N		N		S		S		N		S		N		N
N																								N
N																								N
N		N		S		N		S		N		N		S		S		N		S		N		N
N																								N
N																								N
N		N		S		N		S		N		N		S		R		N		S		N		N
N																								N
N																								N
N		N		S		N		S		N		N		S		R		N		S		N		N
N																								N
N																								N
N		N		S		N		S		N		N		S		S		N		S		N		N
N																								N
N																								N
N		N		S		N		S		N		N		S		R		N		S		N		N
N																								N
N																								N
N		N		S		N		S		N		N		S		S		N		S		N		N
N																								N
N																								N
N	N	N	N	P	N	N	N	P	N	N	N	N	N	P	N	N	N	N	N	N	N	N	N	N

Table C-9: Connection Failure Matrix for Test #9

N	B	N	N	N	N	N	N	N	N	N	N	N	N	N	N	N	N	N	N	N	N	N	N	N
N																								N
N																								N
N	R	R	R	R	R	R	R	R	R	R	R	R	R	R	R	R	R	R	R	R	R	R	R	N
N																								N
N																								N
N	R	R	R	R	R	R	R	R	R	R	R	R	R	R	R	R	R	R	R	R	R	R	R	N
N																								N
N																								N
N	R	R	R	R	R	R	R	R	R	R	R	R	R	R	R	R	R	R	R	R	R	R	R	N
N																								N
N																								N
N	R	R	R	R	R	R	R	R	R	R	R	R	R	R	R	R	R	R	R	R	R	R	R	N
N																								N
N																								N
N	R	R	R	R	R	R	R	R	R	R	R	R	R	R	R	R	R	R	R	R	R	R	R	N
N																								N
N																								N
N	R	R	R	R	R	R	R	R	R	R	R	R	R	R	R	R	R	R	R	R	R	R	R	N
N																								N
N																								N
N	R	R	R	R	R	R	R	R	R	R	R	R	R	R	R	R	R	R	R	R	R	R	R	N
N																								N
N																								N
N	P	N	N	N	N	N	N	N	N	N	N	N	N	N	N	N	N	N	N	N	N	N	N	N

Table C-10: Connection Failure Matrix for Test #10

N	N	N	N	N	N	N	N	N	N	N	N	N	N	N	N	N	N	N	N	N	N	N	N	N
N																								N
N																								N
N		T		T		T		T		T		B		R		R		R		R		B		N
N																								N
N																								N
N		T		T		T		T		T		B		R		B		B		T		T		N
N																								N
N																								N
N		T		T		T		T		T		B		B		R		R		B		R		N
N																								N
N																								N
N		T		T		T		T		T		R		B		R		R		B		R		N
N																								N
N																								N
N		T		T		T		T		T		B		B		R		R		B		R		N
N																								N
N																								N
N		T		T		T		T		T		R		B		B		R		B		R		N
N																								N
N																								N
N		T		T		T		T		T		R		R		R		B		R		B		N
N																								N
N																								N
N	N	N	N	N	N	N	N	N	N	N	N	P	N	N	N	N	N	P	N	N	N	N	N	N

Table C-11: Connection Failure Matrix for Test #11

N	N	N	N	N	N	N	N	N	N	N	N	N	N	N	N	N	N	N	N	N	N	N	N	N
N																								N
N																								N
N		T		R		NA		R		R		R		T		T		T		T		T		N
N																								N
N																								N
N		T		R		NA		R		R		R		T		T		T		T		T		N
N																								N
N																								N
N		T		R		NA		R		R		R		T		T		T		T		T		N
N																								N
N																								N
N		NA		R		T		R		R		R		T		NA		T		T		T		N
N																								N
N																								N
N		T		R		T		R		R		R		T		T		T		T		T		N
N																								N
N																								N
N		NA		R		T		R		R		R		T		T		R		T		T		N
N																								N
N																								N
N		NA		R		T		R		R		R		T		T		T		T		T		N
N																								N
N																								N
N	N	N	N	N	N	N	N	N	N	N	N	N	N	N	N	N	N	N	N	N	N	N	N	N

Table C-12: Connection Failure Matrix for Test #12

N	N	L	N	L	N	L	N	L	N	L	N	L	N	L	N	L	N	L	N	L	N	L	N	N
N		N		N		N		N		N		N		N		N		N		N		N		N
N		N		N		N		N		N		N		N		N		N		N		N		N
N		N		N		N		N		N		N		N		N		N		N		N		N
N		N		N		N		N		N		N		N		N		N		N		N		N
N		N		N		N		N		N		N		N		N		N		N		N		N
N		N		N		N		N		N		N		N		N		N		N		N		N
N		N		N		N		N		N		N		N		N		N		N		N		N
N		N		N		N		N		N		N		N		N		N		N		N		N
N		N		N		N		N		N		N		N		N		N		N		N		N
N		N		N		N		N		N		N		N		N		N		N		N		N
N		N		N		N		N		N		N		N		N		N		N		N		N
N		N		N		N		N		N		N		N		N		N		N		N		N
N		N		N		N		N		N		N		N		N		N		N		N		N
N		N		N		N		N		N		N		N		N		N		N		N		N
N		N		N		N		N		N		N		N		N		N		N		N		N
N		N		N		N		N		N		N		N		N		N		N		N		N
N		N		N		N		N		N		N		N		N		N		N		N		N
N		N		N		N		N		N		N		N		N		N		N		N		N
N		N		N		N		N		N		N		N		N		N		N		N		N
N		N		N		N		N		N		N		N		N		N		N		N		N
N		N		N		N		N		N		N		N		N		N		N		N		N
N		N		N		N		N		N		N		N		N		N		N		N		N
N		N		N		N		N		N		N		N		N		N		N		N		N
N	2	C	N	C	3	C	N	N	N	N	1	N	N	C	N	C	2	C	N	C	1	NP	N	N

Table C-13: Connection Failure Matrix for Test #13

N	N	1	N	N	1	N	1	N	N	1	1	1	1	N	N	N	N	N	N	2	4	N	4	N
N		N		N		N		N		N		N		N		N		N		N		N		N
N		N		N		N		N		N		N		N		N		N		N		N		N
N		N		N		N		N		N		N		N		N		N		N		N		N
N		N		N		N		N		N		N		N		N		N		N		N		N
N		N		N		N		N		N		N		N		N		N		N		N		N
N		N		N		N		N		N		N		N		N		N		N		N		N
N		N		N		N		N		N		N		N		N		N		N		N		N
N		N		N		N		N		N		N		N		N		N		N		N		N
N		N		N		N		N		N		N		N		N		N		N		N		N
N		N		N		N		N		N		N		N		N		N		N		N		N
N		N		N		N		N		N		N		N		N		N		N		N		N
N		N		N		N		N		N		N		N		N		N		N		N		N
N		N		N		N		N		N		N		N		N		N		N		N		N
N		N		N		N		N		N		N		N		N		N		N		N		N
N		N		N		N		N		N		N		N		N		N		N		N		N
N		N		N		N		N		N		N		N		N		N		N		N		N
N		N		N		N		N		N		N		N		N		N		N		N		N
N		N		N		N		N		N		N		N		N		N		N		N		N
N		N		N		N		N		N		N		N		N		N		N		N		N
N		N		N		N		N		N		N		N		N		N		N		N		N
N		N		N		N		N		N		N		N		N		N		N		N		N
N		N		N		N		N		N		N		N		N		N		N		N		N
N		N		N		N		N		N		N		N		N		N		N		N		N
N	N	1	N	1	N	1	2	N	1	N	1	N	N	1	N	1	N	1	N	3	2	N	2	N

Table C-14: Connection Failure Matrix for Test #14

N	N	N	N	N	N	N	N	N	N	N	N	N	N	N	3	N	N	N	N	N	N	N	2	N	N	3	4	N	2	4	4	4	4	4	3	N
N			R			R			R			R			R			R			R			R			R			R			R			N
N			R			R			R			R			R			R			R			R			R			R			R			N
N			R			R			R			R			R			R			R			R			R			R			R			N
N			R			R			R			R			R			R			R			R			R			R			R			N
N			R			R			R			R			R			R			R			R			R			R			R			N
N			R			R			R			R			R			R			R			R			R			R			R			N
N			R			R			R			R			R			R			R			R			R			R			R			N
N			R			R			R			R			R			R			R			R			R			R			R			N
N			R			R			R			R			R			R			R			R			R			R			R			N
N			R			R			R			R			R			R			R			R			R			R			R			N
N			R			R			R			R			R			R			R			R			R			R			R			N
N			R			R			R			R			R			R			R			R			R			R			R			N
N			R			R			R			R			R			R			R			R			R			R			R			N
N			R			R			R			R			R			R			R			R			R			R			R			N
N			R			R			R			R			R			R			R			R			R			R			R			N
N			R			R			R			R			R			R			R			R			R			R			R			N
N			R			R			R			R			R			R			R			R			R			R			R			N
N			R			R			R			R			R			R			R			R			R			R			R			N
N			R			R			R			R			R			R			R			R			R			R			R			N
N			R			R			R			R			R			R			R			R			R			R			R			N
N			R			R			R			R			R			R			R			R			R			R			R			N
N			R			R			R			R			R			R			R			R			R			R			R			N
N			R			R			R			R			R			R			R			R			R			R			R			N
N			R			R			R			R			R			R			R			R			R			R			R			N
N	N	N	N	N	N	N	N	N	N	N	N	N	N	N	N	N	N	N	N	N	N	N	N	N	N	N	N	N	N	N	N	N	N	N	N	N

Table C-15: Connection Failure Matrix for Test #15

N	N	N	N	N	N	N	N	N	N	N	N	N	N	N	N	N	N	N	N	N	N	N	N	N	N	N	N	N	N	N	N	N	N	N	N	N
N			D			D			D			D			D			D			D			D			D			D			D			N
N			D			D			D			D			D			D			D			D			D			D			D			N
N			D			D			D			D			D			D			D			D			D			D			D			N
N			D			D			D			D			D			D			D			D			D			D			D			N
N			D			D			D			D			D			D			D			D			D			D			D			N
N			D			D			D			D			D			D			D			D			D			D			D			N
N			D			D			D			D			D			D			D			D			D			D			D			N
N			D			D			D			D			D			D			D			D			D			D			D			N
N			D			D			D			D			D			D			D			D			D			D			D			N
N			D			D			D			D			D			D			D			D			D			D			D			N
N			D			D			D			D			D			D			D			D			D			D			D			N
N			D			D			D			D			D			D			D			D			D			D			D			N
N			D			D			D			D			D			D			D			D			D			D			D			N
N			D			D			D			D			D			D			D			D			D			D			D			N
N			D			D			D			D			D			D			D			D			D			D			D			N
N			D			D			D			D			D			D			D			D			D			D			D			N
N			D			D			D			D			D			D			D			D			D			D			D			N
N			D			D			D			D			D			D			D			D			D			D			D			N
N			D			D			D			D			D			D			D			D			D			D			D			N
N			D			D			D			D			D			D			D			D			D			D			D			N
N			D			D			D			D			D			D			D			D			D			D			D			N
N			D			D			D			D			D			D			D			D			D			D			D			N
N			D			D			D			D			D			D			D			D			D			D			D			N
N	N	N	N	N	N	N	N	N	N	N	N	N	N	N	N	N	N	N	N	N	N	N	N	N	N	N	N	N	N	N	N	N	N	N	N	N

Table C-16: Connection Failure Matrix for Test #16

N	N	N	N	N	N	N	N	N	N	N	N	N	N	N	N	N	N	N	N	N	N	N	N	N	N	N	N	N	N	N	N	N	N	N	N	N
N			D			D			D			D			D			D			D			D			D			D			D			N
N			D			D			D			D			D			D			D			D			D			D			D			N
N			D			D			D			D			D			D			D			D			D			D			D			N
N			D			D			D			D			D			D			D			D			D			D			D			N
N			D			D			D			D			D			D			D			D			D			D			D			N
N			D			D			D			D			D			D			D			D			D			D			D			N
N			D			D			D			D			D			D			D			D			D			D			D			N
N			D			D			D			D			D			D			D			D			D			D			D			N
N			D			D			D			D			D			D			D			D			D			D			D			N
N			D			D			D			D			D			D			D			D			D			D			D			N
N			D			D			D			D			D			D			D			D			D			D			D			N
N			D			D			D			D			D			D			D			D			D			D			D			N
N			D			D			D			D			D			D			D			D			D			D			D			N
N			D			D			D			D			D			D			D			D			D			D			D			N
N			D			D			D			D			D			D			D			D			D			D			D			N
N			D			D			D			D			D			D			D			D			D			D			D			N
N			D			D			D			D			D			D			D			D			D			D			D			N
N			D			D			D			D			D			D			D			D			D			D			D			N
N			D			D			D			D			D			D			D			D			D			D			D			N
N			D			D			D			D			D			D			D			D			D			D			D			N
N			D			D			D			D			D			D			D			D			D			D			D			N
N			D			D			D			D			D			D			D			D			D			D			D			N
N			D			D			D			D			D			D			D			D			D			D			D			N
N	N	N	N	N	N	N	N	N	N	N	N	N	N	N	N	N	N	N	N	N	N	N	N	N	N	N	N	N	N	N	N	N	N	N	N	N

Table C-17: Connection Failure Matrix for Test #17

N	N	N	N	N	N	N	N	N	N	N	N	N	N	N	N	N	N	N	N	N	N	N	N	N	N	N	N	N	N	N	N	N	N	N	N	N
N			N			N			N			N			N			N			N			N			N			N			N			N
N			N			N			N			N			N			N			N			N			N			N			N			N
N			N			N			N			N			N			N			N			N			N			N			N			N
N			N			N			N			N			N			N			N			N			N			N			N			N
N			N			N			N			N			N			N			N			N			N			N			N			N
N			N			N			N			N			N			N			N			N			N			N			N			N
N			N			N			N			N			N			N			N			N			N			N			N			N
N			N			N			N			N			N			N			N			N			N			N			N			N
N			N			N			N			N			N			N			N			N			N			N			N			N
N			N			N			N			N			N			N			N			N			N			N			N			N
N			N			N			N			N			N			N			N			N			N			N			N			N
N			N			N			N			N			N			N			N			N			N			N			N			N
N			N			N			N			N			N			N			N			N			N			N			N			N
N			N			N			N			N			N			N			N			N			N			N			N			N
N			N			N			N			N			N			N			N			N			N			N			N			N
N			N			N			N			N			N			N			N			N			N			N			N			N
N			N			N			N			N			N			N			N			N			N			N			N			N
N			N			N			N			N			N			N			N			N			N			N			N			N
N			N			N			N			N			N			N			N			N			N			N			N			N
N			N			N			N			N			N			N			N			N			N			N			N			N
N			N			N			N			N			N			N			N			N			N			N			N			N
N			N			N			N			N			N			N			N			N			N			N			N			N
N			N			N			N			N			N			N			N			N			N			N			N			N
N	N	N	N	N	N	N	N	N	N	N	N	N	N	N	P	P	P	P	P	P	P	N	P	P	N	N	N	N	N	N	N	N	N	N	N	N

Table C-18: Connection Failure Matrix for Test #18

N	N	N	N	S	S	N	S	S	N	S	S	S	N	S	N	S	S	S	N	S	N	N	S	N	S	S	N	N	S	N	S	S	N	N	N	N
N			N			N			N			N			N			N			N			N			N			N			N			N
N			N			N			N			N			N			N			N			N			N			N			N			N
N			N			N			N			N			N			N			N			N			N			N			N			N
N			N			N			N			N			N			N			N			N			N			N			N			N
N			N			N			N			N			N			N			N			N			N			N			N			N
N			N			N			N			N			N			N			N			N			N			N			N			N
N			N			N			N			N			N			N			N			N			N			N			N			N
N			N			N			N			N			N			N			N			N			N			N			N			N
N			N			N			N			N			N			N			N			N			N			N			N			N
N			N			N			N			N			N			N			N			N			N			N			N			N
N			N			N			N			N			N			N			N			N			N			N			N			N
N			N			N			N			N			N			N			N			N			N			N			N			N
N			N			N			N			N			N			N			N			N			N			N			N			N
N			N			N			N			N			N			N			N			N			N			N			N			N
N			N			N			N			N			N			N			N			N			N			N			N			N
N			N			N			N			N			N			N			N			N			N			N			N			N
N			N			N			N			N			N			N			N			N			N			N			N			N
N			N			N			N			N			N			N			N			N			N			N			N			N
N			N			N			N			N			N			N			N			N			N			N			N			N
N			N			N			N			N			N			N			N			N			N			N			N			N
N			N			N			N			N			N			N			N			N			N			N			N			N
N			N			N			N			N			N			N			N			N			N			N			N			N
N			N			N			N			N			N			N			N			N			N			N			N			N
N			N			N			N			N			N			N			N			N			N			N			N			N
N	S	S	S	S	S	S	S	S	S	S	S	S	S	S	S	S	S	S	S	S	S	S	S	S	S	S	S	S	S	S	S	S	S	S	S	N

Table C-19: Connection Failure Matrix for Test #19

N	S	S	S	S	S	N	S	S	N	S	N	N	S	N	N	S	N	N	S	N	N	S	N	N	S	N	N	S	N	N	S	N	N	S	N	N
N			N			N			N			N			N			N			N			N			N			N			N			N
N			N			N			N			N			N			N			N			N			N			N			N			N
N			N			N			N			N			N			N			N			N			N			N			N			N
N			N			N			N			N			N			N			N			N			N			N			N			N
N			N			N			N			N			N			N			N			N			N			N			N			N
N			N			N			N			N			N			N			N			N			N			N			N			N
N			N			N			N			N			N			N			N			N			N			N			N			N
N			N			N			N			N			N			N			N			N			N			N			N			N
N			N			N			N			N			N			N			N			N			N			N			N			N
N			N			N			N			N			N			N			N			N			N			N			N			N
N			N			N			N			N			N			N			N			N			N			N			N			N
N			N			N			N			N			N			N			N			N			N			N			N			N
N			N			N			N			N			N			N			N			N			N			N			N			N
N			N			N			N			N			N			N			N			N			N			N			N			N
N			N			N			N			N			N			N			N			N			N			N			N			N
N			N			N			N			N			N			N			N			N			N			N			N			N
N			N			N			N			N			N			N			N			N			N			N			N			N
N			N			N			N			N			N			N			N			N			N			N			N			N
N			N			N			N			N			N			N			N			N			N			N			N			N
N			N			N			N			N			N			N			N			N			N			N			N			N
N			N			N			N			N			N			N			N			N			N			N			N			N
N			N			N			N			N			N			N			N			N			N			N			N			N
N			N			N			N			N			N			N			N			N			N			N			N			N
N	S	S	S	S	S	S	S	N	S	N	S	S	N	N	S	N	S	S	N	N	S	N	S	S	N	S	S	N	N	S	S	N	N	S	N	N

Table C-20: Connection Failure Matrix for Test #20

N	N	N	N	N	N	N	N	N	N	N	N	N	N	N	N	N	N	N	N	N	S	S	S	S	S	S	S	S	S	S	S	S	S	S	S	S
N			N			N			N			N			N			N			N			N			N			N			N			S
N			N			N			N			N			N			N			N			N			N			N			N			S
N			N			N			N			N			N			N			N			N			N			N			N			S
N			N			N			N			N			N			N			N			N			N			N			N			S
N			N			N			N			N			N			N			N			N			N			N			N			S
N			N			N			N			N			N			N			N			N			N			N			N			S
N			N			N			N			N			N			N			N			N			N			N			N			S
N			N			N			N			N			N			N			N			N			N			N			N			S
N			N			N			N			N			N			N			N			N			N			N			N			S
N			N			N			N			N			N			N			N			N			N			N			N			S
N			N			N			N			N			N			N			N			N			N			N			N			S
N			N			N			N			N			N			N			N			N			N			N			N			S
N			N			N			N			N			N			N			N			N			N			N			N			S
N			N			N			N			N			N			N			N			N			N			N			N			S
N			N			N			N			N			N			N			N			N			N			N			N			S
N			N			N			N			N			N			N			N			N			N			N			N			S
N			N			N			N			N			N			N			N			N			N			N			N			S
N			N			N			N			N			N			N			N			N			N			N			N			S
N			N			N			N			N			N			N			N			N			N			N			N			S
N			N			N			N			N			N			N			N			N			N			N			N			S
N			N			N			N			N			N			N			N			N			N			N			N			S
N			N			N			N			N			N			N			N			N			N			N			N			S
N			N			N			N			N			N			N			N			N			N			N			N			S
N	N	N	N	N	N	S	N	N	N	N	N	N	N	N	N	N	N	S	S	S	S	S	S	S	S	S	S	S	S	S	S	S	S	S	S	S

VITA

Jonathan Mitchell Bagwell was born in Clarksville, Tennessee on July 11, 1981 to Mary Anne and Mitchell Bagwell. He then lived in several places finally settling in Gastonia, North Carolina in 1989. He graduated from Ashbrook High School in 1999. Following his high school graduation, Jonathan attended the University of North Carolina at Charlotte. After many struggles with college he finally graduated from UNCC in 2005 with a Bachelors of Science degree in Civil Engineering. Jonathan then pursued a Masters of Science degree in Civil Engineering at Virginia Polytechnic Institute and State University, Virginia Tech, from 2005 to 2007. Upon completion of his Masters degree Jonathan will begin a career in structural design.